DOKUZ EYLÜL UNIVERSITY
GRADUATE SCHOOL OF NATURAL AND APPLIED SCIENCES

INSTANTANEOUS REACTIVE POWER CONTROL AND ITS MODEL FOR SINGLE PHASE LOADS

by

Hossein HAFEZI

October, 2013

İZMİR

INSTANTANEOUS REACTIVE POWER CONTROL AND ITS MODEL FOR SINGLE PHASE LOADS

A Thesis Submitted to the Graduate School of Natural and Applied Sciences of Dokuz Eylül University
In Partial Fulfillment of the Requirements for the Degree of Master of Science in Electric and Electronic Engineering

by
Hossein HAFEZI

October, 2013
İZMİR

M.Sc THESIS EXAMINATION RESULT FORM

We have read the thesis entitled **"INSTANTANEOUS REACTIVE POWER CONTROL AND ITS MODEL FOR SINGLE PHASE LOADS"** completed by **HOSSEIN HAFEZI** under supervision of **PROF. DR. EYÜP AKPINAR** and we certify that in our opinion it is fully adequate, in scope and in quality, as a thesis for the degree of Master of Science.

Prof. Dr. Eyüp AKPINAR

Supervisor

Y. Doç. Dr. Hakkı T. YALAZAN

(Jury Member)

Prof. Dr. Caşkun SARI

(Jury Member)

Prof.Dr. Ayşe OKUR
Director
Graduate School of Natural and Applied Sciences

ACKNOWLEDGEMENT

I would like to express my gratitude to my supervisor Prof. Dr. Eyüp AKPINAR for the useful comments, remarks and engagement through the learning process of this master thesis. The technical background and the research experience I have gained under his care will be valuable asset to me in whole my future carrier and life. Also, I like to thank research assistance Abdül BALIKCI, members of the Electrical Machines and Power Electronics Laboratory Group and other staff of the Department for their assistance. I will be grateful forever for your love.

Finally I would also like to thank my parents and friends who helped me a lot in finishing this thesis within the limited time and for their endless support during my life.

Hossein HAFEZI

INSTANTANEOUS REACTIVE POWER CONTROL AND ITS MODEL FOR SINGLE PHASE LOADS

ABSTRACT

In this thesis, non-active current theory based on average concept and instantaneous reactive power theory (p-q theory) based on Clark transformation have been studied and analyses of reactive power and reactive current calculation of these theories has been represented. Based on analyses limits of both theories by means of case studies has been realized. New switching function of gate pulses has been extracted and has been examined in state space model in MATLAB/Simulink and programming. Based on model investigation and basic reactive power flow concept novel Cascade PI controller has been proposed.

MATLAB simulation of p-q theory with hysteresis current controller, non-active current theory with SPWM controller and proposed cascade PI controller has been established and effectiveness of control methods has been examined. Finally in a laboratory prototype DSP based implementation has been built and by means of C/C++ language represented theories' code have been executed and simulation and analyses results are verified by experimental ones.

Keywords: p-q theory, non-active current theory, power quality, STATCOM, active power filter, reactive power compensation, single-phase system, SPWM, hysteresis current controller

TEK FAZ YÜKLER İÇİN ANLIK REAKTİF GÜÇ KONTROLÜ VE MODELLENMESİ

ÖZ

Bu tezde, ortalamaya dayalı aktif olmayan akım teorisi ve Clark dönüşümüne dayalı anlık reaktif güç teorisi incelenmiş ve bu teorilerin reaktif güç ve reaktif akım hesaplama analizleri sunulmuştur. Analizlere dayanarak, örnek çalışmalar aracılığıyla her iki teorinin de sınırları belirlenmiştir. Kapı darbe sinyallerinin yeni anahtarlama fonksiyonu elde edilmiş ve durum uzay modelinde MATLAB/Simulink ve programlamada incelenmiştir. Model incelemelerine ve temel reaktif güç akış kavramına dayanarak yeni ardışık PI denetleyici önerilmiştir.

p-q teorisi histerezis akım denetleyicili, aktif olmayan akım teorisi sinüsoidal darbe genişliği modülasyonu (SPWM) denetleyici ile birlikte ve önerilmiş ardışık PI denetleyicinin MATLAB benzetimi yapılmış ve bu kontrol yöntemlerinin etkinliği incelenmiştir. Son olarak DSP işlemci tabanlı bir çalişan laboratuvar prototipine C/C++ dilinde, gösterilmiş olan teoriler yüklenerek benzetim ve analiz sonuçları deneysel sonuçlar ile doğrulanmıştır.

Anahtar Sözcükler: p-q teorisi, aktif olmayan akım teorisi, güç kalitesi, Statik Senkron Kampansatör (STATCOM), aktif güç filtresi, reaktif güç kompanzasyonü, tek faz sistem, sinüsoidal darbe genişliği modülasyonu (SPWM), histerezis akım denetleyici

CONTENTS

Pages

LIST OF FIGURES

Page

LIST OF TABLS

Page

CHAPTER ONE
INTRODUCTION

Active power is the useful part of total electric power which is led to net transfer of energy in one direction. However, reactive power is oscillating part of electric power which does not contribute any useful power from/through network and causes losses and heats the cables in the system. Therefore reactive power compensation and power factor correction has been a significant problem and research issue in power systems. Although Passive Filters (PF) have been known as simplest solution to this problem, by introducing and increasing non-linear loads and random variation of reactive power in power electronic devices which draw harmonics and reactive power component e.g. implemented in renewable technologies, HVDC and FACTS; the demand to instantaneously compensate reactive power, an intelligent and adjustable system has been taken attention of researchers and variety of control methods has been designed and introduced to power system society. Despite PFs, STATCOMs and APFs have the ability to compensate reactive power and mitigate harmonic content of system without any energy storage components.

By increasing propagation of power electronics device to daily life and low voltage application or other single-phase harmonic polluted loads like traction systems or arc furnaces the necessity of single phase STATCOM and APF applicable in low or medium voltage has been sensed. Also single-phase configuration is useful for unbalanced three wires or four wires systems where by means of three independent single-phase STATCOM for each phase reactive power burden of each phase can be controlled and the system's balance has been realized.

Control methods and theories which are responsible for reactive power and reactive current calculation is one of the most important components of STATCOMs and APFs for multi-phase or single-phase systems. Commonly this calculation burden has been carried out in digital processors like microprocessor or microcomputer. Standard approach of these theories are based on average concept or

frequency domain calculation, however for fast and instantaneous compensation variety of theories and control methods in time domain has been investigated.

This thesis comprises six chapters. An overview of reactive power and harmonic compensation systems, different configuration and classification based on various parts of systems has been carried out in chapter two. Chapter three deals with analytical approach on two control methods; non-active current theory based on average concept and p-q theory based on Clark transformation and instantaneous concept. Reactive power and reactive current calculation has been studied and some misinterpretation or limits of these theories have been distinguished. Based on Sinusoidal Pulse Width Modulation (SPWM) continuous switching function of gate pulses has been extracted in chapter four. It is implemented in well-known single phase STATCOM and APF model in MATLAB Simulink and programming environments. MATLAB/Simulation model, MATLAB/Simulation co-working with DSP and stand-alone TM320F2812 eZDSP based laboratory prototype configuration and results are came in chapter five. Finally the conclusion has been made in chapter six.

CHAPTER TWO
REVIEW ON REACTIVE POWER AND HARMONIC COMPENSATION

Reactive power compensation was introduced to power system from early days that ac power systems were born, because most of industrial and urban loads absorb inductive current and reactive power from system and this imaginary current not only doesn't contribute any power to the load but also causes excessive power losses in the transmission lines and distribution networks. Traditional solution to compensate reactive power was capacitors that connected to the front end of the loads as close as possible to the load. This scheme fairly satisfied the compensation requirements of early power systems, however, by introducing solid state devices to the electrical engineering, harmonics are came to existence. These harmonics like reactive current led to losses in the power system and beside this effect they cause resonance problems. Harmonic mitigation in power system was became a new challenging problem for electrical engineering and Passive Filters (PF) were introduced to power systems to trap harmonics in a L-C resonance branch and hinder these undesired components to propagate to the system. Varieties of combination of series and parallel L-C branches have used to compensate wide range of harmonics in power systems. Some prevalent schemes of PFs are shown in Figure 2.1.

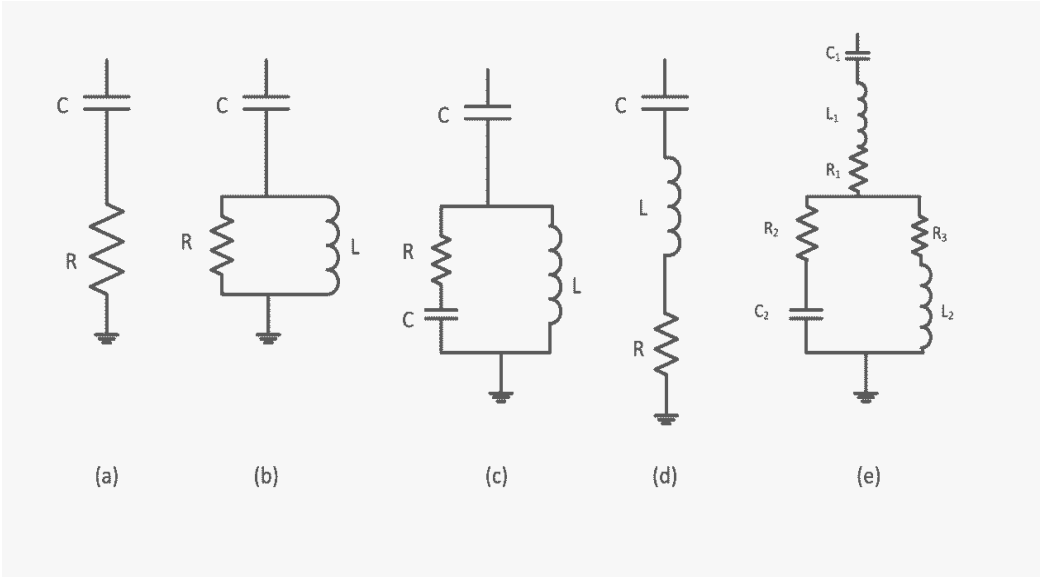

Figure 2.1 Passive filter schemes

Proliferation of solid state devices such as thyristors, Bipolar Junction Transistors (BJT), Metal–Oxide–Semiconductor Field-Effect Transistors (MOSFET), Gate-Turn-Off thyristors (GTO) and Insulated Gate Bipolar Transistors (IGBT) led to flourish the power electronics and this thriving intrinsically propagated harmonics to the network. Passive filters not only were not able to compensate those wide range harmonics but also might cause resonance problems. Also complexity and size of PFs became another major problem. High technology solid state devices make it possible to control current and voltage instantaneously and 70-80 decades of twentieth century was turning point in reactive power and harmonic compensation where Static Synchronous Compensator (STATCOM) and Active Power Filter introduced to power systems. (Gyugyi, & Strycula, 1976), (Harashima, Inaba & Tsuboi, 1976), (Epstein, Yair & Alexandrovitz, 1979) and (Akagi, Kanazawa & Nabae, 1984) were pioneers in instantaneous reactive and harmonic compensation.

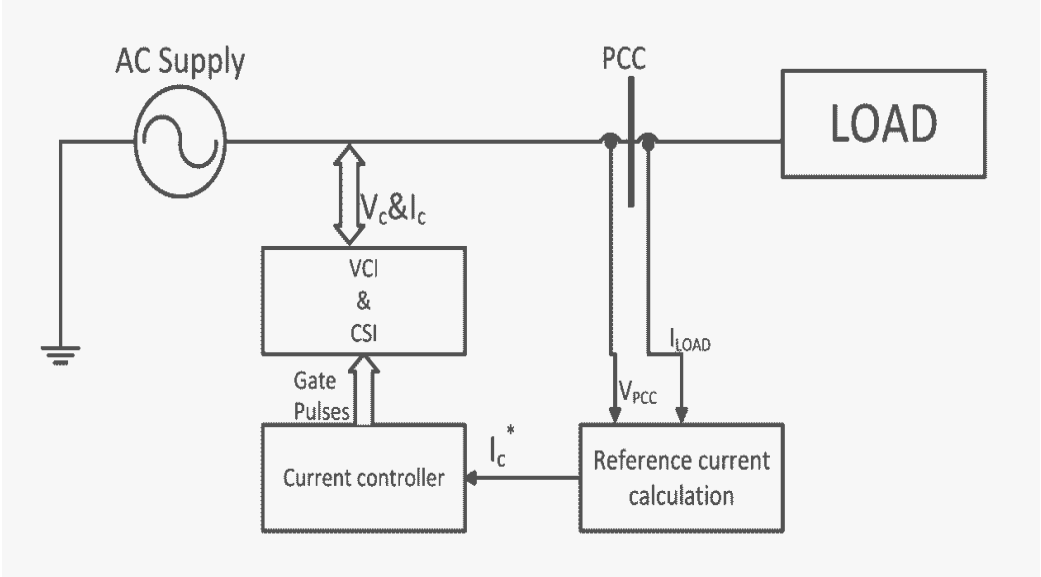

Figure 2.2 Generic scheme of instantaneous reactive power and harmonic compensation

Figure 2.2 represented the generic scheme of instantaneous reactive and harmonic compensation where in Point of Common Coupling (PCC) load current and voltage are measured continuously and by using a proper calculation method, active power, reactive power, active current and reactive current are calculated instantaneously and the reference current for compensation purpose is extracted. Then by means of a current control strategy gate pulses are generated in order to force Voltage Source

Invertor (VSI) or Current Source Invertor (CSI) to follow reference current. Classification of STATCOMs and APFs is based on these three basic parts that are shown in Figure 2.2.

Aim of this chapter is to represent a brief review of instantaneous reactive and harmonic compensation and its classification based on invertor type, topology, supply system, reference current calculation theory or method and current control strategy.

2.1 Classification Based on Inverter Type

2.1.1 Voltage Source Invertor

The most dominant and wide accepted invertor type that is used in instantaneous reactive power and harmonic compensation is Voltage Source Invertor (VSI) because it is lighter than CSI, cheaper and expandable to multilevel versions to enhance the performance and decrease the switching frequency which is very important factor in design and implementing the STATCOMs and APFs. Figure 2.3 shows a shunt STATCOM with VSI that utilized a capacitor as storage device to provide DC voltage for invertor and also supplies switching losses. A series inductance X_c at the input of a VSI bridge is normally used as the buffer between supply terminal voltage and PWM voltage generated by the STATCOM. In this figure VSI is represented based on IGBTs and free wheeling diodes. Configuration of VSI differs depending on application, voltage level, switching frequency and other features of system and circuit that is comprised.

2.1.2 Current Source Invertor

Current Source Invertor (CSI) is another invertor type that is used in STATCOM applications. Figure 2.4 represents a shunt scheme of STATCOM with CSI as

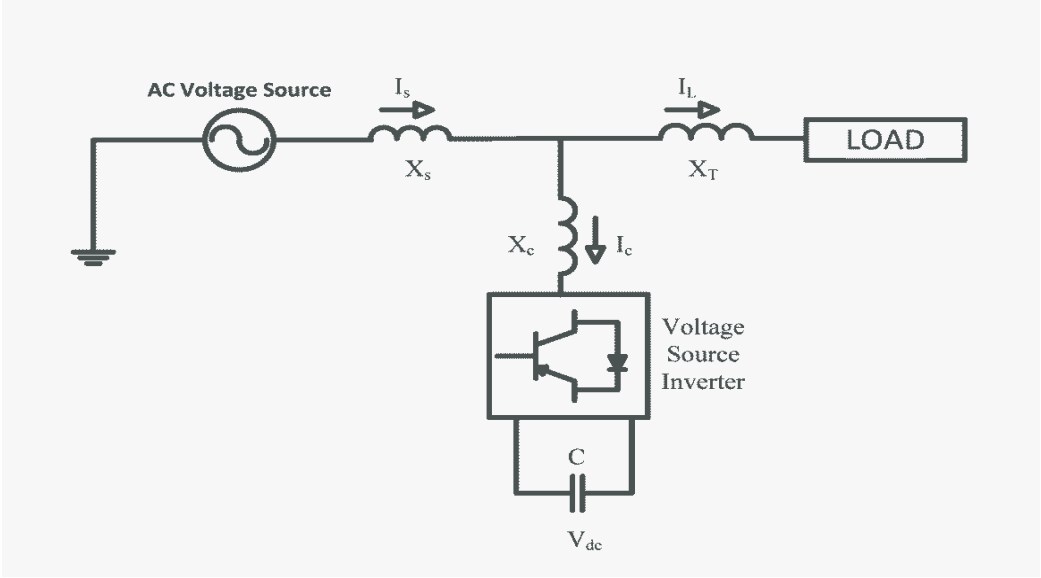

Figure 2.3 Active power filter with voltage source inverter

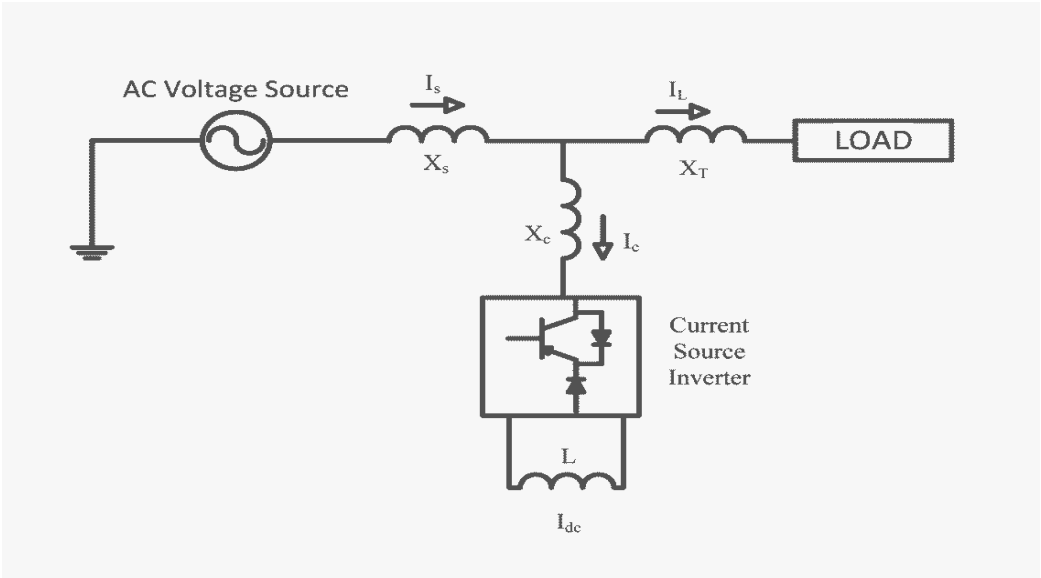

Figure 2.4 Active power filter with current source inverter

compensation current controller. In this scheme CSI behaves as nonlinear current source that produce nonlinear current or reactive current requirement of load thus source voltage just needs to supply active current for load. In Figure 2.4 a diode is used in series with IGBTs for reverse voltage blocking. However, GTO-based configurations do not need these series diode but they have restricted switching frequency (Singh, Al-Haddad & Chandra, 1999). CSIs are considered reliable structure for STATCOMs and APFs (Hayashi, Sato & Takahashi, 1988) but they are

heavier than VSI because they comprised inductances and also they produce higher losses and require higher value of parallel capacitors. Moreover they cannot be used in multilevel modes to decrease switching frequency and improve performance in higher voltage rating.

2.2 Classification Based on Topology of Circuit

Based on topology of the circuit and the way that STATCOMs and AFPs are connected to main system, they are classified to shunt or series, the combination of both shunt and series which is known as Unified Power Quality Conditioner (UPQC) and combination of passive filters with APFs which is named hybrid filter. Generally a passive ripple filter is used at the terminal of the supply system, which compensates for switching harmonics and improves the THD of the supply voltage and current based on the type of filter and compensation purpose of the filter that was chosen.

2.2.1 Shunt STATCOM and Active Power Filters

As introduced earlier a three-phase or single-phase invertor is used as STATCOM or APF. In shunt scheme, ac side of three-phase or single-phase invertor is connected in parallel with load and supply through a snubber inductance to compensate undesired components of current or voltage. Figure 2.3 and Figure 2.4 represent schematic of shunt STATCOM or APF with VSI and CSI respectively. Shunt APFs are used for current harmonics and reactive power compensation, balancing unbalanced currents and also they are implemented in Uninterruptable Power Supply (UPS) utilities to enhance the efficiency and reliability of power supply (Choi, Park & Dewan, 1995). As discussed in (Akagi, Watanabe & Aredes, 2007) most effective performance of shunt APF is reached when it is installed at the end of a radial feeder.

2.2.2 Series Active Power Filter

Series APF is using a matching transformer which is connected in series with load and supply to eliminate voltage harmonics, balance and regulate terminal voltage of the load or line, reduce negative sequence voltage and regulate the voltage that supplies the load. Without matching transformer higher voltage rate switches are needed in order to endure line voltage press (Nastran & et al. 1994).

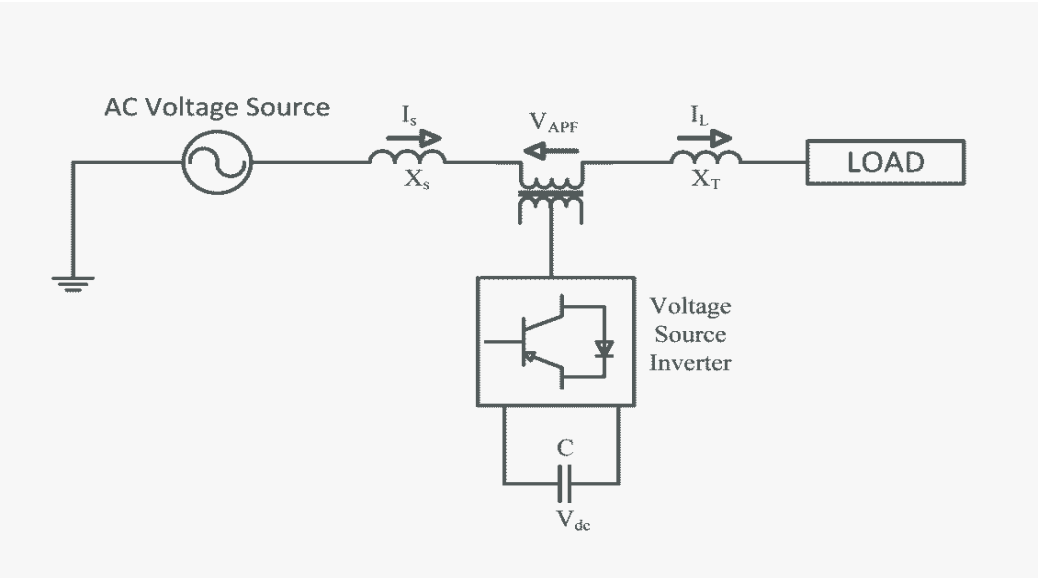

Figure 2.5 Series active power filter with voltage source invertor

Figure 2.5 represents a series APF with VSI which is responsible for undesired voltage components like harmonics, spikes, sags, notches, etc. Instead of VSI a CSI can be used as PWM invertor to produce desired voltage and current in APF as represented in Figure 2.6. The V_{APF} is injected to the system in a way that satisfies the systems requirement.

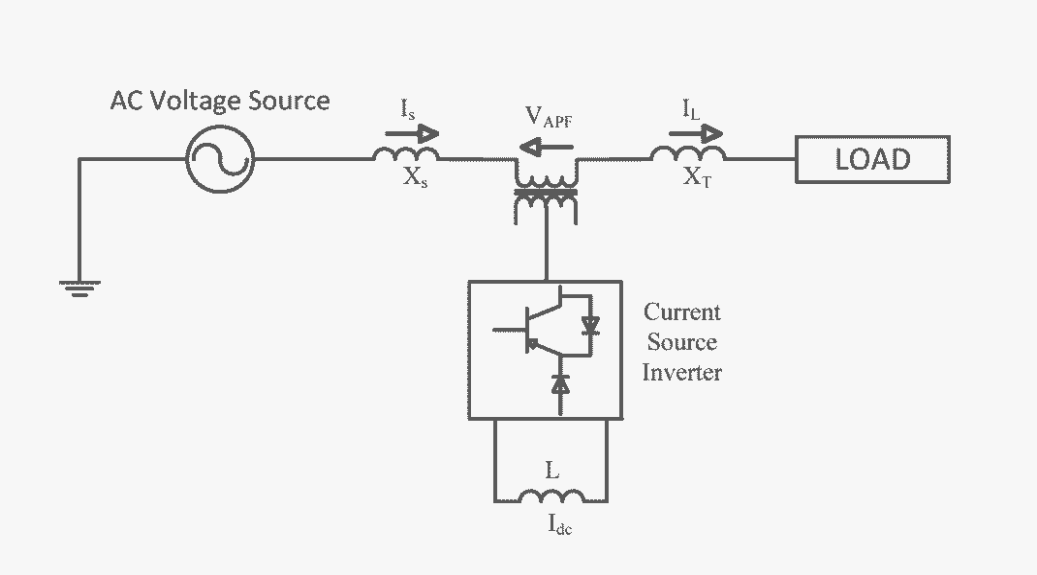

Figure 2.6 Series active power filter with current source invertor

2.2.3 Unified Power Quality Conditioner

A combination of series APF and shunt APF where two inverters are connected back to back and share the same dc link component either capacitor or inductor is titled in literatures as Unified Power Quality Conditioner (UPQC). In this configuration as shown in Figure 2.7 series APF eliminates voltage harmonics, balance any distortion in supply power and attenuates any other undesired components of voltage and shunt APF is responsible for reactive power, current harmonics, unbalance and hinder other current polluted components. Consequently it could be considered as an ideal APF which eliminate both voltage and current impureness and it is capable to give clean power to critical and harmonic-prone loads and isolate harmonic sensitive loads such as computers and medical equipment. Also it has been implemented in UPS system effectively (Kamran & Habetler, 1998).

Both VSI and CSI are applicable however, VSI structure has been preferred in most literatures because it is more economical in terms of component cost and availability.

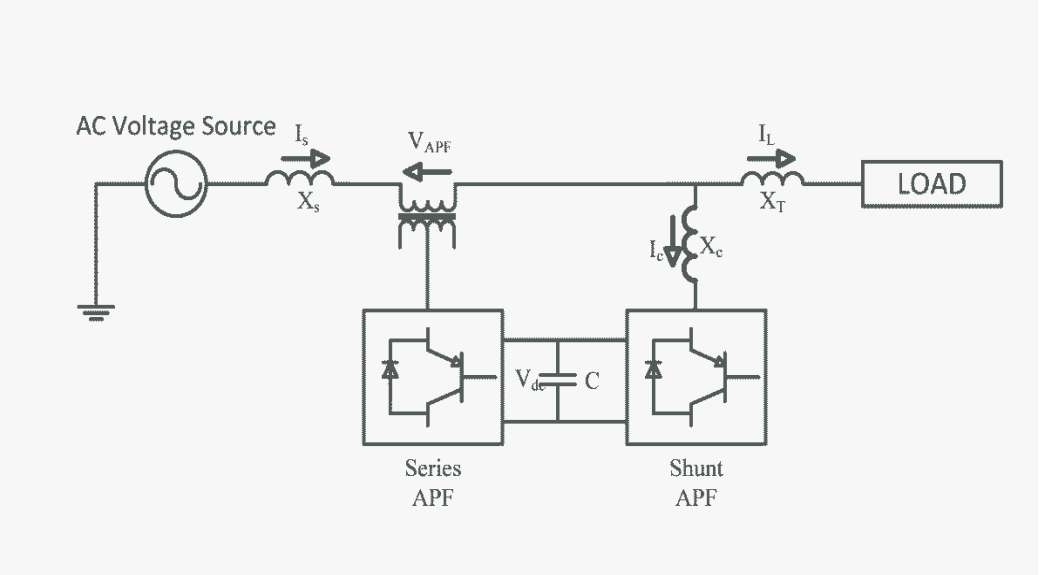

Figure 2.7 UPQC using capacitor as DC link component

In configurations that are shown in Figure 2.7 & Figure 2.8 the switching devices must have uni-directional current and bi-directional voltage capability (Moran, 1989). UPQC main drawbacks are its large cost and control complexity because of the large number of solid-state devices involved.

2.2.4 Hybrid Power Filter

The APFs consisting of VSI or CSI have such a problem that they are inferior in initial cost and efficiency to passive filters. Therefore, it is rational that attention has been paid to combine APF with passive filters under classification of hybrid power filter. In configuration that is represented in Figure 2.9 the function of series APF is not directly compensate reactive power or current harmonics however, by suppressing the voltage harmonics it enhance the performance of passive filter (Akagi, 1994).

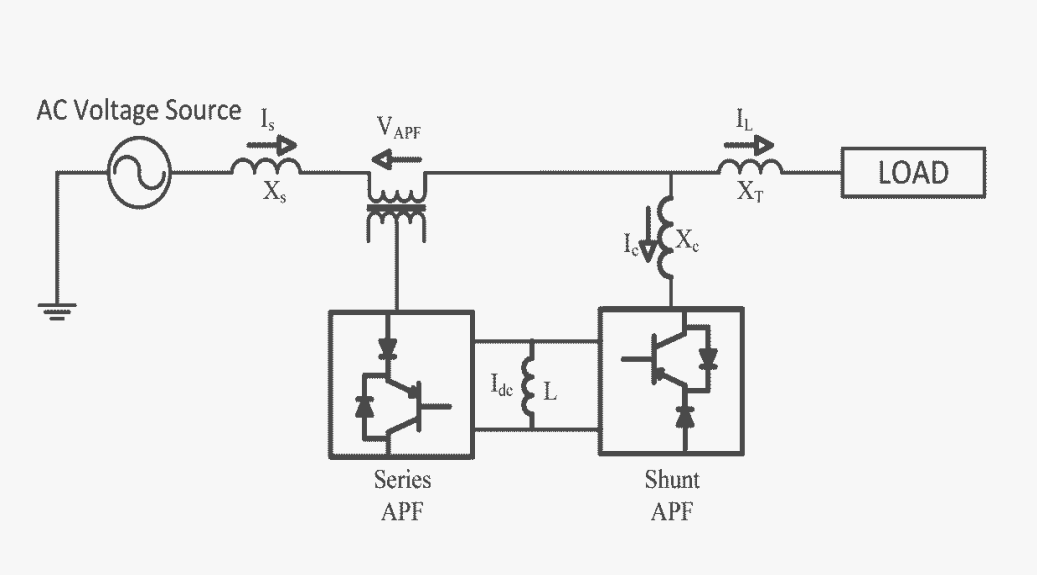

Figure 2.8 UPQC using inductance as DC link component

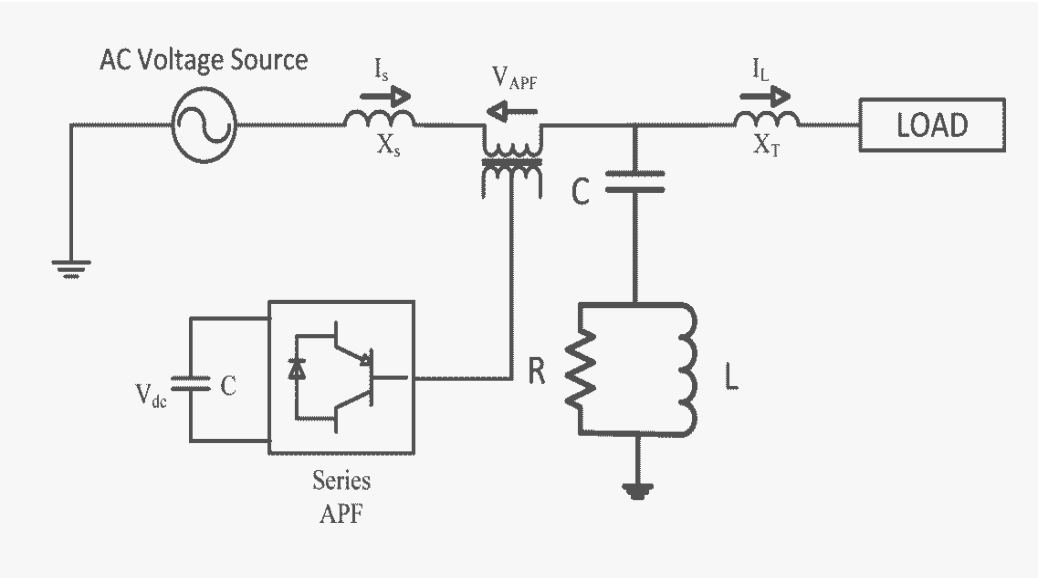

Figure 2.9 Hybrid filter with series APF

Passive filters are quite popular because the solid-state devices used in APF can be of reduced size and cost (about 5% of the load size) and a major part of the hybrid filter is made of the passive shunt L-C filter used to eliminate lower order harmonics (Bhattacharya & Divan, 1995). Figure 2.10 represents hybrid filter with shunt APF which is less common than configuration that is represented in Figure 2.9.

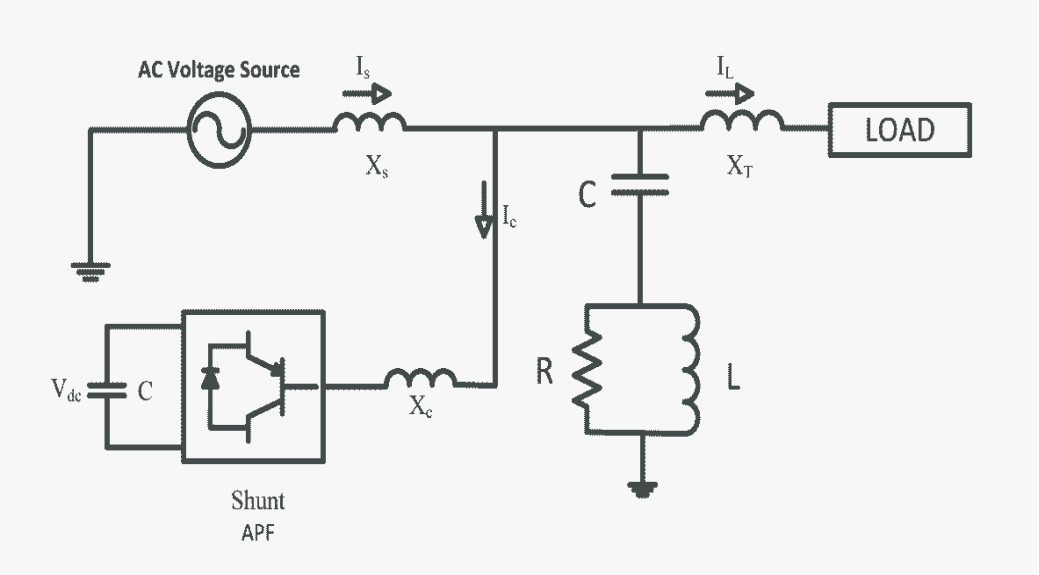

Figure 2.10 Hybrid filter with shunt APF

2.3 Classification Based on Supply System

From power supply or the load point of view STATCOMs and APFs are classified to single-phase, three-phase three wire and three-phase four wire configurations.

2.3.1 Single Phase Active Power Filter

In applications such as in electric traction and in several large manufacturing plants, it is common that a large portion of the load is comprised single-phase type. Also large numbers of domestic nonlinear loads exist and they propagate reactive, harmonic and unbalanced currents to the networks. Power system administrator has established penalties to end users who exceed standard's maximum limit for harmonic, reactive power and unbalanced current that are allowed to be injected to the system. Then, single-phase STATCOM and APF is attracted high attention in recent years. All configurations like shunt, series, UPQC and hybrid can be implemented in single-phase consideration. In some cases, active filtering is included in the power conversion stage (Chen & Divan, 1991) to improve input characteristic at supply end.

2.3.2 Three Phase Three Wire

Most industrial three-phase loads like Adjustable Speed Drives (ASD) are fed by three wire systems. These facilities are used to enhance controllability and efficiency of induction motors or other motor types, however beside wide range advantages that have introduced to power system, they propagate reactive current and harmonics to networks. Three-phase three wires APF with three wires on the ac side and two wires in dc side, are used in front end of these equipment to attenuate problems of these loads. In some configuration three single-phase APFs are considered to prepare independent controllability in each phase and reliable compensation with unbalanced systems.

2.3.3 Three Phase Four Wire

A large number of residential and industrial single phase loads are supplied from three phase mains with neutral conductor where single phase load is connected between phase to neutral. Although single phase loads try to be distributed equally between phases, however, they cause excessive neutral current, harmonic and reactive power burden, and unbalance that sum up in neutral conductor and produce high neutral current with harmonics in system. Three-phase three wires STATCOMs and APFs are not able to deal with this problem then, three-phase four wires scheme was investigated and well-designed to accompany with neutral current.

There exist two major configurations for this APF type: Capacitor midpoint type and four-pole switch type which are represented in Figure 2.11 and Figure 2.12. Also three single-phase bridge configuration is possible but the number of switches are the dominant drawback of this scheme. Capacitor midpoint type has implemented in smaller ratings while the ac neutral wire is directly connected to the electrical midpoint of the dc bus (Moran & et al. 1995). Four legs type has better controllability (Quinn, Mohan & Mehta, 1993) and can be implemented in higher ratings.

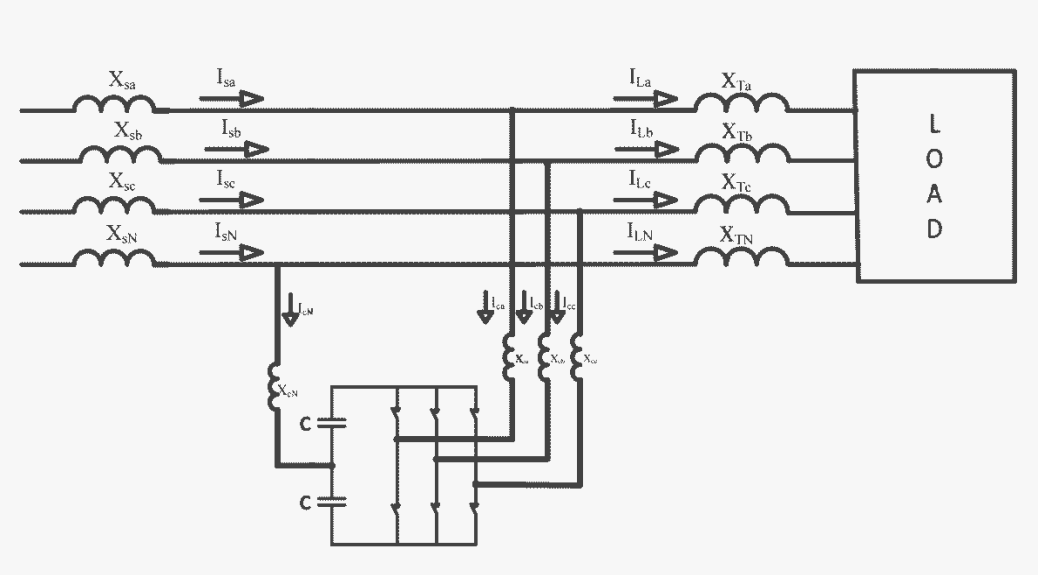

Figure 2.11 Three-phase four wire APF capacitor midpoint type

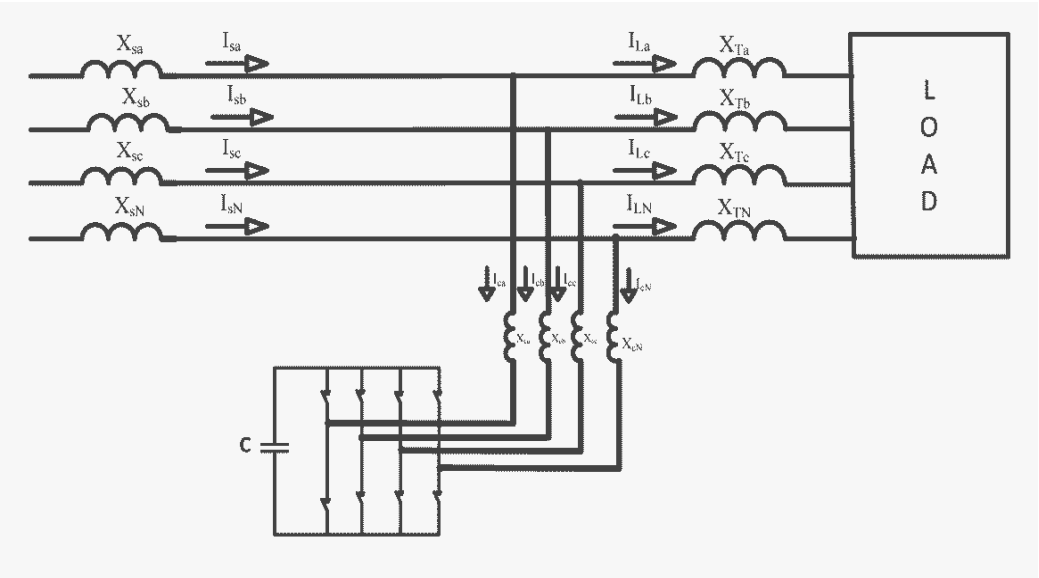

Figure 2.12 Three-phase four wire APF four legs type

2.4 Classification Based on Control Strategy

Control strategy is the most important part and heart of the STATCOMs and APFs and development of compensation signals either in terms of voltages or currents is taken place in control block and it can affect their rating, transient as well as steady state characteristic. From this point of view two major classifications are possible for methods that are being used in STATCOMs and APFs which in both

categories variety of methods and implementations are exist in literatures and have been taken to practice.

2.4.1 Frequency Domain Methods

Fast Fourier Transform (FFT) is a powerful tool to compute frequency components of current or voltage signal. Most frequency domain methods have used FFT and once the FFT is taken, desired and undesired components are separated to produce the gate signals for inverter switching function. Frequency domain methods are accomplished by using either predetermined methods (similar to passive filters) or cancellation-of-M-harmonics methods. The device switching frequency of the APF is kept generally more than twice the highest compensation harmonic frequency for effective compensation (Grady, Samotyj & Noyola, 1990).

These methods due to comprise cumbersome calculations and requirement of at least one period to compute compensation current or voltage components are considered sluggish and unsuitable for systems that need fast response. Also they are highly sensitive to frequency variation and for those load currents or systems that vary every period or at least in few periods, may not lead to proper compensation results.

2.4.2 Time Domain Methods

Large computation time of frequency domain methods and complexity of them led researchers to look for effective methods in time domain to decrease execution time of signal processors and attain fast responses. The greatest advantage of time domain methods is their fast response to changes in the power system. Also, they are easy to implement and has little computational burden. These methods are based on instantaneous measurement of voltage and current and computation of reference signal in the form of either voltage or current for compensation purpose. There exist variety of methods and theories that were represented in literatures which

controllability, cogency and validity of them were examined and have been taken to practice, here some popular methods are represented:

1. Instantaneous Reactive Power Theory
2. Instantaneous Non-Active Current Theory
3. Synchronous d-q Reference Frame (Bhattacharya, Veltman, Divan & Lorenz, 1995), (Wang, X & et al. 2008).
4. Synchronous Detection Method (Jou, 1995).
5. Notch Filter Based Method (Yazdani, Bakhshai, Joos & Mojiri 2008).
6. Sliding Mode Controller (Bandal, & Madurwar, 2012) and (Fei, Li & Zhang, 2012).
7. Neural Network Based Method (Cirrincione, Pucci, Vitale, & Miraoui, 2009).
8. Adaptive Linear Neuron (ADALINE) Method (Avik & Chandan, 2009), (Hong, & et al. 2010).
9. Adaptive Filter Method (Singh, & Solanki, 2009).

In this thesis instantaneous reactive power and instantaneous non-active current theories will be discussed in detail and Simulink and experimental examinations are based on these methods.

2.4.2.1 Instantaneous Reactive Power Theory

Instantaneous reactive power theory or p-q theory was born in 1980s by (Akagi, Kanazawa & Nabae, 1984). It is based on transformation of voltage and current signals to α-β coordinate by means of Clarke transformation. The instantaneous active and reactive power can be computed in terms of transformed voltage and current signals. From instantaneous active and reactive powers, harmonic active power and reactive powers are extracted using low-pass and high-pass filters respectively. From harmonic active and reactive powers, using reverse transformation, compensating commands in terms of either currents or voltages are derived. Figure 2.13 shows the block diagram of control method based on instantaneous reactive power theory to produce reference current. The dual method

which generate reference voltages for compensation purposes is applicable (Akagi, Watanabe & Aredes, 2007).

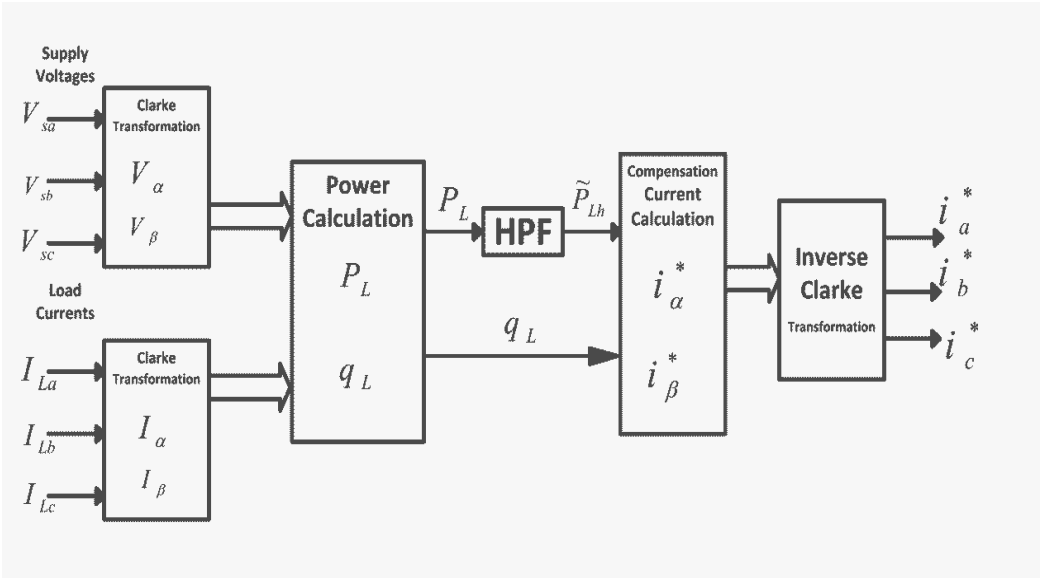

Figure 2.13 Instantaneous reactive power and harmonic compensation based on p-q theory

Instantaneous reactive power or p-q theory is originally developed for three-phase systems however, it was extended to single-phase system and single-phase implementation is also possible. Detailed discussion on this theory is represented in chapter three.

2.4.2.2 Instantaneous Non-Active Current Theory

Instantaneous non-active current theory is based on (Fryze, 1932) traditional active power calculation. Real-time voltage and current are sensed and average active power is calculated. Then this average active power is divided to rms value of reference voltage which in most case is the positive sequence of source voltage, and again is multiplied by reference voltage to be in phase with it (Xu, Tolbert, Chiasson & et al., 2007) and (Xu, Tolbert, Kueck & Rizy, 2010) This procedure's block diagram is represented in Figure 2.14 and is discussed in detail in chapter three. The resulted active current is in phase with reference voltage and non-active current is defined as difference of load current and active current which is used for compensation purposes.

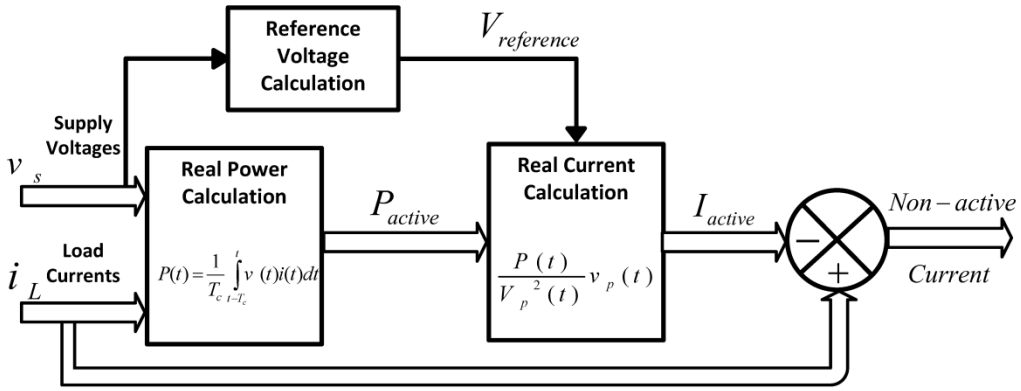

Figure 2.14 Block diagram of instantaneous non-active current theory

this method can be implemented either in three-phase system if the input voltages and currents are considered as vectors in Figure 2.14 and in single-phase systems if those signals are considered as single-phase source voltage and load current.

2.5 Classification Based on Current Controller

Most STATCOM and APF control strategies produce reference current for compensation purpose and a proper current controller is needed to be implemented in order to satisfy compensation function. Important characteristics of an appropriate current controller are its simplicity to implement, fast response and reliability to properly and delayless follow the reference current. Some well-suited current controller methods are:

1. Hysteresis Current Control
2. PWM Current or Voltage Control
3. Deadbeat Current Control (Kawabata, Miyashita & Yamamoto, 1990) and (Martin & Santi, 2012)
4. Fuzzy Based Current Controller (Aghanoori, Mohseni & Masoum, 2011)
5. Delta Modulation Current Control (Jeraldine Viji, Pushpalatha & Rekha, 2011)
6. Linear (Ramp-Comparison) Current Control (Raymond, 1993)

2.5.1 Hysteresis Current Control Method

The hysteresis-type current controller is the most popular current controller because of its simplicity in implementation, inherently limiting the current and very fast response. This current control method has investigated in literature for convertor, invertor, power quality issues, smart grids and so many fields and purposes. Single-band hysteresis current control method is the simplest form which is illustrated in Figure 2.15. In this case, the inverter will produce a positive output voltage when the current error touches the lower hysteresis limit. On the other hand, a negative output voltage is produced when the current error touches the upper hysteresis limit.

Double-band hysteresis current controller (Dahono, 2008) and some other adaptive hysteresis current controllers (Bose, 1990) and (Dahono, 2008) have been represented and implemented in APF and STATCOM application.

2.5.2 PWM Current or Voltage Control Method

In this method the produced reference current or its PI controller modified signal is considered as control signal to be compared with triangular carrier signal. The most important advantage of it is its predefined switching frequency which is centered around the carrier frequency. Also its robustness and easy implementation make it suitable current controller method for power electronics devices. Since the control signal variation is dependent on load and other parameters of system then adaptive models and techniques may be needed to enhance controllability and effectiveness of the method. Basic and well-known concept of the method is represented in Figure 2.16. Multireference and multicarrier implementations applicable for multi-level invertors and other applications which are available in literatures (Cataliotti, Genduso, Raciti & Galluzzo, 2007) and (Saeedifard, Iravani & Pou, 2007).

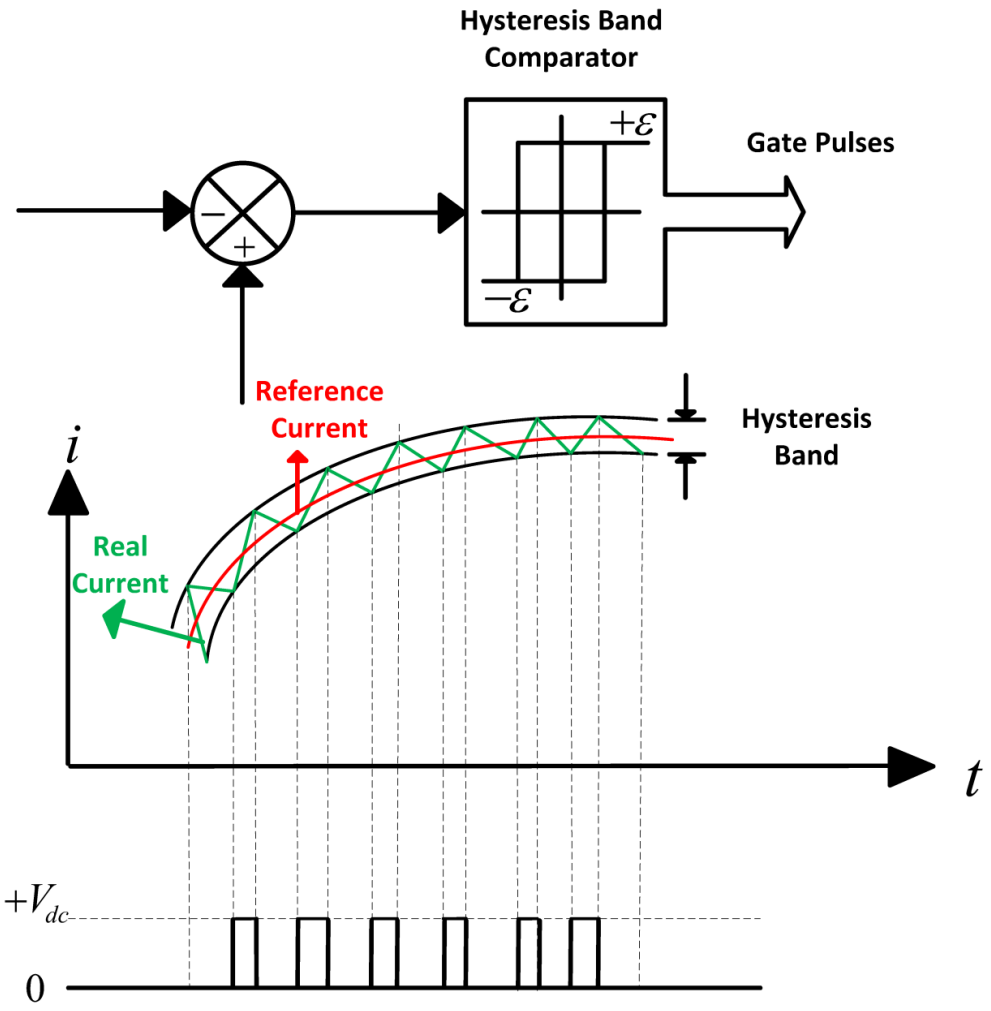

Figure 2.15 Principle of hysteresis current controller

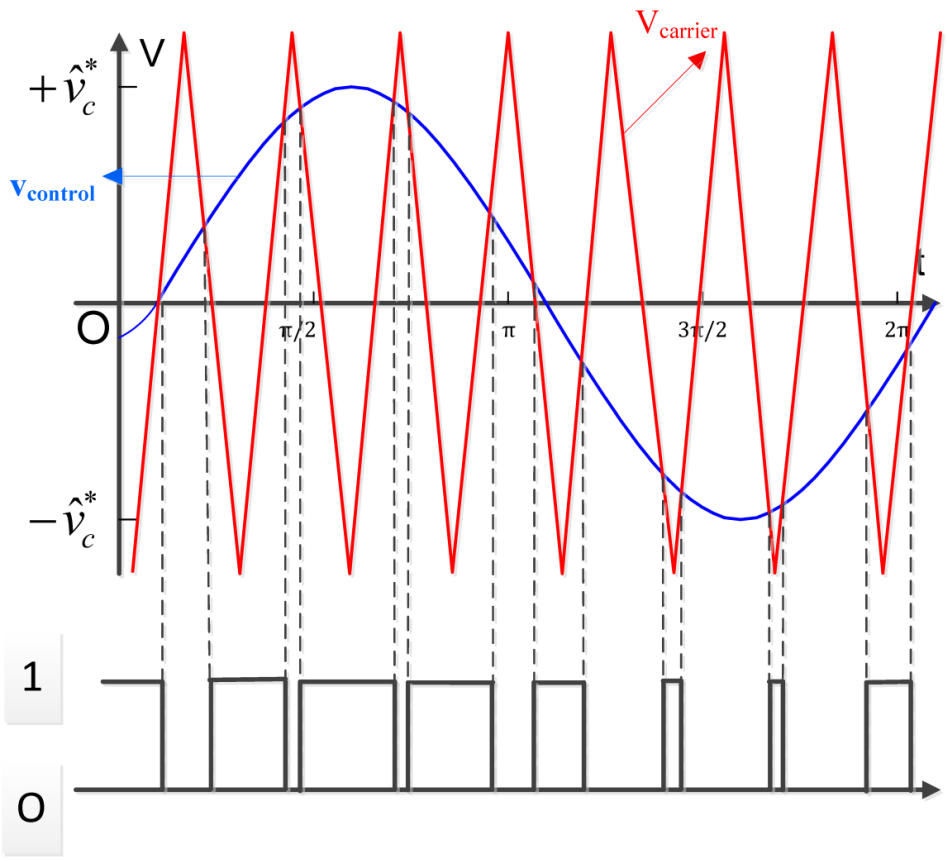

Figure 2.16 Principle of SPWM current controller

CHAPTER THREE
ANALYTICAL APPROACH ON LIMITATION AND FEASIBLE REGION FOR IMPLEMENTATION OF REACTIVE POWER THEORIES

Power electronics equipment beside wide range advantages that introduced to power system, caused some major problems in these systems by injecting non-periodic, unbalanced and highly distorted current to the network. In order to tackle these distorted current and also reactive power, Active Power Filter (APF), Static Var Compensation (STATCOM) and Unified Power Quality Conditioner (UPQC) were introduced to power systems since late 70s (Gyugyi & Strycula, 1976). Two popular control methods for instantaneous reactive power compensation and harmonic mitigation for three phase and single phase systems which are investigated here are presented in several literatures accompanied by Simulink and experimental results. Most of works claimed that the control strategy is general and works under sinusoidal, non-sinusoidal, distorted, periodic, non-periodic, balanced and unbalanced condition, however, lack of analytical approach and consistency of those analyses by standard (IEEE Standard 1459, 2010) is evident and sensible. This chapter presents the Instantaneous Non-active Current Theory and p-q Theory as two wide accepted theories, analyses and compares these theories by standard to identify limitation and find feasible region for implementing these theories in instantaneous reactive power compensation and harmonic mitigation.

3.1 Instantaneous p-q Theory

Instantaneous p-q Theory originally developed for three phase systems first by (Akagi & et al., 1984) where by means of Clarke transformation voltages and currents in abc coordinate transform to αβ0 stationary reference frame:

$$\begin{bmatrix} V_0 \\ V_\alpha \\ V_\beta \end{bmatrix} = \sqrt{\frac{2}{3}} \begin{bmatrix} \frac{1}{\sqrt{2}} & \frac{1}{\sqrt{2}} & \frac{1}{\sqrt{2}} \\ 1 & \frac{1}{2} & \frac{1}{2} \\ 0 & \frac{\sqrt{3}}{2} & \frac{\sqrt{3}}{2} \end{bmatrix} \begin{bmatrix} V_a \\ V_b \\ V_c \end{bmatrix} \tag{3.1}$$

$$\begin{bmatrix} I_0 \\ I_\alpha \\ I_\beta \end{bmatrix} = \sqrt{\frac{2}{3}} \begin{bmatrix} \frac{1}{\sqrt{2}} & \frac{1}{\sqrt{2}} & \frac{1}{\sqrt{2}} \\ 1 & \frac{1}{2} & \frac{1}{2} \\ 0 & \frac{\sqrt{3}}{2} & \frac{\sqrt{3}}{2} \end{bmatrix} \begin{bmatrix} I_a \\ I_b \\ I_c \end{bmatrix} \tag{3.2}$$

in three wire systems or four wire balance systems there is no zero-sequence current and voltage, then, above equations can be simplified to

$$\begin{bmatrix} V_\alpha \\ V_\beta \end{bmatrix} = \sqrt{\frac{2}{3}} \begin{bmatrix} 1 & \frac{1}{2} & \frac{1}{1} \\ 0 & \frac{\sqrt{3}}{2} & \frac{\sqrt{3}}{2} \end{bmatrix} \begin{bmatrix} V_a \\ V_b \\ V_c \end{bmatrix} \tag{3.3}$$

and if Clarke transformation matrix in above equation is defined as

$$C = \sqrt{\frac{2}{3}} \begin{bmatrix} 1 & \frac{1}{2} & \frac{1}{1} \\ 0 & \frac{\sqrt{3}}{2} & \frac{\sqrt{3}}{2} \end{bmatrix} \tag{3.4}$$

then

$$I_{\alpha\beta} = C * I_{abc} \tag{3.5}$$

Instantaneous active and reactive power in α-β coordinate are defined as

$$\begin{bmatrix} p \\ q \end{bmatrix} = \begin{bmatrix} V_\alpha & V_\beta \\ -V_\beta & V_\alpha \end{bmatrix} \begin{bmatrix} I_\alpha \\ I_\beta \end{bmatrix} \tag{3.6}$$

which in existence of zero sequence current and voltage, zero sequence power represented by below equation. It indicates that α and β coordinate voltages and currents do not contribute any effect on zero-sequence power.

$$P_0 = V_0 \cdot I_0 \tag{3.7}$$

By inverse operation of equation (3.6) it will be possible to calculate reference current for reactive power and harmonic compensation purpose.

$$\begin{bmatrix} I_\alpha \\ I_\beta \end{bmatrix} = \begin{bmatrix} V_\alpha & V_\beta \\ -V_\beta & V_\alpha \end{bmatrix}^{-1} \begin{bmatrix} p \\ q \end{bmatrix} \tag{3.8}$$

from equation (3.6) active and reactive power can be calculated. Also p-q theory has the property to separate active and reactive power in α and β coordinates or by means of highpass or lowpass filter explicit dc components of active and reactive power ($\overline{p}$,$\overline{q}$) which stand for average power and oscillating components of active and reactive power ($\tilde{p}$, $\tilde{q}$) which stand for harmonic power. Then by using equation (3.8) p-q theory makes it selective whether reactive power, oscillating power or both of them simultaneously be compensated. The following relation provides the reference currents creating $\overline{q}$, $\tilde{p}$ and $\tilde{q}$.

$$\begin{bmatrix} I_\alpha^* \\ I_\beta^* \end{bmatrix} = \begin{bmatrix} V_\alpha & V_\beta \\ -V_\beta & V_\alpha \end{bmatrix}^{-1} \begin{bmatrix} 0 \\ \overline{q} \end{bmatrix} + \begin{bmatrix} V_\alpha & V_\beta \\ -V_\beta & V_\alpha \end{bmatrix}^{-1} \begin{bmatrix} \tilde{p} \\ \tilde{q} \end{bmatrix} \tag{3.9}$$

3.1.1 Single Phase p-q Theory

The concept of original three phase p-q theory was extended to single phase by (Liu, Yang & Wang, 1999). This implication based on instantaneous $\frac{\pi}{2}$ lag or lead of

original voltage and current to establish pseudo orthogonal two phase system in similarity to Clarke transformation results. Thus by this approach original single phase system can be represented in α-β coordinate. The original voltage and current are considered as α axis components and the $\frac{\pi}{2}$ lead or lag fiction quantities are considered as β axis components. With these definitions voltages and currents can be written as

$$\begin{bmatrix} V_\alpha(\omega t) \\ V_\beta(\omega t) \end{bmatrix} = \begin{bmatrix} V_s(\omega t) \\ V_s(\omega t + \frac{\pi}{2}) \end{bmatrix} \tag{3.10}$$

$$\begin{bmatrix} I_\alpha(\omega t) \\ I_\beta(\omega t) \end{bmatrix} = \begin{bmatrix} I_s(\omega t) \\ I_s(\omega t + \frac{\pi}{2}) \end{bmatrix} \tag{3.11}$$

where V_s and I_s are the original single phase voltage and current magnitudes. Now by this procedure α-β coordinate voltage and current are obtained and instantaneous active power and reactive power can be calculated.

$$\begin{bmatrix} p(\omega t) \\ q(\omega t) \end{bmatrix} = \begin{bmatrix} V_\alpha(\omega t) & V_\beta(\omega t) \\ -V_\beta(\omega t) & V_\alpha(\omega t) \end{bmatrix} \begin{bmatrix} I_\alpha(\omega t) \\ I_\beta(\omega t) \end{bmatrix} \tag{3.12}$$

Again instantaneous active and reactive powers can be expressed as their average and oscillating components

$$p(\omega t) = \bar{p}(\omega t) + \tilde{p}(\omega t) \tag{3.13}$$

$$q(\omega t) = \bar{q}(\omega t) + \tilde{q}(\omega t) \tag{3.14}$$

and compensation reference current can be calculated by reverse operation of equation (3.12).

$$\begin{bmatrix} I_\alpha^*(\omega t) \\ I_\beta^*(\omega t) \end{bmatrix} = \begin{bmatrix} V_\alpha(\omega t) & V_\beta(\omega t) \\ -V_\beta(\omega t) & V_\alpha(\omega t) \end{bmatrix}^{-1} \begin{bmatrix} -\tilde{p}(\omega t) \\ -q(\omega t) \end{bmatrix} \quad (3.15)$$

3.2 Instantaneous Non-active Current Theory

The instantaneous non-active current theory is based on (Fryze, 1932) traditional active power definition and can be implemented in single phase and multi-phase systems. Active power is calculated by averaging method on pre-defined averaging interval and then by using rms values of voltage the instantaneous active current is defined.

For a three phase system if instantaneous voltages and currents defined as

$$v(t) = \begin{bmatrix} v_a(t) & v_b(t) & v_c(t) \end{bmatrix}^T \quad (3.16)$$

$$i(t) = \begin{bmatrix} i_a(t) & i_b(t) & i_c(t) \end{bmatrix}^T \quad (3.17)$$

the instantaneous power p(t) and the average power (P) over the averaging interval [t-T_c , t] are defined as

$$p(t) = v^T(t)i(t) = \sum_{k=1}^{3} v_k(t)i_k(t) \quad (3.18)$$

$$P = \frac{1}{T_c} \int_{t-T_c}^{t} p(\tau)d\tau \quad (3.19)$$

Theoretically, the averaging interval T_c can be chosen arbitrarily from zero to infinity and as discussed in (Xu & et al., 2007) the active power, active and non-active currents will have different features depending on T_c. In practice for a periodic system with period T, T_c is chosen as the integer multiple of $\frac{T}{2}$ and for a system with non-periodic current, which has a periodic voltage with fundamental period T and a completely non-periodic current, the theoretical value for averaging

interval, T_c is infinitive however, a few multiple of fundamental period T will be fine enough to mitigate most of undesirable component in current. Actually selecting the T_c is a crucial decision in this method and will affect active power, rms values of voltage and current and consequently will affect active and non-active current that is calculated for compensation purpose and have been investigated in literatures deeply.

From average active power definition in (3.19) the active current $i_a(t)$ and non-active current $i_n(t)$ can be defined as

$$i_a(t) = \frac{P}{V_p{}^2} v_p(t) \tag{3.20}$$

$$i_n(t) = i(t) - i_a(t) \tag{3.21}$$

in (3.20) $v_p(t)$ is the reference voltage, which is chosen based on system characteristics and compensation purpose. Commonly it is chosen as positive sequence of fundamental component of the system source voltage. Another important factor in this theory is selecting $v_p(t)$, which indicated the compensation purpose and will affect active current and non-active current. V_p is the rms value of reference voltage $v_p(t)$, that is

$$V_p = \sqrt{\frac{1}{T_c} \int_{t-T_c}^{t} v_p{}^T(\tau) v_p(\tau) d\tau} \tag{3.22}$$

Similar to p-q theory where by means of average and oscillating component of active and reactive power equations (3.13) and (3.14) the compensation features can be selective, in instantaneous non-active current theory two important elements in calculation of compensation current are T_c and $v_p(t)$. By appropriate choosing averaging interval T_c and the reference voltage $v_p(t)$ different compensation goals

can be achieved, for instance, if compensating of odd or even harmonic would be desired the reference voltage should be selected as the desired voltage components or if the system is pure sinusoidal, periodic or non-periodic it will affect averaging interval selection.

Equations (3.18) - (3.22) can be applied for single phase system simply by substituting single phase voltage and current instead of voltage and current vectors in those equations.

3.3 Analytical Approach on Active and Reactive Power Definition in single phase p-q Theory

Based on (3.10), (3.11) and (3.12) equations active and reactive power in single phase p-q theory is defined as

$$p(t) = \frac{1}{2}[v(\omega t)i(\omega t) + v(\omega t + \frac{\pi}{2})i(\omega t + \frac{\pi}{2})] \tag{3.23}$$

$$q(t) = \frac{1}{2}[v(\omega t)i(\omega t + \frac{\pi}{2}) - v(\omega t + \frac{\pi}{2})i(\omega t)] \tag{3.24}$$

then for a typical system with second and third harmonics in voltage and current waveforms as

$$v(t) = \sqrt{2}V_1 \sin(\omega t) + \sqrt{2}V_2 \sin(2\omega t) + \sqrt{2}V_3 \sin(3\omega t) \tag{3.25}$$

$$i(t) = \sqrt{2}I_1 \sin(\omega t - \varphi_1) + \sqrt{2}I_2 \sin(2\omega t - \varphi_2) + \sqrt{2}I_3 \sin(3\omega t - \varphi_3) \tag{3.26}$$

where the V_n and I_n (for $n = 1,2,3$) are rms values for consequent harmonic components, then active and reactive power definition of equations (3.23) and (3.24) leads to

$$p(t) = V_1 I_1 \cos(\varphi_1) + V_2 I_2 \cos(\varphi_2) + V_3 I_3 \cos(\varphi_3)$$
$$+ V_1 I_2 \cos(-\omega t + \varphi_2) + V_1 I_3 \cos(-2\omega t + \varphi_3) + V_2 I_1 \cos(\omega t + \varphi_1)$$
$$+ V_2 I_3 \cos(-\omega t + \varphi_3) + V_3 I_1 \cos(2\omega t + \varphi_1) + V_3 I_2 \cos(\omega t + \varphi_2) \quad (3.27)$$

And

$$q(t) = V_1 I_1 \sin(\varphi_1) + V_2 I_2 \sin(\varphi_2) + V_3 I_3 \sin(\varphi_3)$$
$$+ V_1 I_2 \sin(-\omega t + \varphi_2) + V_1 I_3 \sin(-2\omega t + \varphi_3) + V_2 I_1 \sin(\omega t + \varphi_1)$$
$$+ V_2 I_3 \sin(-\omega t + \varphi_3) + V_3 I_1 \sin(2\omega t + \varphi_1) + V_3 I_2 \sin(\omega t + \varphi_2) \quad (3.28)$$

first three terms in equations (3.27) and (3.28) are multiplication of voltage and current in the same harmonics and are coincided with Budeanu's traditional active and reactive power definitions in frequency domain. (see Appendix A) and here after we use this notation instead

$$P_1 = V_1 I_1 \cos(\varphi_1); P_2 = V_2 I_2 \cos(\varphi_2); P_3 = V_3 I_3 \cos(\varphi_3), \ldots \quad (3.29)$$

$$Q_1 = V_1 I_1 \sin(\varphi_1); Q_2 = V_2 I_2 \sin(\varphi_2); Q_3 = V_3 I_3 \sin(\varphi_3), \ldots \quad (3.30)$$

also for cross multiplications of voltage and currents in different harmonics, instantaneous cross product active and reactive power can be defined as

$$P_{12} = V_1 I_2 \cos(-\omega t + \varphi_2); P_{13} = V_1 I_3 \cos(-2\omega t + \varphi_3); P_{21} = V_2 I_1 \cos(\omega t + \varphi_1), \ldots \quad (3.31)$$

$$Q_{12} = V_1 I_2 \sin(-\omega t + \varphi_2); Q_{13} = V_1 I_3 \sin(-2\omega t + \varphi_3); Q_{21} = V_2 I_1 \sin(\omega t + \varphi_1), \ldots \quad (3.32)$$

by replacement equations (3.29) - (3.32) in equations (3.27) and (3.28) and rewriting those equation

$$p(t) = P_1 + P_2 + P_3 + P_{12} + P_{13} + P_{21} + P_{23} + P_{31} + P_{32} \quad (3.33)$$

$$q(t) = Q_1 + Q_2 + Q_3 + Q_{12} + Q_{13} + Q_{21} + Q_{23} + Q_{31} + Q_{32} \quad (3.34)$$

If the p-q theory applied to nonsinusoidal voltage and current that have wide range of harmonic content like

$$v(t) = \sqrt{2}\sum_{h=1}^{n} V_h \sin(h\omega t) \tag{3.35}$$

$$i(t) = \sqrt{2}\sum_{h=1}^{n} I_h \sin(h\omega t - \varphi_h) \tag{3.36}$$

equations (3.33) and (3.34) can be extended and rewritten as

$$p(t) = \sum_{h=1}^{n} P_h + \sum_{l=1}^{n}\sum_{\substack{m=1 \\ m\neq l}}^{n} P_{lm} \tag{3.37}$$

$$q(t) = \sum_{h=1}^{n} Q_h + \sum_{l=1}^{n}\sum_{\substack{m=1 \\ m\neq l}}^{n} Q_{lm} \tag{3.38}$$

These results indicated that single phase p-q theory's definitions under nonsinusoidal condition for active and reactive power include arithmetically summation of each harmonic active and reactive power and inter action of different harmonics.

3.4 Analysis of Active and Reactive Power Definition in Instantaneous Non-active Current Theory

As it could be educed from equations (3.18) to (3.21) instantaneous non-active current theory does not have a definition for reactive power and in this method compensation current is extracted by subtracting active current (3.20) from load current which is shown in (3.21). Thus here active power analysis according to equation (3.19) is represented and other definitions of reactive power are represented in next section.

If the average approach of active power definition in instantaneous non-active current theory is applied to system having the voltage and current waveforms with equations (3.25) and (3.26) respectively, it will yield the average active power

$$P = V_1 I_1 \cos(\varphi_1) + V_2 I_2 \cos(\varphi_2) + V_3 I_3 \cos(\varphi_3) \tag{3.39}$$

and by using the notation that suggested in (3.29)

$$P = P_1 + P_2 + P_3 \tag{3.40}$$

again if this procedure extended to general system that represented in (3.35) and (3.36) total active power that transferred by such system will be

$$P = \sum_{h=1}^{n} P_h \tag{3.41}$$

3.5 Comparison of Reactive Power Definition with IEEE 1459 Standard

3.5.1 Single-phase Nonsinusoidal Definitions in IEEE Std 1459^{TM}-2010

According to IEEE standard a nonsinusoidal instantaneous voltage or current has two distinct components: the system frequency components v_1 and i_1 and the remaining term v_H and i_H, respectively.

$$v = v_1 + v_H \qquad and \qquad i = i_1 + i_H \tag{3.42}$$

where

$$v_1 = \sqrt{2}V_1 \sin(\omega t - \alpha_1) \tag{3.43}$$

$$i_1 = \sqrt{2}I_1 \sin(\omega t - \beta_1) \tag{3.44}$$

$$v_H = V_0 + \sqrt{2}\sum_{h\neq 1} V_h \sin(h\omega t - \alpha_h) \tag{3.45}$$

$$i_H = I_0 + \sqrt{2}\sum_{h\neq 1} I_h \sin(h\omega t - \beta_h) \tag{3.46}$$

the corresponding rms values squared are as follows

$$V^2 = \frac{1}{kT}\int_{\tau}^{\tau+kT} v^2 dt = V_1^2 + V_H^2 \tag{3.47}$$

$$I^2 = \frac{1}{kT}\int_{\tau}^{\tau+kT} i^2 dt = I_1^2 + I_H^2 \tag{3.48}$$

where

$$V_H^2 = V_0^2 + \sum_{h\neq 1} V_h^2 = V^2 - V_1^2 \tag{3.49}$$

and

$$I_H^2 = I_0^2 + \sum_{h\neq 1} I_h^2 = I^2 - I_1^2 \tag{3.50}$$

are the squares of the rms values of v_H and i_H, respectively.

The standard explicitly argues that selecting averaging interval is crucial in nonsinusoidal systems in order to voltage and current's rms values are measured correctly (IEEE Std 1459™-2010). If the distorted voltage and current waveforms consist of harmonics only, then an averaging time interval kT enables the correct

calculation of rms and power values. If the mentioned waveforms consist an interharmonic, the measurement time interval kT, which is needed to correctly calculate rms values and powers, is the least common multiple of the periods of the fundamental component and the interharmonic component otherwise the rms values of interharmonic as well as the power associated with it are incorrectly measured and this error is reflected in the measurement accuracy of the total rms and powers values.

Additional, if at least one of the interharmonics of order h is an irrational number, then the observed waveform is not periodic (it is called nearly periodic). In such a case, the averaging time interval kT should be infinitely large to have a correct measurement of the rms and power. In practice when dominant power is carried by fundamental components, such errors are small. The larger the measurement interval kT becomes, the less significant the errors become.

Based on these definitions, instantaneous power is defined as

$$p = vi \tag{3.51}$$

$$p = p_a + p_q \tag{3.52}$$

where the first term

$$p_a = V_0 I_0 + \sum_h V_h I_h \cos\theta_h [1 - \cos(2h\omega t - 2\alpha_h)] \tag{3.53}$$

is the part of the instantaneous power that is equal to the sum of harmonic active powers. The harmonic active power of order h is caused by the harmonic voltage of order h and the component of the harmonic current of order h in-phase with the harmonic voltage of order h. Each instantaneous active power of order h has two terms: an active or real, harmonic power $p_h = V_h I_h \cos\theta_h$, and the intrinsic harmonic

power $- p_h \cos(2h\omega t - 2\alpha_h)$, which does not contribute to net transfer of energy or to additional power loss in conductor.

The second term p_q is a term that does not represent a net transfer of energy (i.e., its average value is nil); nevertheless, the current related to these nonactive component causes additional loss in conductors.

$$\begin{aligned} p_q &= -\sum_h V_h I_h \sin\theta_h \sin(2h\omega t - 2\alpha_h) \\ &+ 2\sum_n \sum_{\substack{m \\ m\neq n}} V_m I_n \sin(m\omega t - \alpha_m)\sin(n\omega t - \beta_n) \\ &+ \sqrt{2}V_0 \sum_h I_h \sin(h\omega t - \beta_h) + \sqrt{2}I_0 \sum_h V_h \sin(h\omega t - \alpha_h) \end{aligned} \tag{3.54}$$

the angle $\theta_h = \beta_h - \alpha_h$ is the phase angle between the phasors V_h and I_h.

Active power is defined as average value of p in (3.51) where the averaging interval discussed earlier

$$P = \frac{1}{kT}\int_{\tau}^{\tau+kT} p\,dt = \frac{1}{kT}\int_{\tau}^{\tau+kT} p_a\,dt \tag{3.55}$$

$$P = P_1 + P_H \tag{3.56}$$

where P_1 and P_H are fundamental active power and harmonic active power (nonfundamental active power) respectively and are defined as

$$P_1 = \frac{1}{kT}\int_{\tau}^{\tau+kT} v_1 i_1\,dt = V_1 I_1 \cos\theta_1 \tag{3.57}$$

$$P_H = V_0 I_0 + \sum_{h\neq 1} V_h I_h \cos\theta_h = P - P_1 \tag{3.58}$$

in these equations if harmonic active power contain subharmonic or interharmonic, again it is important that averaging interval be selected appropriately in order to lead correct measurement.

Fundamental reactive power is defined as average value of product of current and $\frac{\pi}{2}$ degree shifted voltage by means of an integrator

$$Q_1 = \frac{1}{kT}\int_{\tau}^{\tau+kT} i_1\left[\int v_1 dt\right]dt = V_1 I_1 \sin\theta_1 \tag{3.59}$$

apparent power is defined as product of rms value of voltage and current

$$S = VI \tag{3.60}$$

also, nonactive power is defined as difference of squared values of apparent power and active power, consequently

$$N = \sqrt{S^2 - P^2} \tag{3.61}$$

3.5.2 Analytical Comparison over Reactive Power Definitions in the Presence of Distorted Waveforms

In the presence of distorted voltage and current waveforms, according to analysis that presented in (3.34) and (3.38) single phase p-q theory definition for total reactive power, arithmetically add reactive powers in each harmonic plus cross products of currents and voltages in different frequencies. This equation represented here for simplicity

$$q(t) = \sum_{h=1,2,3}^{n} Q_h + \sum_{l=1,2,3}^{n}\sum_{\substack{m=1,2,3 \\ m\neq l}}^{n} Q_{lm} \tag{3.62}$$

first term of this equation completely coincide with Budeanu's traditional equations (see Appendix A) and as discussed in (Czarnecki, 1987) and (Lyon, 1935) Budeanu's definition for reactive power under nonsinusoidal condition do not contribute to correct calculation for reactive power and cannot be used for compensation purpose while it suggested to simply add the generalized Q_h of the instantaneous power alternating components of all harmonics. But each of these components has a different frequency and may have different phase angle φ_h. Therefore, this sum does not specify the reactive power component of the whole instantaneous power (3.51).

3.5.2.1 Case Study One

The following numerical example is meant to facilitate the understanding of the problem. Consider a parallel RLC load that is shown in Figure 3.1 with $R = 12\Omega$, $L = 15.5mH$, $C = 200\mu F$. When this circuit is supplied with highly distorted source voltage, by means of p-q theory these results are obtained:

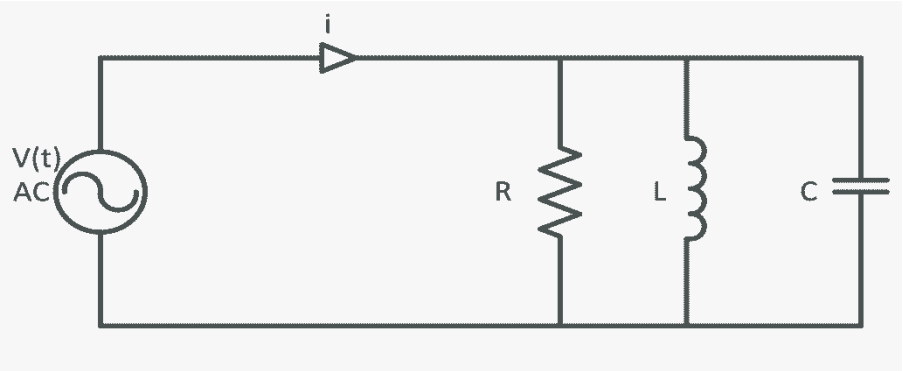

Figure 3.1 RLC load supplied by distorted voltage source

the instantaneous voltages and currents are

$$\begin{aligned} v(t) &= v_1(t) + v_3(t) + v_7(t) + v_{11}(t) + v_{13}(t) \\ i(t) &= i_1(t) + i_3(t) + i_7(t) + i_{11}(t) + i_{13}(t) \end{aligned} \tag{3.63}$$

$$
\begin{aligned}
v_1(t) &= \sqrt{2}220\sin(\omega t - 0^\circ) & i_1(t) &= \sqrt{2}36.32\sin(\omega t - 59.68^\circ) \\
v_3(t) &= \sqrt{2}60\sin(3\omega t - 120^\circ) & i_3(t) &= \sqrt{2}8.77\sin(3\omega t - 64.77^\circ) \\
v_7(t) &= \sqrt{2}40\sin(7\omega t - 18^\circ) & i_7(t) &= \sqrt{2}16.75\sin(7\omega t + 60.53^\circ) \\
v_{11}(t) &= \sqrt{2}35\sin(11\omega t - 40^\circ) & i_{11}(t) &= \sqrt{2}23.73\sin(11\omega t + 42.94^\circ) \\
v_{13}(t) &= \sqrt{2}30\sin(13\omega t - 20^\circ) & i_{13}(t) &= \sqrt{2}24.18\sin(13\omega t + 64.06^\circ)
\end{aligned} \qquad (3.64)
$$

the calculated total impedance, phase difference between voltage and current and reactive powers in each harmonic are summarized in Table 3.1. It has shown that single phase p-q theory in accordance to Budeanu's traditional definitions may lead to incorrect calculations of reactive power value and it can be equal to zero at nonzero values of the terms , i.e., despite the reciprocating energy transmission between the source and the load.

Table 3.1 Impedances, power angels and reactive powers

	ω_1	ω_3	ω_7	ω_{11}	ω_{13}
Z_T	3.057+j5.228	3.9-j5.6214	0.4745-j2.34	0.181-j1.464	0.128-j1.235
φ_h	59.68°	-55.23°	-78.52°	-82.94°	-84.06°
Q_h	6898.68	-432.2	-656.94	-824.26	-721.6

In this numeric example almost 30% of fundamental component reactive power, despite the fact that these reactive powers have different frequencies, is canceled by third, seventh, eleventh and thirteenth harmonic's reactive powers, because the total impedance in fundamental frequency is inductive but by increasing the frequency the total impedance becomes capacitive and negative reactive powers in Table 3.1 illustrated this fact.

MATLAB/Simulink model is implemented for configuration shown in Figure 3.1 based on instantaneous reactive power theory (p-q theory) and results gave credibility to represented analysis. Simulation result is given in Figure 3.2 clearly

shows that p-q theory failed to compensate this parallel RLC load and source current is not completely harmonic free and in-phase with source voltage.

Based on analytical approach that is represented in this chapter and the fact that φ_h in equations (3.36) and (3.38) can pose negative and positive values in different frequencies and under different loads, reactive power definition of single phase p-q theory does not contribute the reliable result in all situations and it may cause incorrect calculations of reactive power for compensation purpose and also may cause failures in system.

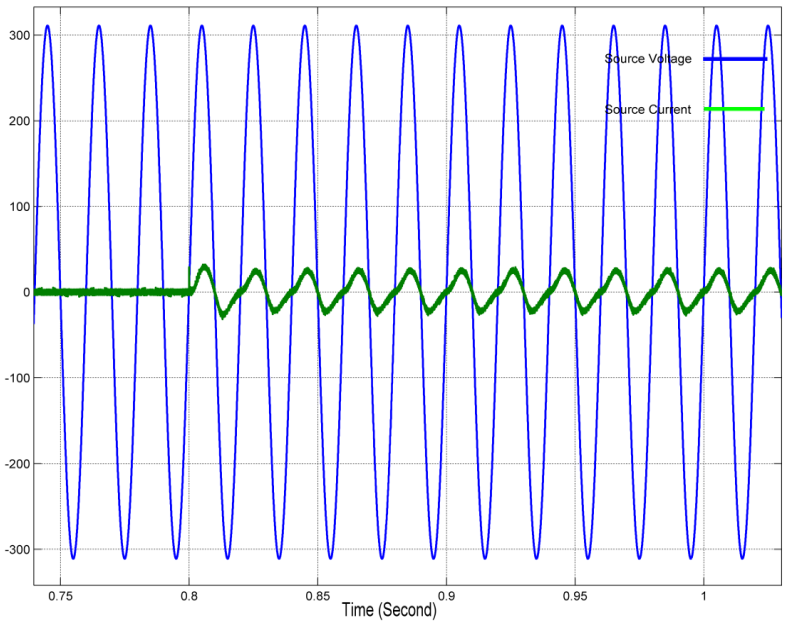

Figure 3.2 Source voltage & current waveforms

3.5.2.2 Case Study Two

In the system that contain subharmonics or interharmonics in voltage or current, p-q theory in the terms of cross multiplications of harmonics may produce harmonic orders that neither voltage nor current waveforms do not include, and as discussed in the case of non-active current theory if the system contain subharmonics or interharmonics, this theory's calculations are highly affected by selecting proper averaging interval and in the case of including irrational order harmonic the

averaging interval theoretically should be infinitive to contribute the correct value for rms value of voltage and also active power, active current and non-active current.

As a numerical example in existence of subharmonic and interharmonic let's consider the hypothetical system with voltage

$$v(t) = v_1 + v_{0.73} + v_{1.34} + v_3 + v_5 \tag{3.65}$$

where the subscripts indicate the order of harmonics and

$$\begin{aligned} v_1(t) &= \sqrt{2}220\sin(\omega t) \\ v_{0.73}(t) &= \sqrt{2}10\sin(0.73\omega t + 20^\circ) \\ v_{1.34}(t) &= \sqrt{2}20\sin(1.34\omega t - 8^\circ) \\ v_3(t) &= \sqrt{2}30\sin(3\omega t - 70^\circ) \\ v_5(t) &= \sqrt{2}15\sin(5\omega t + 140^\circ) \end{aligned} \tag{3.66}$$

for a linear load instantaneous current similar to example that represented in (IEEE Std 1459^{TM}-2010) and by calculation, is

$$i(t) = i_1 + i_{0.73} + i_{1.34} + i_3 + i_5 \tag{3.67}$$

where

$$\begin{aligned} i_1(t) &= \sqrt{2}100\sin(\omega t - 30^\circ) \\ i_{0.73}(t) &= \sqrt{2}4.5\sin(0.73\omega t - 3^\circ) \\ i_{1.34}(t) &= \sqrt{2}8\sin(1.34\omega t - 45^\circ) \\ i_3(t) &= \sqrt{2}7.5\sin(3\omega t - 130^\circ) \\ i_5(t) &= \sqrt{2}2.5\sin(5\omega t + 70^\circ) \end{aligned} \tag{3.68}$$

for simplicity in p-q theory calculation if just first two component of voltage and current are considered

$$v(t) = v_1 + v_{0.73} \tag{3.69}$$

$$i(t) = i_1 + i_{0.73} \tag{3.70}$$

reactive power calculation in single phase p-q theory from equations (3.34) and (3.38) led to

$$q = 22000\sin(30^\circ) + 40\sin(23^\circ) + 1000\cos(-0.27\omega t - 40^\circ) + 880\cos(0.27\omega t - 87^\circ) \tag{3.71}$$

and according to equation(3.15) reactive component of compensation current is defined as

$$I^*_{\alpha q}(\omega t) = \frac{-V_\beta}{V_\alpha^2 + V_\beta^2} q \tag{3.72}$$

by substituting (3.69)-(3.71) in this equation, $I^*_{\alpha q}(\omega t)$ introduce $1.27\omega t$, $0.46\omega t$ order harmonics for synthesized reactive current where neither source voltage nor original load did not contain these harmonics. Figure 3.3 shows the compensation current that is extracted by p-q theory for proposed system with original reactive current that should be calculated. Figure 3.3 clearly represents that harmonic content of original reactive current and the compensation current that is calculated by p-q theory does not coincide.

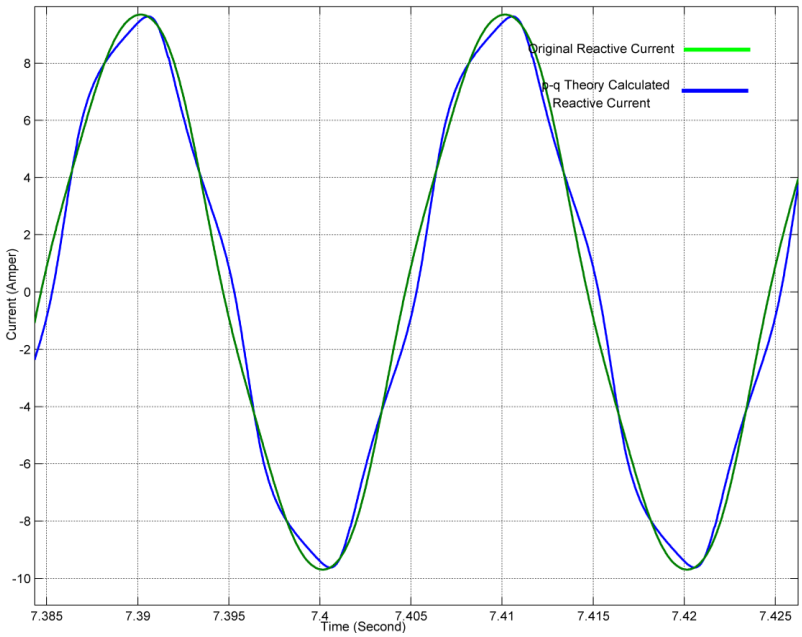

Figure 3.3 Calculated & original reactive currents

The problem goes to be severe if the whole system in (3.65) and (3.67) is considered. In this example when source voltage and load current contain one subharmonic order, one interharmonic and two very common harmonic orders in power systems (third and fifth orders) p-q theory introduce more than 20 completely irrelevant harmonics order for reactive current component where most of them are subharmonics or in a very close frequency to fundamental component and cannot filter out by means of parallel High Pass Filters (HPF) that are very common in APF systems to filter out high frequency components that are produced by switching devices and have frequency content close to switching frequency. This example clearly illustrates that p-q theory led to incorrect calculation of instantaneous reactive current for compensation purpose in presence of subharmonic and interharmonic.

And if the same example is implemented by instantaneous non-active current theory as discussed earlier, voltage rms and active power values highly affected by averaging interval selection, and to reach the correct value, the averaging interval should be least common multiplier of harmonic orders. If the averaging interval is chosen $T = \frac{1}{f_1}$ where f_1 is fundamental frequency, the voltage rms value variation is

represented in Figure 3.4 by using MATLAB Simulink for source voltage introduced in (3.66) and (3.68)

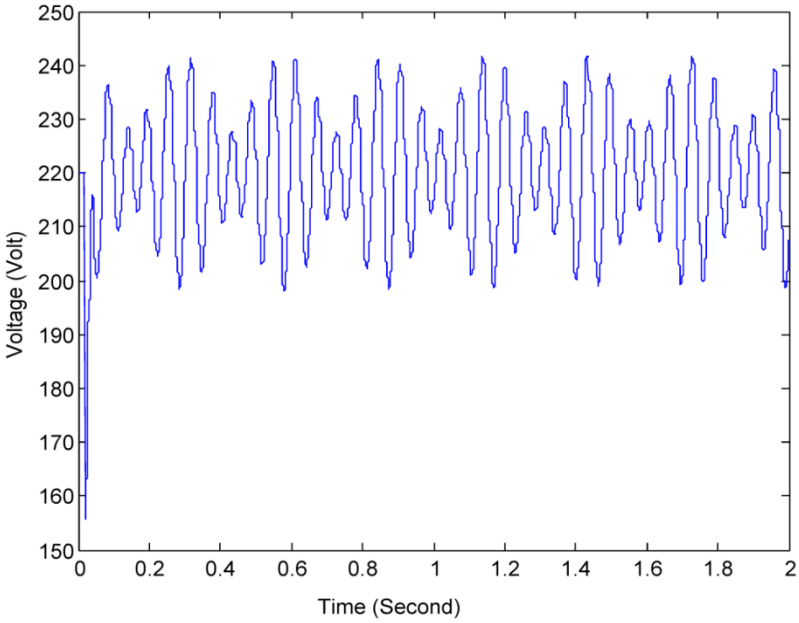

Figure 3.4 Voltage RMS variation averaging interval equal to fundamental period

Active power variation is represented in Figure 3.5, which make it clear that by this configuration both voltage rms and active power's variation is effectively high and they lost their linearity to produce a reliable non-active current for compensation purpose.

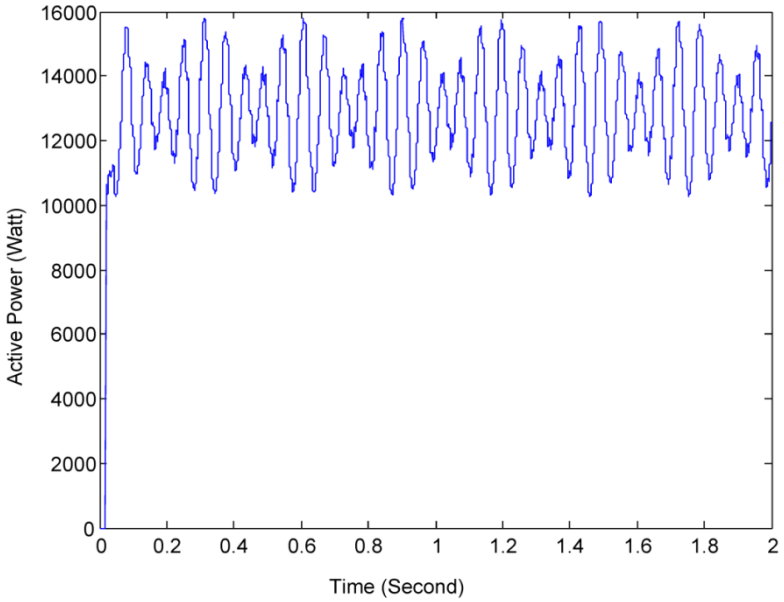

Figure 3.5 Active power variation averaging interval equal to fundamental frequency

If the averaging interval is equal to $10T$ where $T = \frac{1}{f_1}$ voltage rms and active power led to better results

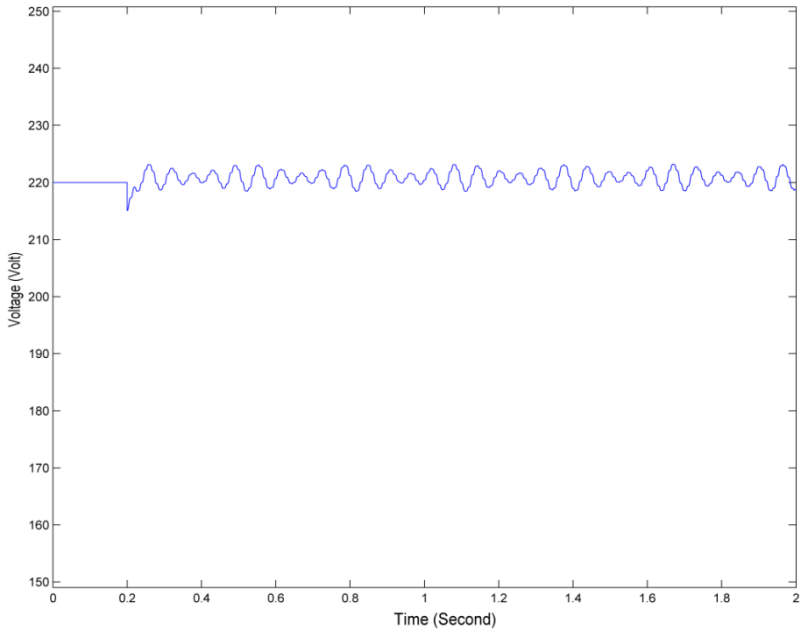

Figure 3.6 Voltage RMS variation averaging interval equal to 10T

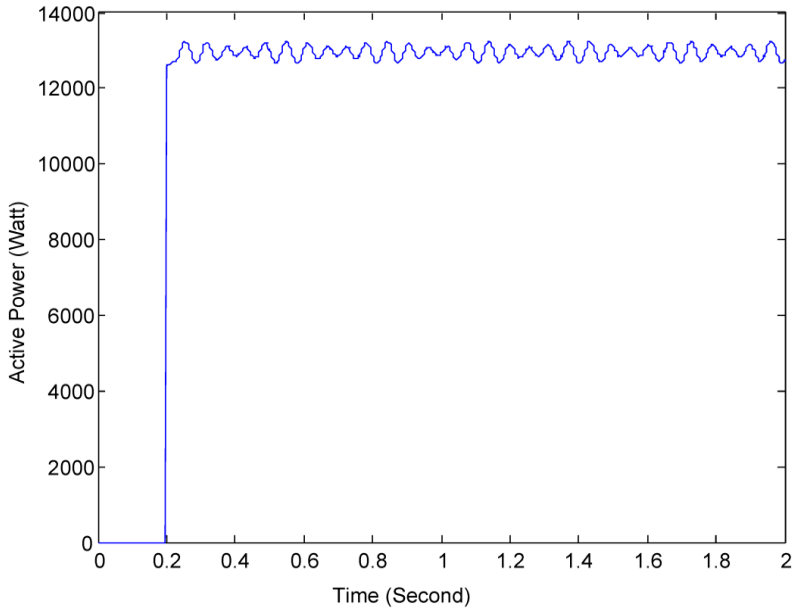

Figure 3.7 Active power variation averaging interval equal to 10T

It is obvious from Figure 3.4 to Figure 3.7 that averaging interval is very important in non-active current calculation and choosing the proper averaging interval for a system with distorted source voltage is a cumbersome and time consuming calculation, also in the presence of subharmonics and interharmonics this interval should be around 10-20 times of fundamental component period for reliable calculation, and this makes the system so sluggish for transient responses and this control method impractical.

All in all and according to (IEEE Std 1459^{TM}-2010) single phase p-q theory and non-active current theory do not yield to a correct value for reactive power in a system that voltage or the current waveforms are highly distorted. Thus a control method that satisfy all compensation requirements under nonsinusoidal voltage and current, is tangible in reactive power compensation and other FACTS devices because power electronics devices penetrate wide range of harmonics to network and single phase form of these equipment increasingly exist in everyday life and also interconnecting renewable energies like Photovoltaic (PV), Wind Farm, Thermovoltaic, Ocean Wave Energy (OWE) and other new technologies is an important issue in power electronics engineering.

CHAPTER FOUR
MATHEMATICAL MODEL OF SINGLE PHASE STATCOM

Analyzing and scrutinizing of models and theories plays crucial role in design, simulation and implementation of systems. Models gave deep insight and understanding of systems and have assisted researcher to analyze systems and engineers to select system's parameters or fine-tune its settings.

This chapter represents the well-suited single-phase STATCOM or shunt APF model in state-space form. The switching function of solid state devices is extracted utilizing analytical approach based on Sinusoidal Pulse Width Modulation (SPWM) control strategy and extracted switching function is carried out in model by employing both MATLAB script programming and MATLAB Simulink.

4.1 Switching Function Calculation

Based on Sinusoidal Pulse Width Modulation (SPWM) control strategy the difference between reference current that was produced by one of the methods that are represented in 2.4 and real VSI current is fed to a PI controller as error in order to control voltage of SPWM calculate. The control voltage is compared with a triangular carrier waveform in the sake of gate signals of solid state devices are generated. The block diagram is illustrated in Figure 4.1.

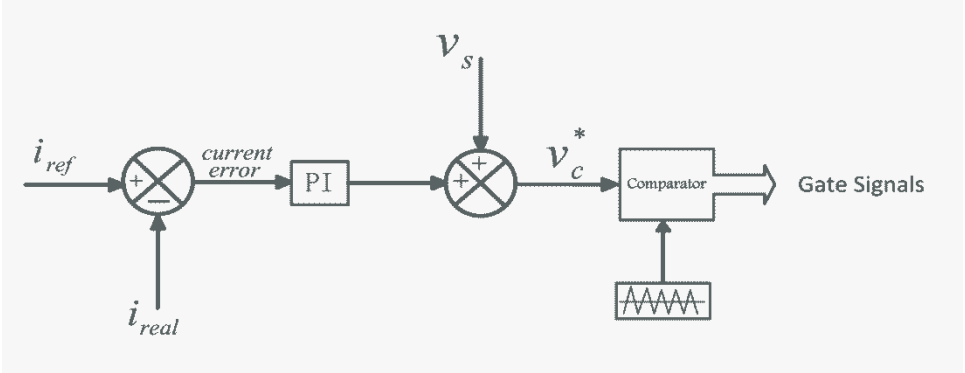

Figure 4.1 Block diagram of SPWM current controller

Let's system's fundamental frequency, fundamental angular frequency, carrier frequency and carrier angular frequency are defined as

$$f : fundamental\ frequency, \quad \omega = 2\pi f \tag{4.1}$$

$$f_c : carrier\ frequency, \quad \omega_c = 2\pi f_c \tag{4.2}$$

as Figure 4.1 illustrate current error signal is fed to PI controller in order to meet proper current controlling. Reference current that is calculated by means of one of control strategies that are represented in 2.4 and the current that is produced by VSI are

$$i_{c-ref} \rightarrow i_c^* \tag{4.3}$$

$$i_{c-real} \rightarrow i_c \tag{4.4}$$

then, the current error signal should be

$$\Delta i_c = i_c^* - i_c \tag{4.5}$$

if by means of an appropriate current controller, either hysteresis current controller or SPWM current controller, VSI's current properly follows the reference current, the frequency of Δi_c should be approximately f_c as Figure 4.2 illustrates.

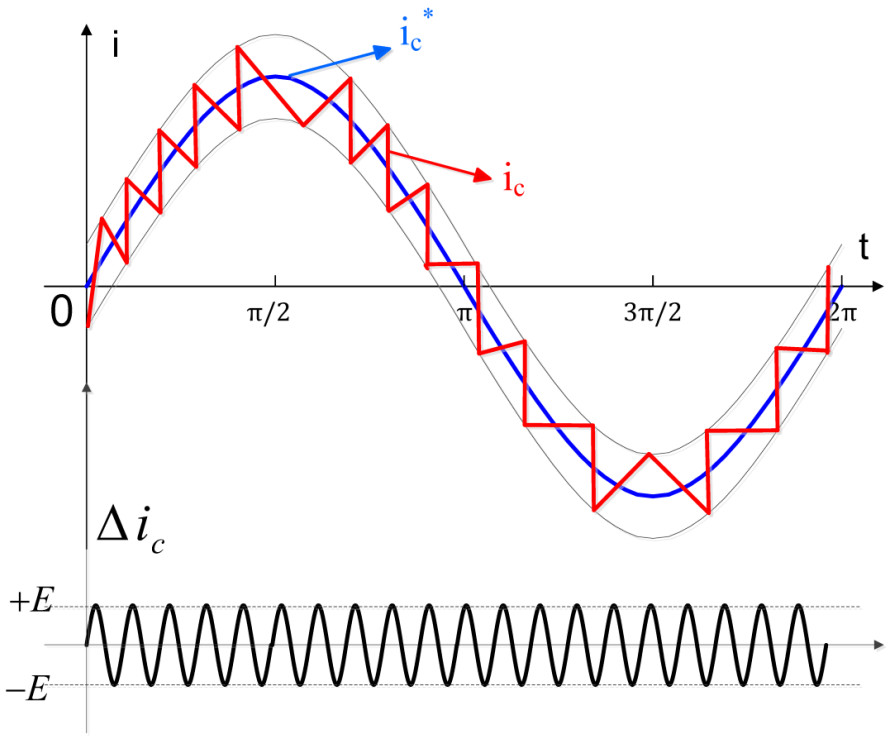

Figure 4.2 Reference current, real current and error current

where

$$i_c^* = \sqrt{2} I_m \sin(\omega t + \alpha) \tag{4.6}$$

$$i_c = \sqrt{2} I_m \sin(\omega t + \alpha) + E \sin(\omega_c t) \tag{4.7}$$

I_m is the rms value of reference current, E is the approximate magnitude of error current and α is the phase deviation of reference current regards to reference source voltage. Then, Δi_c can be written as

$$\Delta i_c = E \sin(\omega_c t) \tag{4.8}$$

this error signal is fed to PI controller and output of PI controller as illustrated in Figure 4.1 is considered as control signal to be implemented in SPWM current control strategy. As it can be seen from Figure 4.1 a feedforward source voltage

signal is added up to PI controller output in order to enhance controller stability and speed.

$$v_{c\_ref} \rightarrow v_c^* \tag{4.9}$$

$$v_s : Source \quad Voltage = \sqrt{2}V_m \sin(\omega t) \tag{4.10}$$

where V_m is the rms value of source voltage and v_c^* is the output of PI controller and is used as control voltage in SPWM which is

$$v_c^* = v_s + k_p \Delta i_c + k_I \int \Delta i_c dt \tag{4.11}$$

where k_p and k_I are proportional gain and integration gain of PI controller respectively.

By substituting (4.8) and (4.10) in (4.11) and simplification is led to

$$\hat{v}_c^* = V_m \sin(\omega t) + k_p E \sin(\omega_c t) - \frac{k_I E}{\omega_c} \cos(\omega_c t) \tag{4.12}$$

If the values of k_p and k_I are significantly high (as in our model are and it is an important factor to VSI's real current follows the reference current properly), the high frequency components of $\hat{v}_c^*$ in (4.12) not only cause change in amplitude of fundamental component of that, but also, cause phase shifting which is a substantial concept of STATCOM and is investigated in 4.2 in detail. Then the control voltage can be approximated by

$$\hat{v}_c^* = A \times V_m \sin(\omega t + \delta) \tag{4.13}$$

where A is defined as magnitude coefficient which is affected by modulation index of SPWM that is defined as

$$m_a = \frac{\hat{V}_{control}}{\hat{V}_{tri}} \tag{4.14}$$

SPWM generated complementary gate signals are shown in Figure 4.3.

If the carrier frequency is much larger than the frequency of the control signal (50 Hz), at any given time, the exact switching functions of Figure 4.3 can be approximated by their instantaneous values of control signal (Saeedifard, Iravani & Pou, 2007). Thus, the exact switching functions of Figure 4.3, i.e., S_1 and S_2 are mathematically expressed by equivalent continuous switching functions $\hat{S}_1$ and $\hat{S}_2$, as shown in Figure 4.3 by dashed blue lines and mathematical expressions are

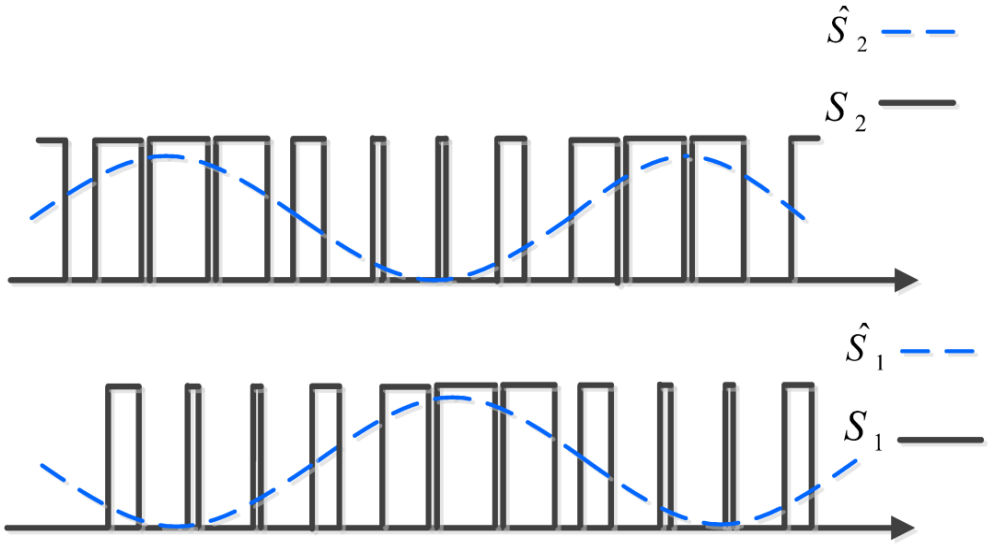

Figure 4.3 SPWM generated gate signals

$$\hat{S}_1 = -\frac{1}{2} m_a \sin(\omega t + \delta) + \frac{1}{2} \tag{4.15}$$

$$\hat{S}_2 = +\frac{1}{2} m_a \sin(\omega t + \delta) + \frac{1}{2} \tag{4.16}$$

where complementary property of $\hat{S}_1$ and $\hat{S}_2$ necessitate that

$$\hat{S}_1 + \hat{S}_2 = 1 \tag{4.17}$$

4.2 Single-Phase STATCOM Dedicated Model

Continuous switching functions that are driven in previous section, are implemented in dedicated model of a shunt single-phase either APF or STATCOM (Nasiri & Emadi, 2003) and (Marco, Alejandro & Marving, 2003), which electrical circuit is represented in Figure 4.4.

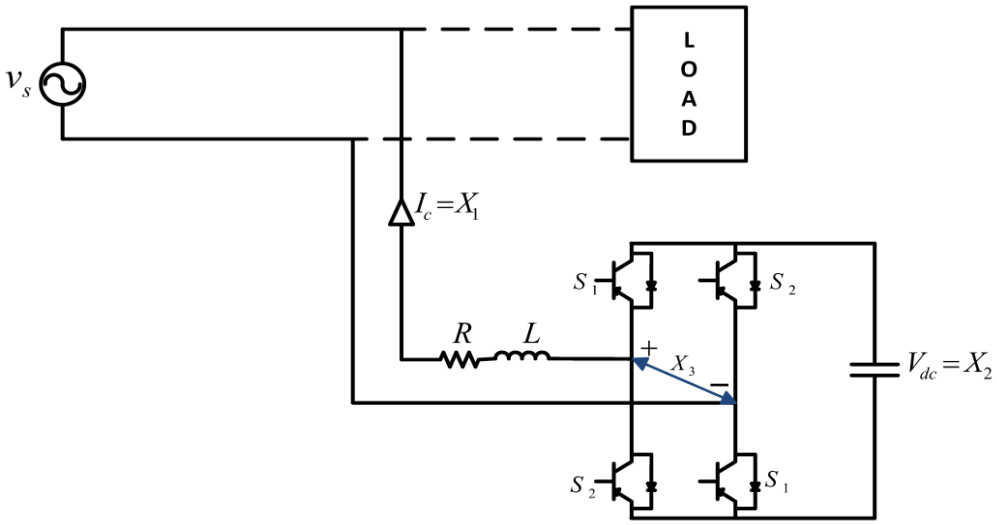

Figure 4.4 Shunt scheme circuit of single-phase STATCOM

From state space analysis of this circuit, KVL in the main loop led to

$$-L\frac{dx_1(t)}{dt} - Rx_1(t) + v_s(t) - \hat{S}_1 x_2(t) + \hat{S}_2 x_2(t) = 0 \tag{4.18}$$

where $x_1(t)$ and $x_2(t)$ are state space variables of compensation current and capacitor voltage respectively. And capacitor voltage $x_2(t)$ and inverter's output voltage which is represented as $x_3(t)$ in Figure 4.4 are illustrated is equation 4.19 and 4.20 respectively.

$$C\frac{dx_2(t)}{dt} = \hat{S}_1 x_1(t) - \hat{S}_2 x_1(t) \tag{4.19}$$

$$x_3(t) = \hat{S}_1 x_2(t) - \hat{S}_2 x_2(t) \tag{4.20}$$

by using (4.17) and rewriting equations (4.18)-(4.20) in the form of state space equations in term of $\hat{S}_2$

$$\begin{cases} X_1^{\bullet} = -\frac{R}{L} X_1 - \frac{1}{L} X_2 + \frac{2\hat{S}_2}{L} X_2 + \frac{1}{L} V_s \\ X_2^{\bullet} = \frac{1-2\hat{S}_2}{C} X_1 \\ X_3 = (1-2\hat{S}_2) X_2 \\ Y = X_1 \end{cases} \tag{4.21}$$

this non-linear set of equations is modeled the shunt APF or STATCOM.

4.2.1 Principle of Reactive Power Flow in STATCOM

Now that by continuous form of switching functions in (4.15) and (4.16), the (4.21) model is completed, it can infer that the invertor output voltage which is represented by $x_3(t)$ in the model is in-phase with $\hat{S}_2$ and $\hat{v}_c^*$ in (4.13) and this is the principle of proper working of STATCOM or a distributed line and network model. Figure 4.5 represented the equivalent circuit (Saadat, 2004).

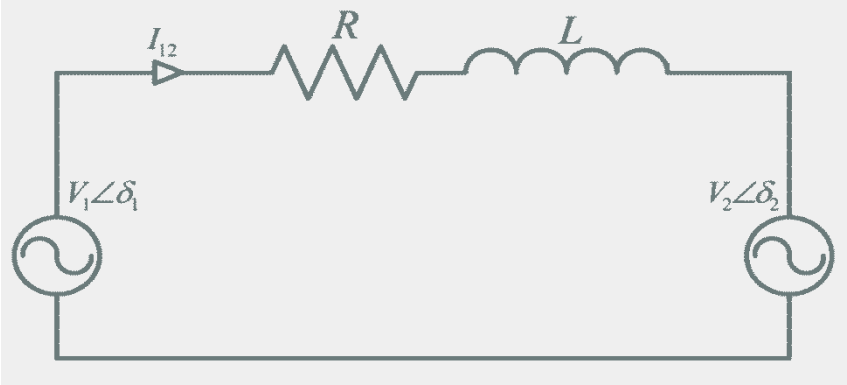

Figure 4.5 Equivalent circuit of STATCOM

$$I_{12} = \frac{|V_1|}{|Z|}\angle(\delta_1 - \gamma) - \frac{|V_2|}{|Z|}\angle(\delta_2 - \gamma) \tag{4.22}$$

where

$$Z = R + j\omega L \qquad \& \qquad \gamma = \tan^{-1}(\frac{j\omega L}{R}) \tag{4.23}$$

The complex power flow from V_1 to V_2

$$S_{12} = V_1 I_{12}^* = \frac{|V_1|^2}{|Z|}\angle\gamma - \frac{|V_1||V_2|}{|Z|}\angle\gamma + \delta_1 - \delta_2 \tag{4.24}$$

where * superscript in above equation stands for conjugate operator. Thus, the real and reactive powers at the sending end are

$$P_{12} = \frac{|V_1|^2}{|Z|}\cos(\gamma) - \frac{|V_1||V_2|}{|Z|}\cos(\gamma + \delta_1 - \delta_2) \tag{4.25}$$

$$Q_{12} = \frac{|V_1|^2}{|Z|}\sin(\gamma) - \frac{|V_1||V_2|}{|Z|}\sin(\gamma + \delta_1 - \delta_2) \tag{4.26}$$

in distributed networks R is much lower than X and approximately it could be inferred that $\gamma \cong 90$ and this led to well-known power flow equation of power system

$$P_{12} = \frac{|V_1||V_2|}{|Z|}\sin(\delta_1 - \delta_2) \tag{4.27}$$

This representation illustrated that by properly controlling the magnitude and phase shifting of the invertor's output voltage in Figure 4.4 model, the reactive power and active power flow of APF or STATCOM can effectively be controlled.

4.2.2 Case Study and Simulation Results

As a numeric example and case study, represented model in (4.21) is implemented in a system which parameters are shown in Table 4.1.

Table 4.1 Circuit parameters

Source Voltage RMS	V_s(rms) = 220 volt
Resistive Load	P = 1500 watt
Inductive Load	Q = 1500 VAR
Coupling Inductance	L = 5mH
Coupling Resistance	R = 0.5 Ω
DC Link Capacitor	C = 4700 μF

block diagram of proposed example is shown in Figure 4.6

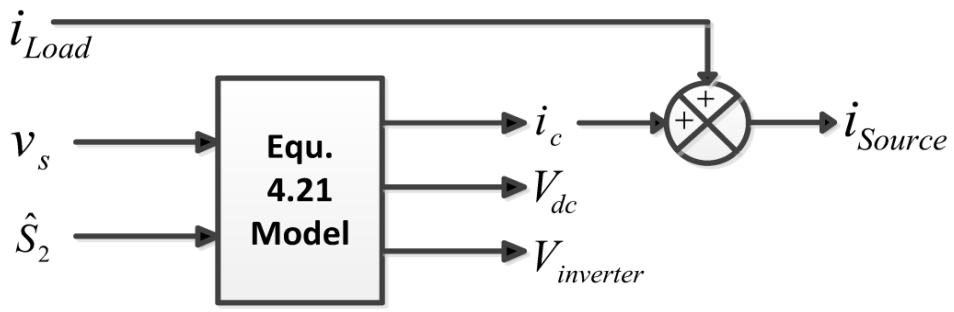

Figure 4.6 Block diagram of proposed example

Nonlinear equation (4.21) is implemented in MATLAB/Simulink by means of function block and also it has been solved in MATLAB/Script programming by implementing basic concept of derivative in discrete mode. Switching functions which are fed to model are calculated in no-load condition as

$$\hat{S}_2 = +\frac{1}{2} \times 0.861 \sin(\omega t + 3.138^{rad}) + \frac{1}{2} \tag{4.28}$$

and under load

$$\hat{S}_2 = +\frac{1}{2} \times 0.892 \sin(\omega t + 3.126^{rad}) + \frac{1}{2} \tag{4.29}$$

variation in modulation index in (4.28) and (4.29) is because of variation in amplitude of control signal according to (4.14) since carrier signal's amplitude is kept constant. DC link voltage, invertor's compensation current and source compensated current versus source voltage are shown in Figure 4.7 and Figure 4.8 respectively.

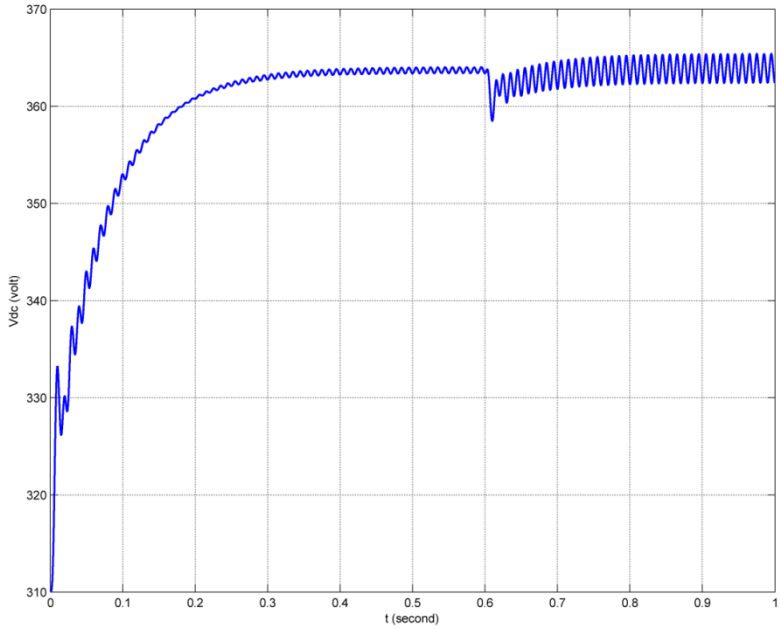

Figure 4.7 DC link capacitor voltage variation. open-loop control

Simulation has been made under no-load condition until t = 0.6s and load has been connected after t = 0.6s and DC link voltage drop around t = 0.6s is because of connection of load. Also compensation current and compensated source current variation are obvious in Figure 4.8 and Figure 4.9.

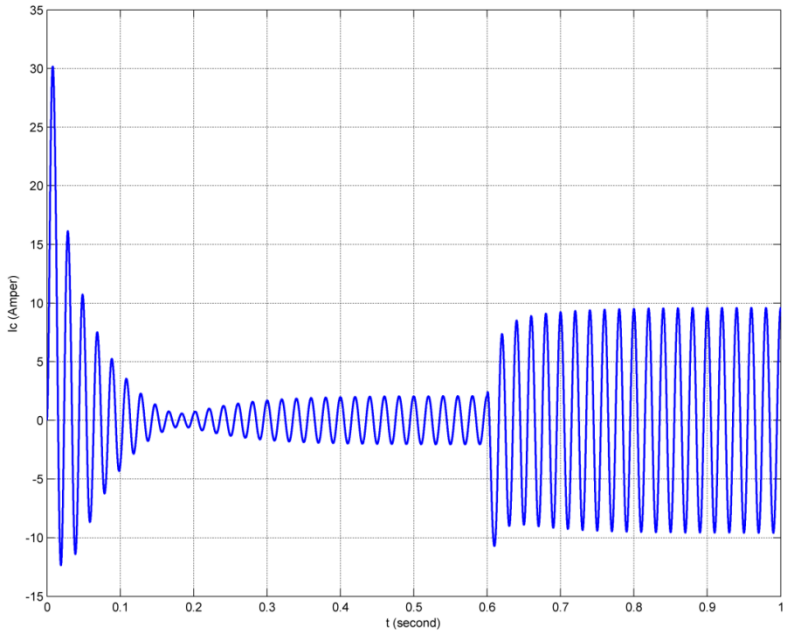

Figure 4.8 Invertor's compensation current, open-loop control

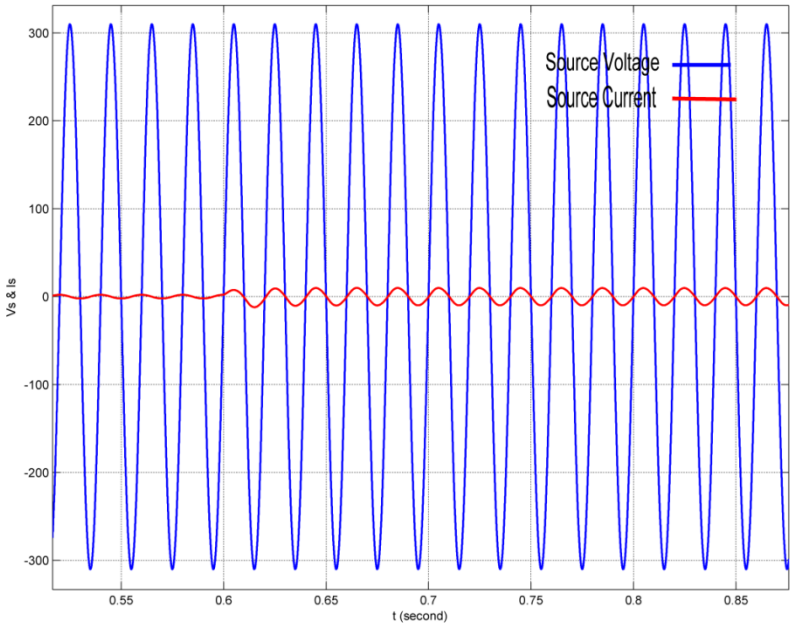

Figure 4.9 Source voltage and source current waveforms, open-loop control

4.3 Close-loop Cascade PI Controller

The proposed model in previous section is open-loop control method by pre-calculated switching function which is not applicable for a real system, however, it is instructive to study the impacts of various factors in control loop to design and obtain a close-loop control method.

Analysis has clarified that dc link voltage control is very critical in this system. First of all, the power converter of the shunt APF or STATCOM is a boot-type converter, this means that the dc voltage must be kept higher than the peak value of the ac-bus voltage. Also dc link voltage value and its variation highly affect control voltage magnitude ($\hat{v}_c^*$) and its phase displacement (δ) regards to source voltage and consequently it affects modulation index (m_a) and δ in (4.15) and (4.16). Actually, based on principle of STATCOM and reactive power compensation (4.2.1), VSI invertor is not responsible to produce any real power and in the case of harmonic compensation it absorbs just the amount of real power that is needed to compensate harmonic losses. By the other means constant dc link voltage can guarantee that harmonic losses be compensated and there is no any real power exchange between

VSI and main circuit. Proposed control method by inspiring from (Tsang & Chan, 2005 and 2006) is based on this fact and it suggests that constant dc link voltage can guarantee proper VAR and harmonic compensation and there is no need to such calculation to find reference current which is proposed in p-q theory and non-active current theory or other control methods.

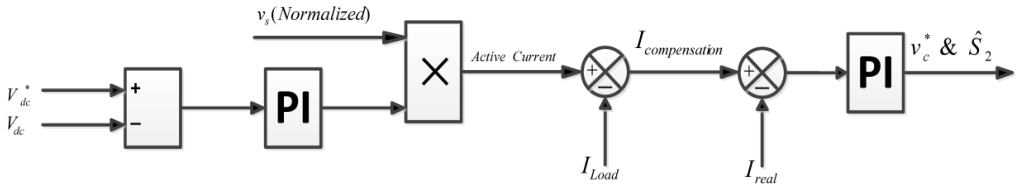

Figure 4.10 Close-loop control method

In (Tsang, Chan & Tang, 2013). Cascade PI Controller is implemented for multi-level shunt active power filter and here almost the same control method implemented for single-phase STATCOM control. In the suggested control method output of dc voltage PI controller is multiplied by normalized source voltage to be in phase with source voltage and will be considered as active current. Active current simply subtracted from load current in order to compensation reference current for current controller be calculated. The error of this reference current and filter current is fed to PI controller to produce control voltage which here in mathematical model is considered as switching function.

Proposed close-loop control method is implemented in the same case study that is represented in previous section and results are almost the same and even better. DC link voltage, invertor's compensation current and source compensated current versus source voltage are shown in Figure 4.11 to Figure 4.13 for comparison with Figure 4.7 to Figure 4.9. These results with Simulink and experimental results which are represented in next chapter gave credibility to proposed novel control method.

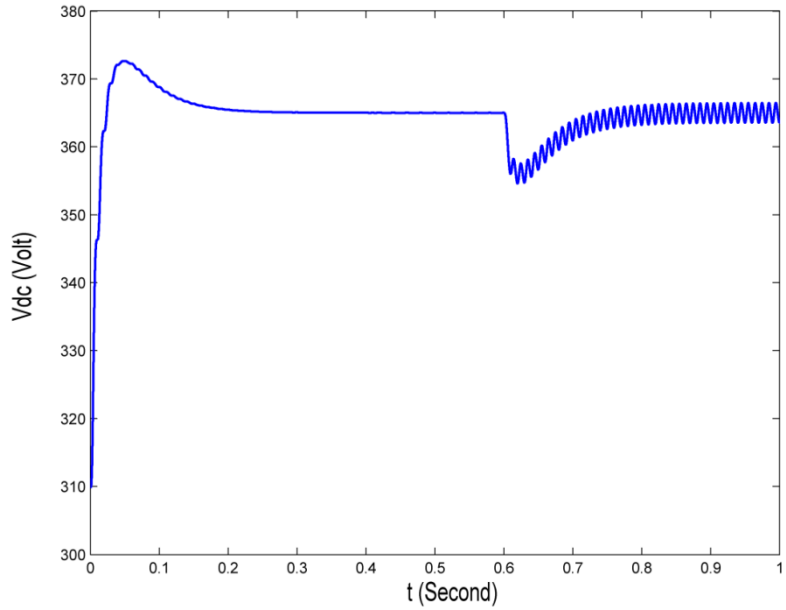

Figure 4.11 DC link capacitor voltage variation, close-loop control

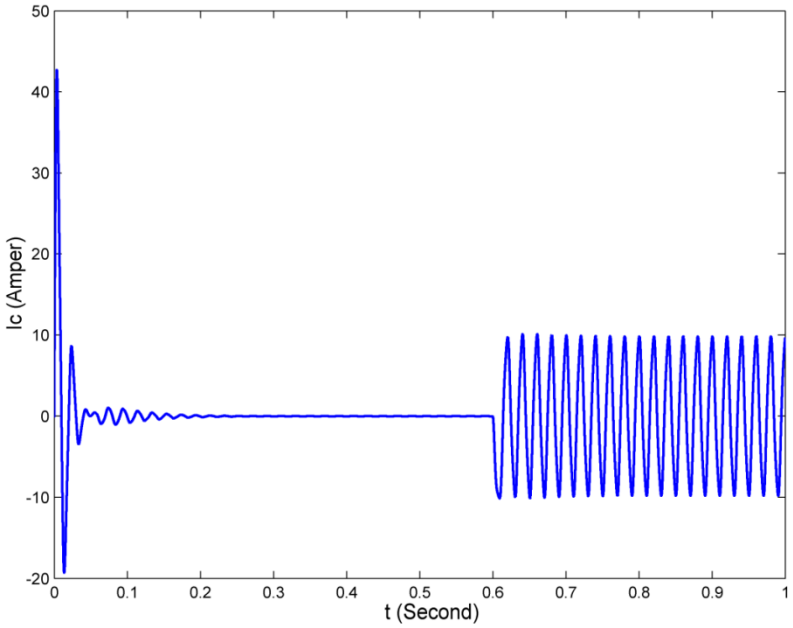

Figure 4.12 Invertor's compensation current, close-loop control

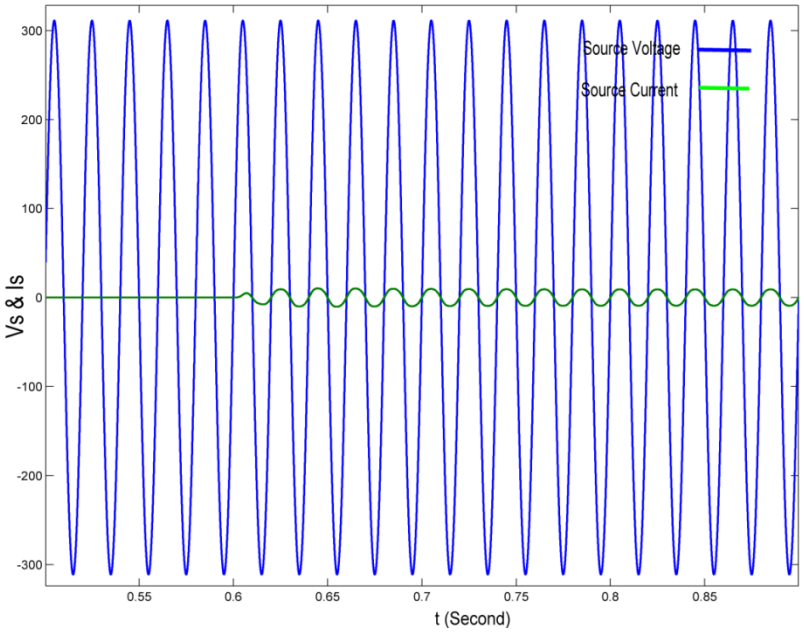

Figure 4.13 Source voltage and source current waveforms, close-loop control

CHAPTER FIVE
MATLAB SIMILATION AND EXPERIMENTAL IMPLEMENTATION

MATLAB\Simulink is a very powerful tool to simulate systems which utilize in most engineering fields in order to design systems prior to implementation. In this chapter MATLAB/Simulink power electronics toolbox is utilized to create simulation circuits for p-q theory, non-active current theory with current controllers that are discussed in 2.5 and novel Cascade PI Controller, the capability of MATLAB/Simulink to co-work with Texas Instruments^{TM} Digital Signal Processors (eZDSP) is used and validity of simulation circuits is proven by MATLAB/Simulink co-working by TMS320F2812 eZDSP platform. Finally TMS320F2812 eZDSP stand-alone flash programming is carried out in a laboratory prototype and experimental results gave credibility to effectiveness of theories.

5.1 MATLAB/Simulink Set Up

5.1.1 p – q Theory with Hysteresis Current Controller

The proposed single-phase p-q Theory is simulated to confirm the performance of reactive power compensation. The SimPowerSystems block sets of MATLAB/ Simulink has been utilized as the simulation tool. Solver options have been set to fixed step, discrete time with no continuous states which is adjusted by means of sampling time. In the control strategy output of DC link PI controller is multiplied by normalized source voltage in order to be in-phase with it and then it is added to the reactive current that is calculated by p-q theory and the summation is considered as reference current which should be produced by VSI. Then the reference current is fed to hysteresis current controller. Complete control block diagram is illustrated in Figure 5.1 and PI controller configuration with hysteresis controller is summarized in Table 5. 1.

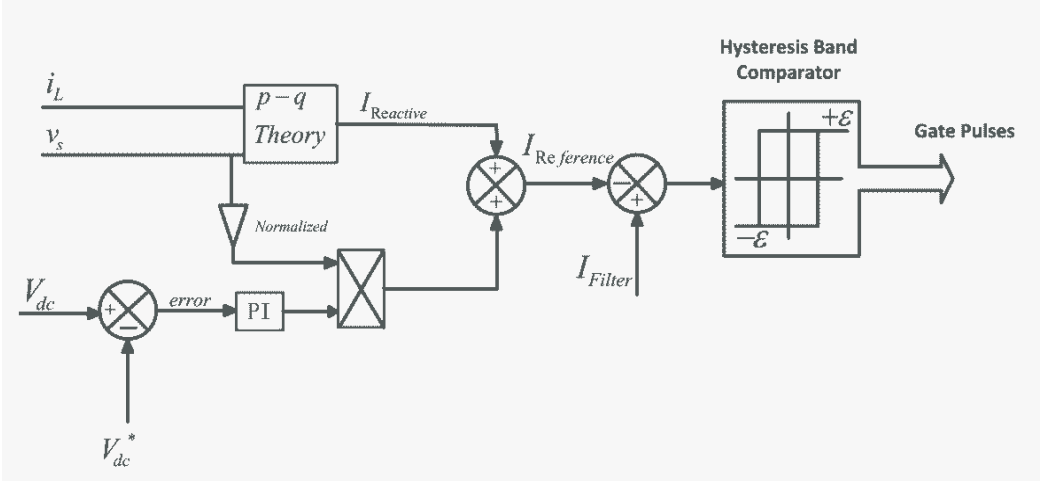

Figure 5.1 p-q theory with hysteresis current controller block diagram

Table 5. 1 p-q theory with hysteresis controller parameters

DC link PI controller	$K_i = 80$
	$K_p = 1.6$
Hysteresis Band	0.2 A

The supply voltage is considered as ideal with pure sinusoidal waveform. The load on the system is resistive-inductive load drawing lagging current from network with power factor close to 0.71 and ideal IGBTs with antiparallel diode are implemented in H-bridge single-phase boost type inverter topology. Sampling time is set to 83.33 µs which is the same with DSP based stand-alone experimental set up. The design specifications and circuit parameters used in the simulated system are given in Table 5.2. Simulation results show that p-q theory can instantaneously calculate and produce reactive power and reactive current and by means of proper implementation of hysteresis current controller constant DC link voltage and reactive power compensation can be guaranteed. DC link voltage, source voltage versus the current that is absorbed from source (source current) and source voltage versus the current that is produced by VSI (filter current) are shown in Figure 5.2, Figure 5.3, Figure 5.4 respectively.

Table 5.2 Simulated system's parameters

AC Supply Voltage	30V(RMS)
Fundamental Frequency	50 HZ
Reference DC Bus Voltage	50 V
Resistive Load	75 Watt
Inductive Load	75 VAR
Coupling Inductance	5 mH
Coupling Resistance	0.5 Ohm
Sampling Time	83.33 µs
Inverter Switching Frequency	Between 1.5 and 2 kHz

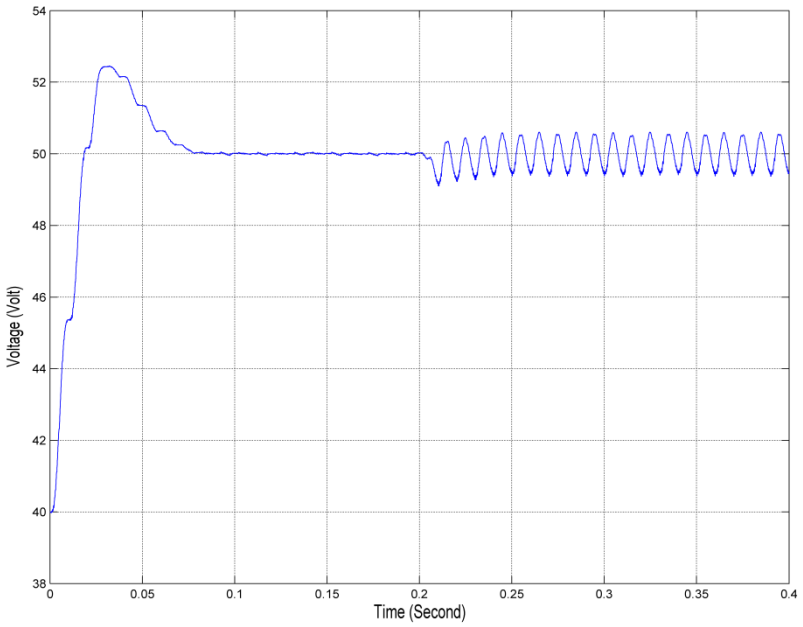

Figure 5.2 p-q theory with hysteresis controller, DC link voltage variation, MATLAB Simulink

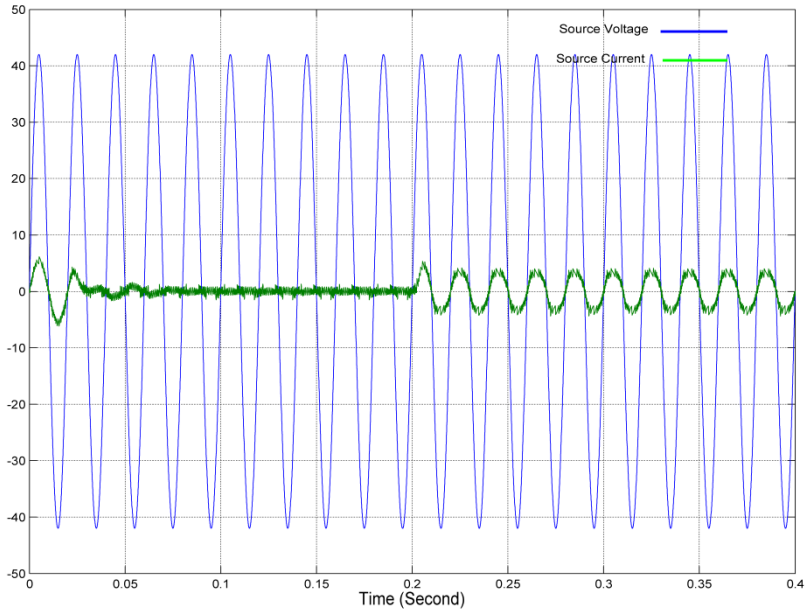

Figure 5.3 p-q theory with hysteresis controller, source voltage versus source current, MATLAB Simulink

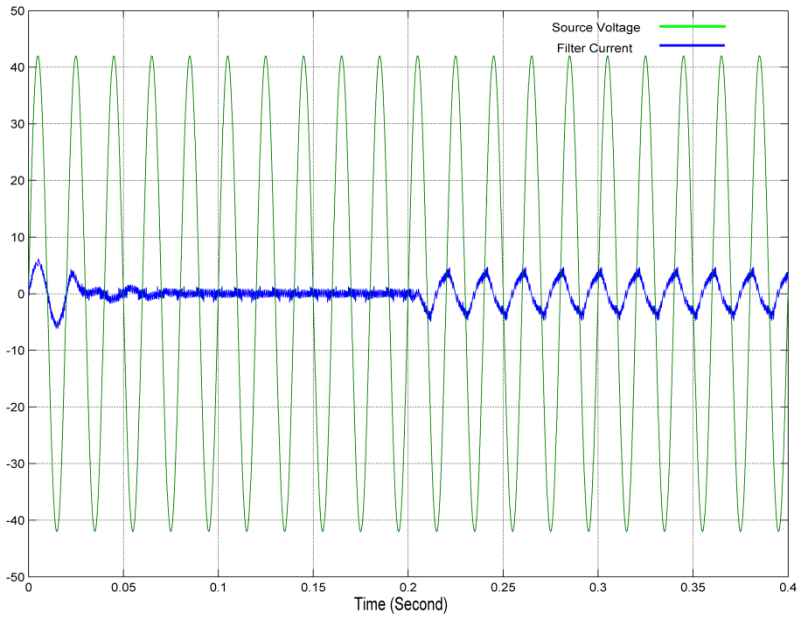

Figure 5.4 p-q theory with hysteresis controller, source voltage versus filter current, MATLAB Simulink

Simulation has been done under no-load until t=0.2s and load has been connected at that time. Figure 5.4 explicitly depicts that the current that produced by VSI (filter current) 90º leading the source voltage (capacitive current) in order to compensate

inductive part of load which 90º lagging source voltage. Also before load connected to the system, VSI absorbs just the amount of current which satisfies DC link voltage stability and it is oscillating around zero except at the starting or in transient situation (when the load is connected or the reference DC link changes). Under load condition DC link has oscillation around 1V peak to peak.

Fast Fourier Transform (FFT) analyses of source current is represented in Figure 5.5 which explicitly shows that switching frequency is around 1.5-2 kHz. Figure 5.6 is represented a zoomed version of FFT analyses output of the same signal in lower frequency range where the dominant harmonic is third harmonic and it is because less number of switching in cress of source current which injects low order odd harmonics to the source current. Less switching occurs in cress regions because hysteresis current control technique cannot properly track reference current in the regions that the polarity of derivative change (cress regions).

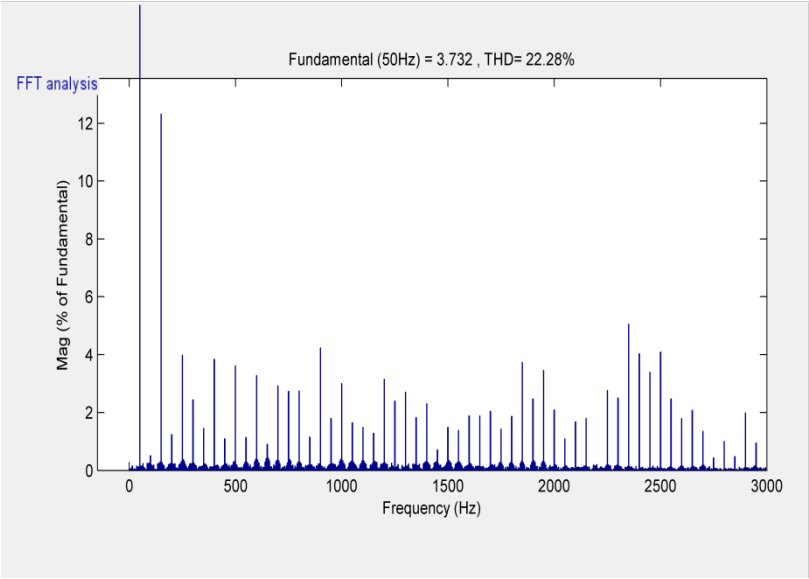

Figure 5.5 p-q theory with hysteresis controller, source current FFT analyses

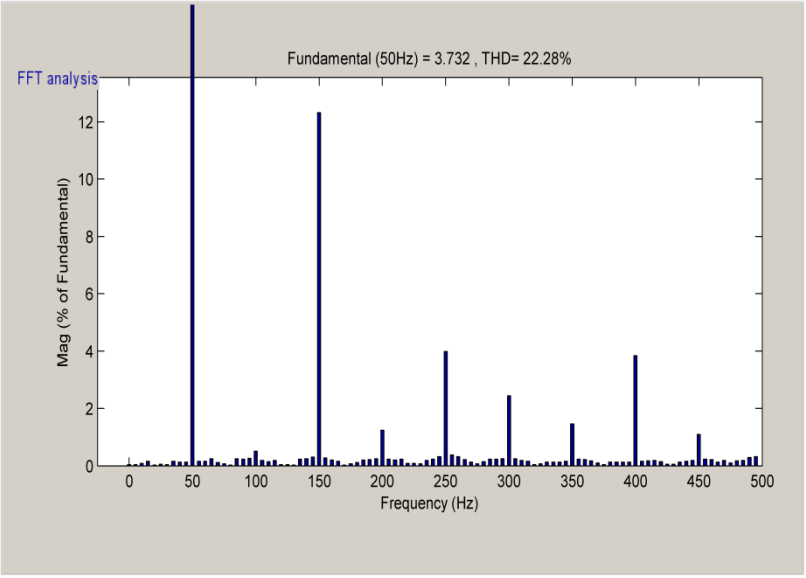

Figure 5.6 p-q theory with hysteresis controller, source current FFT analyses in low frequency range

5.1.2 Non-Active Current Theory with SPWM Current Controller

Instantaneous non-active current theory which is proposed in Figure 2.14 has been implemented in order to produce non-active current, output of DC link PI controller which is multiplied with normalized source voltage in order to be in phase with it, added to non-active current and the summation is considered as reference current. This reference current instantaneously compared with VSI produced current (filter current) and the difference is considered as error which is fed to second PI controller in the sake of generating of reference voltage. The reference voltage instantaneously compared with triangular carrier voltage and gate pulse signals are generated. Complete control strategy is represented in Figure 5.7

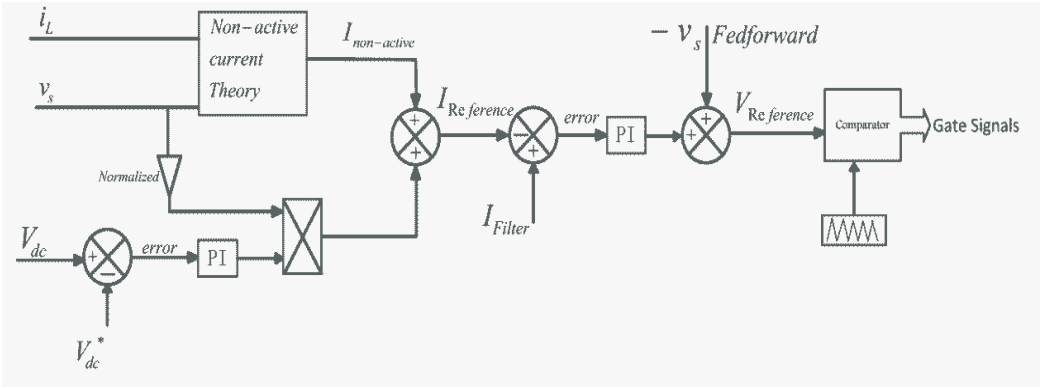

Figure 5.7 Non-active current theory with SPWM controller block diagram

In (Xu, Tolbert, Chiasson, 2007) and (Xu, Tolbert, Kueck, 2010) it is suggested that original source voltage forwardly feed to second PI controller output however, deep investigation in model and simulation depicted that VSI output voltage and consequently reference voltage in the control method is almost in opposite phase of source voltage, then adding original source voltage to reference voltage forwardly can disfigure reference voltage on peak values and this can deteriorate controller performance on peak values and add some odd harmonics to the source current. Here as it can be inferred from Figure 5.7, 180º shifted form of source voltage is considered as feedforward signal and the results both in simulink and experimental are satisfactory.

Above mentioned instantaneous non-active current theory is implemented in the same system with parameters that is represented in Table 5.2, simulation has been made in the same condition except the sampling time which is set to 100µs in this method to completely coincide with experimental implementation because execution time of this control method with SPWM current controller in DSP based implementation is longer than p-q theory with hysteresis current controller. Controller set up is summarized in Table 5.3.

Table 5.3 Non-active current theory with SPWM controller set up parameters

DC link PI controller	$K_i = 60$
	$K_p = 1.2$
Second PI controller	$K_i = 5$
	$K_p = 40$
PWM carrier frequency	1.25 kHz
PWM carrier peak value	25 V

Results demonstrate effectiveness of control strategy and instantaneous reactive current compensation has been achieved. DC link voltage, source voltage versus source current and source voltage versus filter current are shown in Figure 5.8, Figure 5.9 and Figure 5.10 respectively.

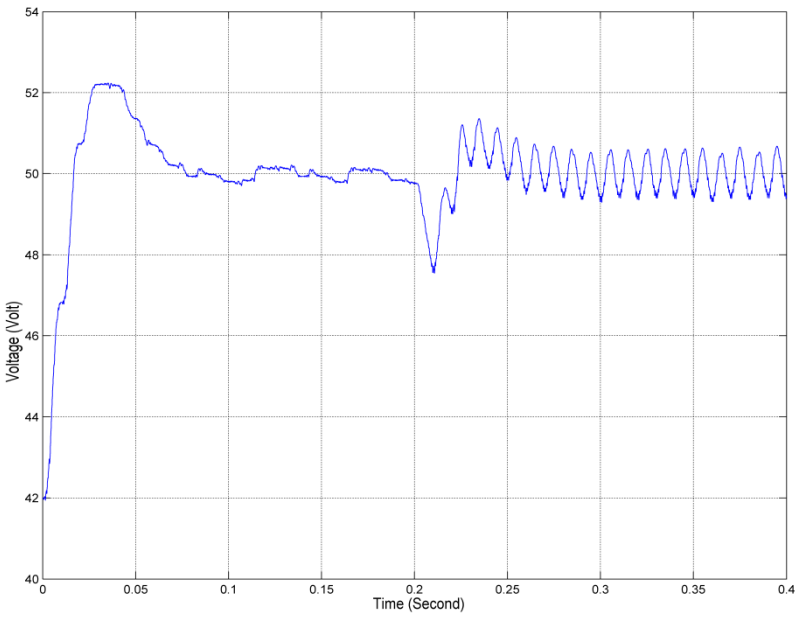

Figure 5.8 Non-active current theory with SPWM controller, DC link voltage variation, MATLAB Simulink

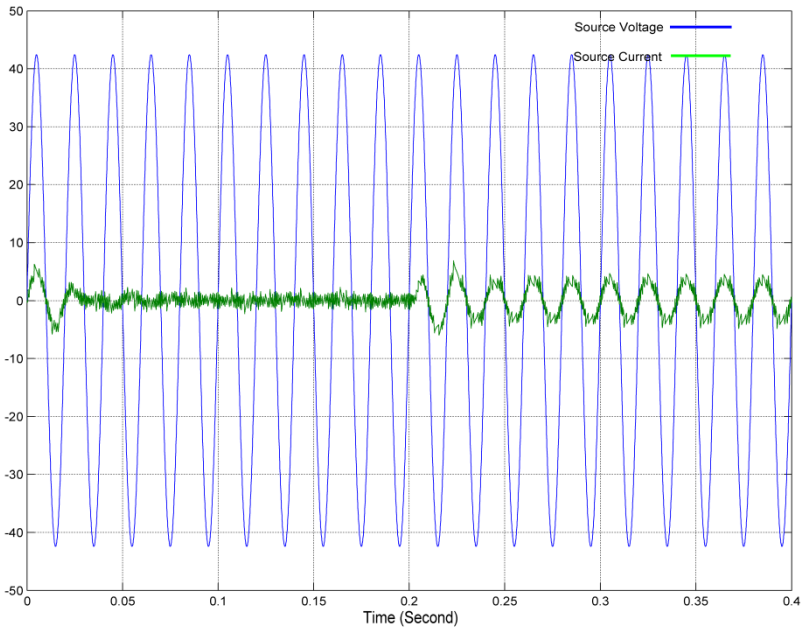

Figure 5.9 Non-active current theory with SPWM controller, source voltage versus source current, MATLAB Simulink

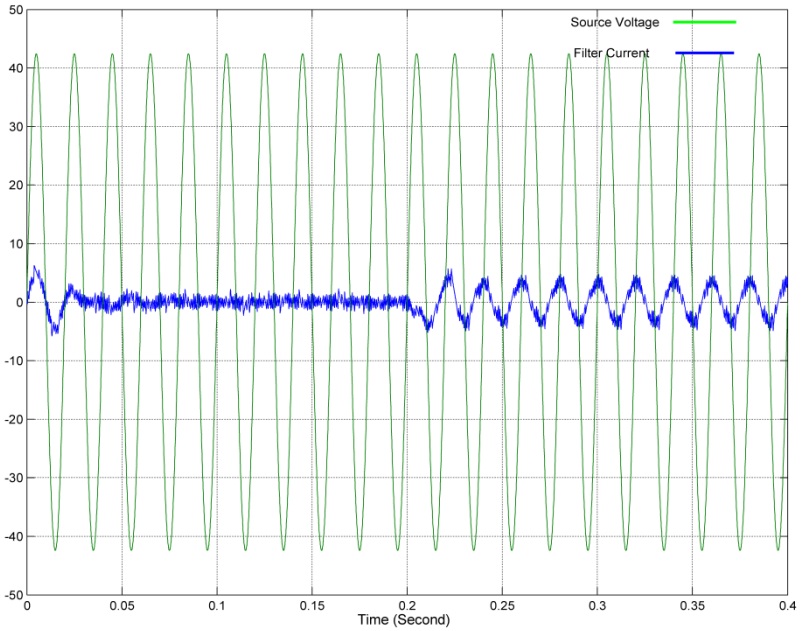

Figure 5.10 Non-active current theory with SPWM controller, source voltage versus filter current, MATLAB Simulink

Again, simulation has been made under no-load condition until t=0.2s and until this time it can be realized from Figure 5.10 that VSI produces just the amount of current that is satisfied constant DC link and under inductive load, VSI by means of

non-active current theory and proper SPWM controller produced capacitive current (90º leading the source voltage) in order to compensate inductive current. DC link variation under no-load is neglectable and under load is around 1V peak to peak.

FFT analyses of source current is represented in Figure 5.11 switching frequency exactly is around PWM carrier frequency (1.25 kHz) and this is one of the advantages of this control method against hysteresis current controller. Some odd harmonics are observed and again in this control method the dominant harmonic order is third harmonic and the reason of it because reference voltage in this method completely exceeds the carrier signal in cress regions and there is no intersection between reference voltage and PWM carrier signal, consequently in cross regions there is no or at least less switching occur and this causes insertion of some odd harmonic orders especially third harmonic. In Figure 5.12 this phenomenon is observable.

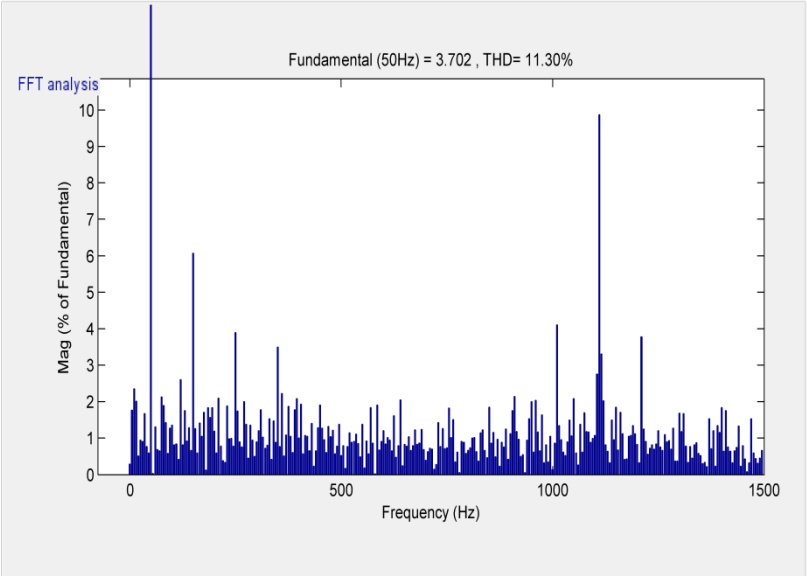

Figure 5.11 Non-active current theory with SPWM controller, source current FFT analyses

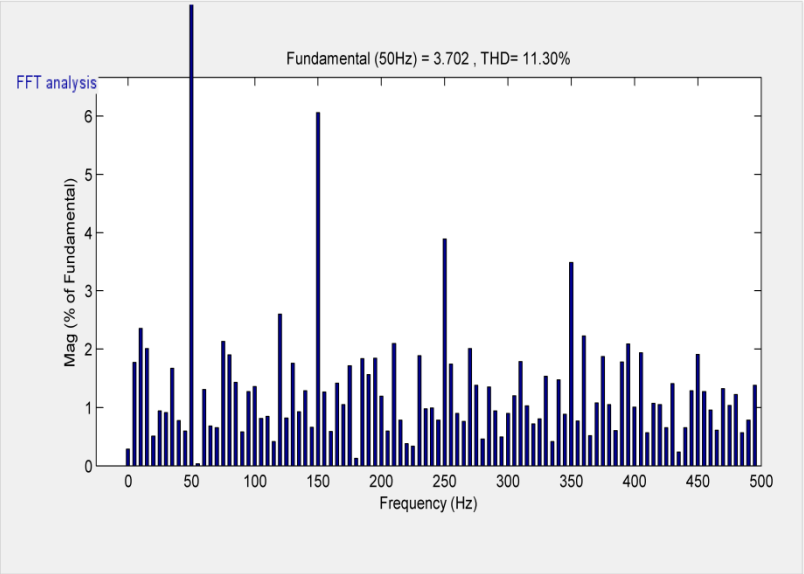

Figure 5.12 Non-active current theory with SPWM controller, source current FFT analyses in low frequency range

5.1.3 Cascade PI controller method

Proposed cascade PI controller which is represented in Figure 4.10 is simulated in MATLAB/Simulink environment. In the proposed method difference between actual DC link voltage and DC reference voltage (error) is fed to first (DC link) PI controller, output of the PI controller multiplied by normalized source voltage to be in-phase with source voltage and it is considered as active current that should be absorbed from source, then without any extra calculation non-active or compensation current is obtained by simply subtracting load current from active current. This compensation current is compared with filter current and the error is fed to second (current controller) PI controller. Output of PI controller is added up with 180º degree shifted form of source voltage (feedforward) and reference voltage is obtained. This reference voltage instantaneously compared with triangular waveform in order to gate pulse signals generate. Complete control block diagram is shown in Figure 5.13.

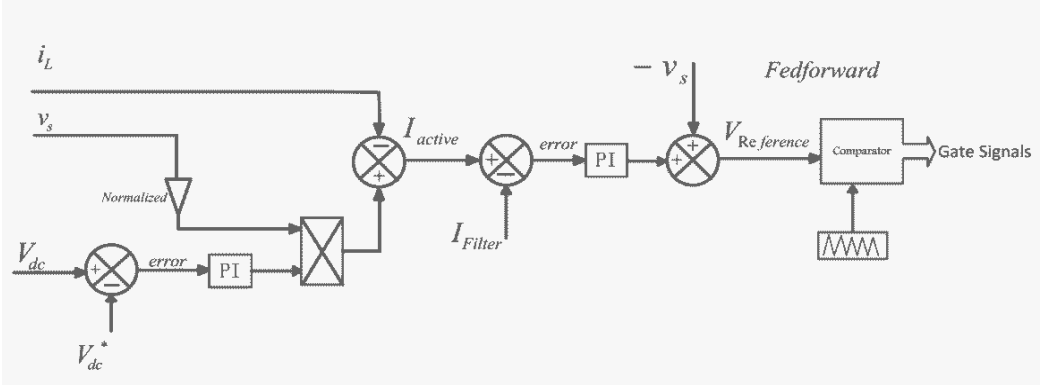

Figure 5.13 Cascade PI controller block diagram

Simulation has been made in 30V (RMS) to match with experimental setup. Simulated system's parameters are shown in Table 5.4.

Table 5.4 Cascade PI control method simulated system parameters

AC Supply Voltage	30V(RMS)
Fundamental Frequency	50 HZ
Reference DC Bus Voltage	50 V
Resistive Load	60 Watt
Inductive Load	75 VAR
Coupling Inductance	5 mH
Coupling Resistance	0.5 Ohm
Sampling Time	100 µs
Inverter Switching Frequency	Around 1.25 kHz

PI controllers and SPWM set up parameters are summarized in Table 5.5. Simulation results depict that the control method can adequately deals with reactive power and assure constant DC link voltage. DC link voltage, source voltage versus source current and source voltage versus filter current are represented in Figure 5.14, Figure 5.15 and Figure 5.16 respectively.

Table 5.5 Cascade PI controller setup parameters

DC link PI controller	$K_i = 50$
	$K_p = 1.2$
Second PI controller	$K_i = 2$
	$K_p = 80$
PWM carrier frequency	1.25 kHz
PWM carrier peak value	150 V

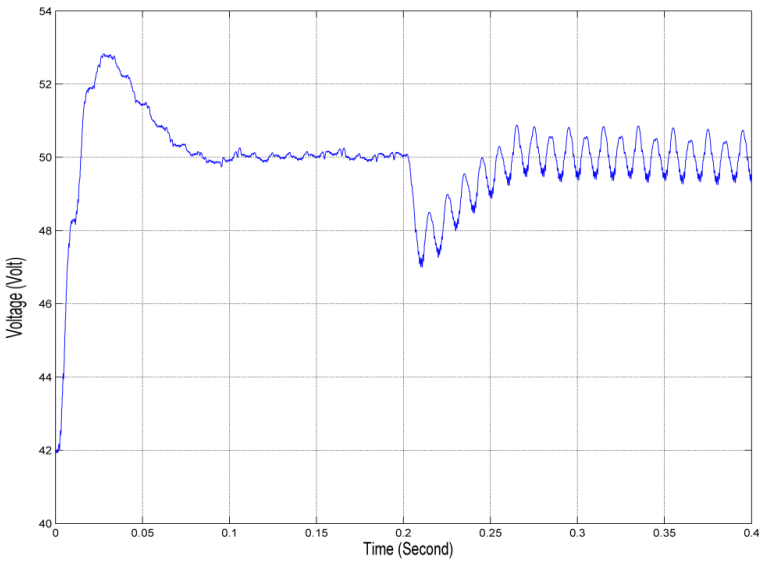

Figure 5.14 Cascade PI controller, DC link voltage variation, MATLAB Simulink

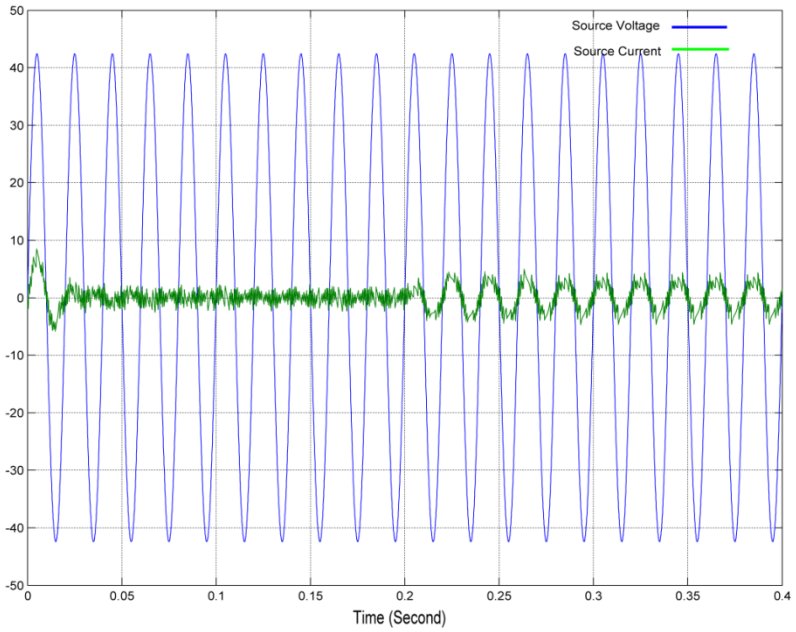

Figure 5.15 Cascade PI controller, source voltage versus source current, MATLAB Simulink

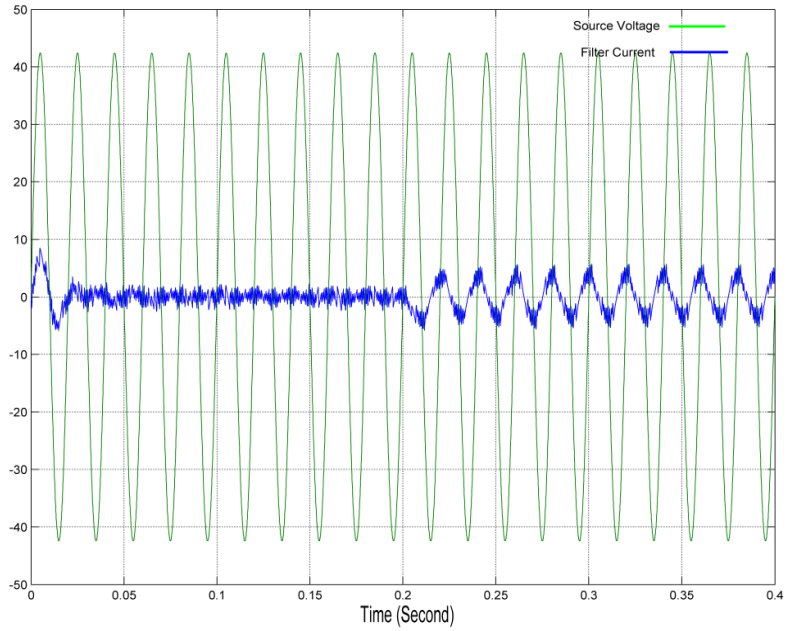

Figure 5.16 Cascade PI controller, source voltage versus filter current, MATLAB Simulink

Like previous cases simulation has been made to work under no-load until t=0.2s and the load is connected to the source at t=0.2s, simulation results clearly show that source current is in phase with source voltage and reactive power compensation is achieved. Figure 5.16 shows that filter current 90º leads the source voltage which is

capacitive in order to compensate inductive load. DC link has 1V oscillation under load and with no-load DC link oscillation is neglectable.

FFT analyses of source current in the same manner are represented in Figure 5.17 and Figure 5.18. In this method likewise SPWM method the switching frequency is around PWM carrier signal frequency (1.25 kHz) and dominant harmonic is third harmonic order because of the above mentioned reason.

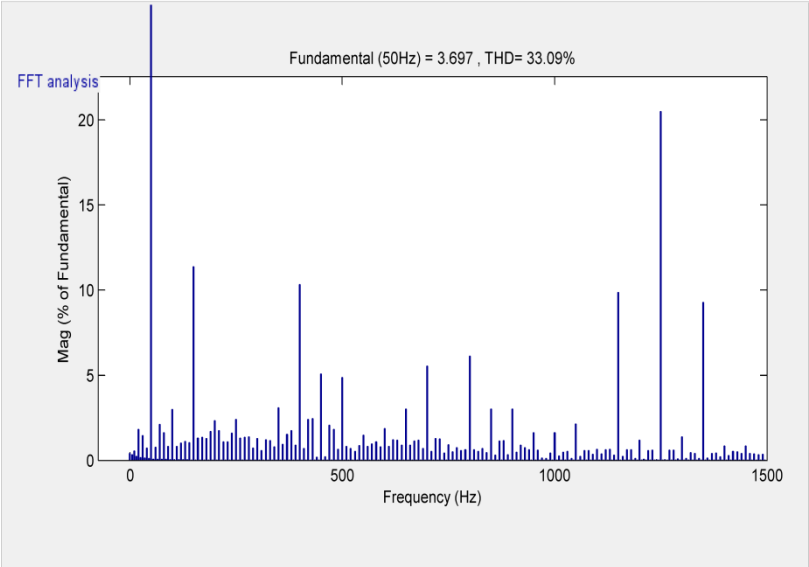

Figure 5.17 Cascade PI controller, source current FFT analyses

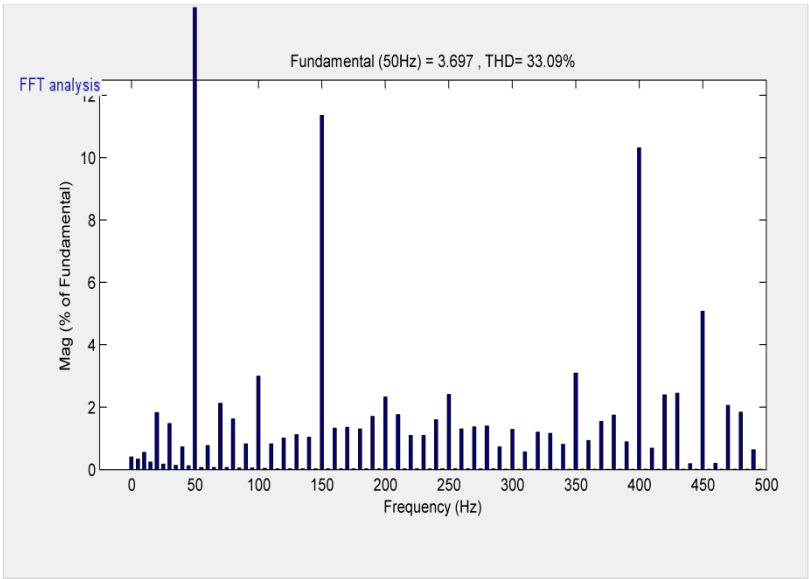

Figure 5.18 Cascade PI controller, source current FFT analyses in low frequency range

5.2 MATLAB/Simulink Co-working with Texas Instruments™ eZDSP

The capability of MATLAB/Simulink to co-work with Texas Instruments™ (TI) eZDSP is utilized in order to check the validity of control method before stand-alone DSP based experiment. By employing Simulink Coder/Embedded IEDs tool box features it is possible to generate Code Composer Studio (CCS) C code for Simulink models. Integrated Development Environment (IDE) Link of MATLAB software provides tools that help users verify their code during development by enabling them to run portions of simulations on their hardware and profiling the executing code. Processor-in-the-Loop (PIL) simulation is used to run part of the application on DSP while the rest is run in Simulink. For this purpose proper Target Preferences from MATLAB library is added to the "control block" subsystem and it is configured for F2812 platform. Then from "Simulation" > "Configuration Parameters" in the model menu, under "Code Generation" > "IDELink", Build action is set to "Create_Processor_In_the_Loop _project".

Right-clicked the "control block" subsystem, and "Code Generation" > "Build Subsystem" from the context menu is selected, "Build" button on the opened dialog box is selected, build process in the MATLAB® command window is completed and PIL subsystem which is CCS compatible C code form of the control block, is created in new Simulink window. New PIL control block subsystem is replaced by original MATLAB control block on the model. The simulated model is illustrated in Figure 5.19.

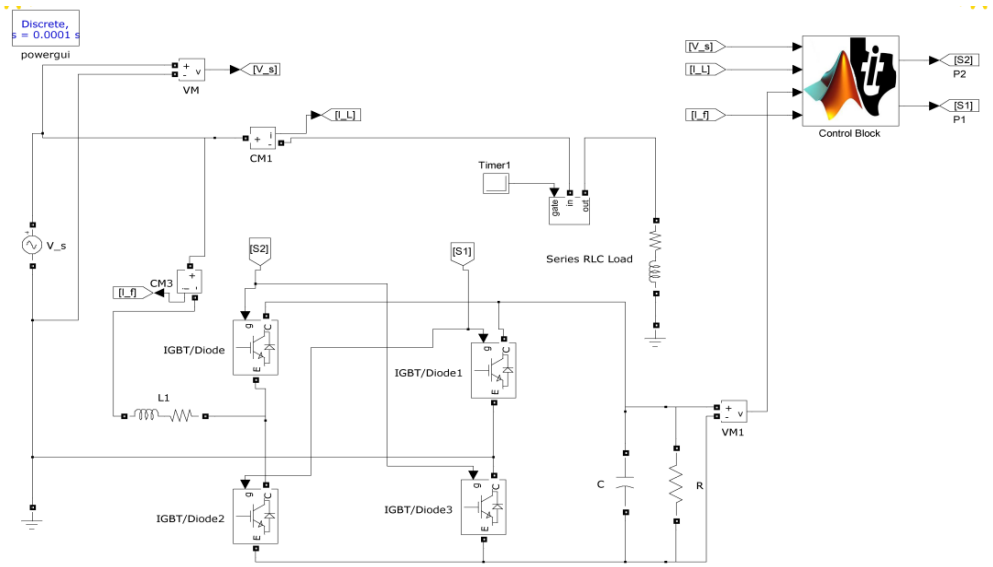

Figure 5.19 MATLAB/Simulation model with TI eZDSP

By this configuration control part of Simulink model is performed in DSP while other part of model is run from Simulink. Performance of the DSP to calculate compensation current and gate pulses is proven; results for three methods are represented.

Similar to simulation; DC link variation, source current versus source voltage and filter current versus source voltage are recorded for represented three methods and recorded results are identical with simulation ones.

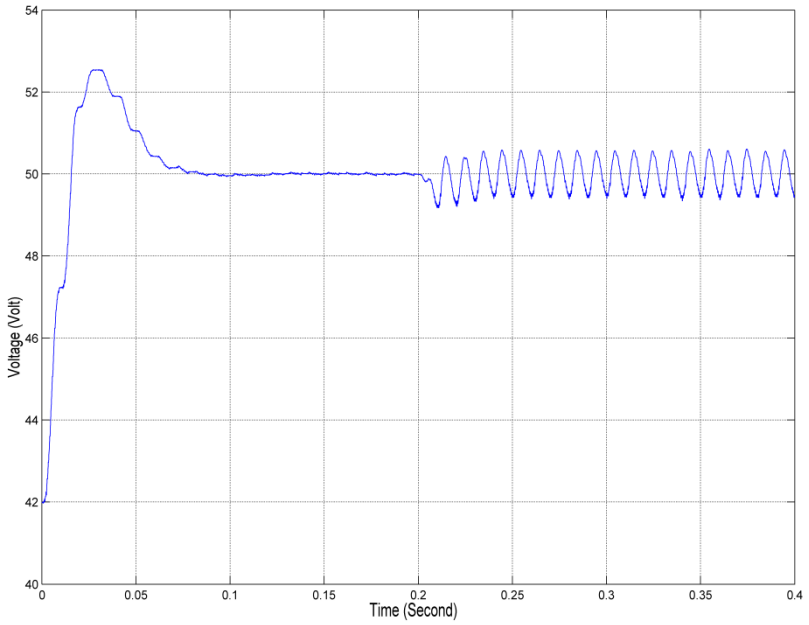

Figure 5.20 p-q theory with hysteresis current controller, DC link variation, DSP co-working with MATLAB

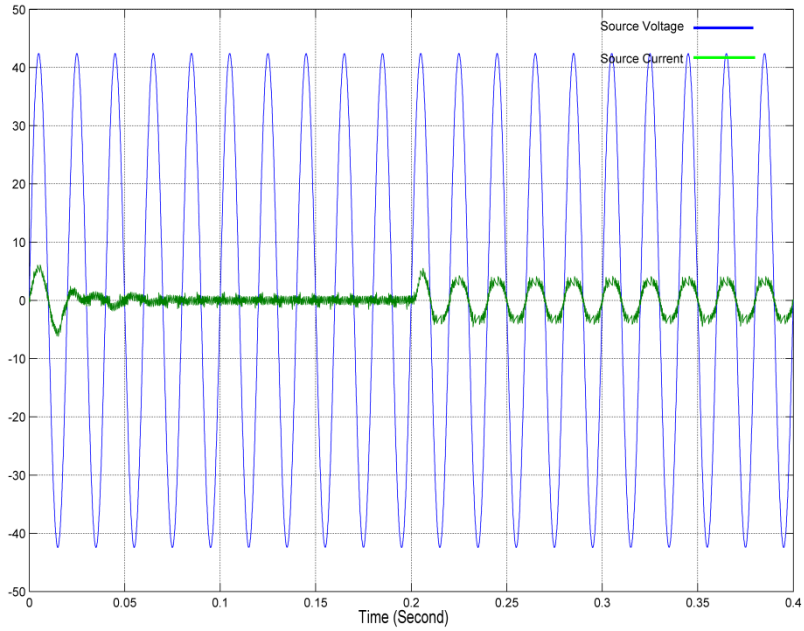

Figure 5.21 p-q theory with hysteresis current controller, source current versus source voltage, DSP co-working with MATLAB

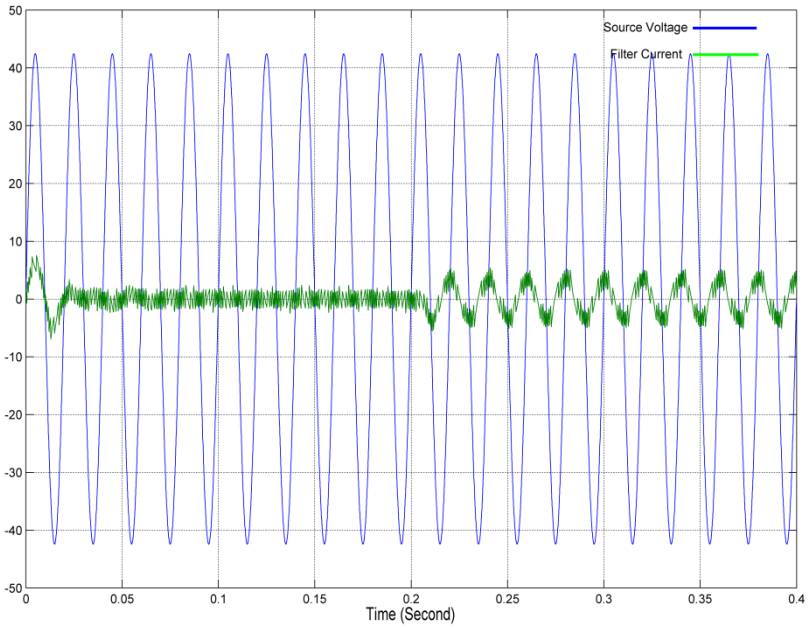

Figure 5.22 p-q theory with hysteresis current controller, filter current versus source voltage, DSP co-working with MATLAB

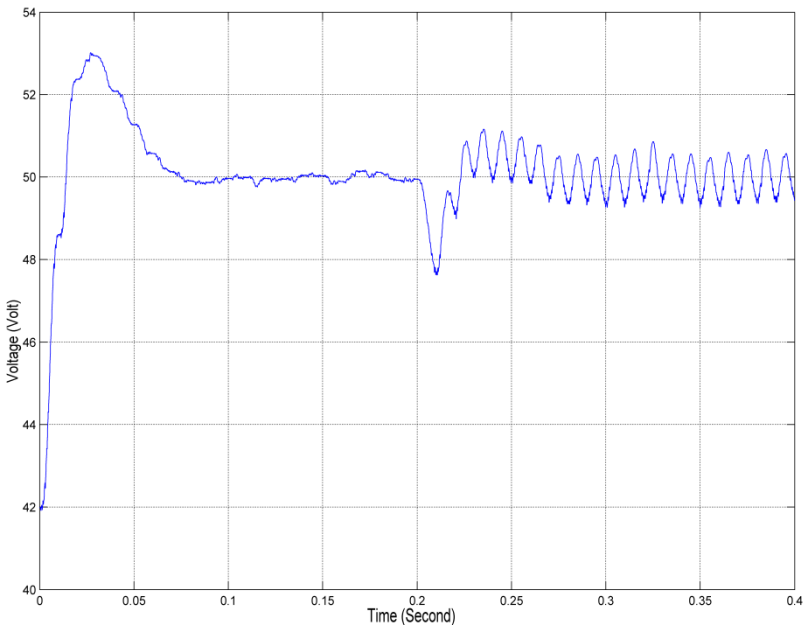

Figure 5.23 Non-active current theory with SPWM controller, DC link variation, DSP co-working with MATLAB

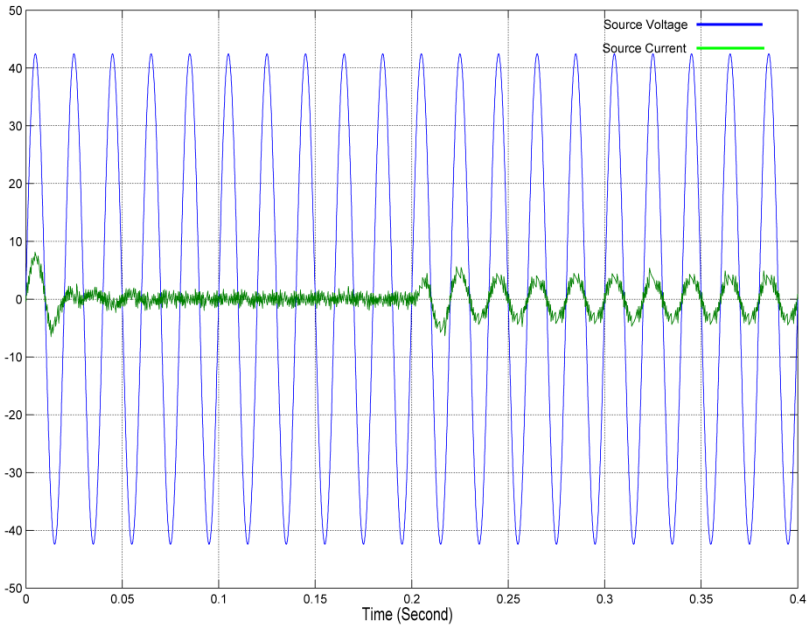

Figure 5.24 Non-active current theory with SPWM controller, source current versus source voltage, DSP co-working with MATLAB

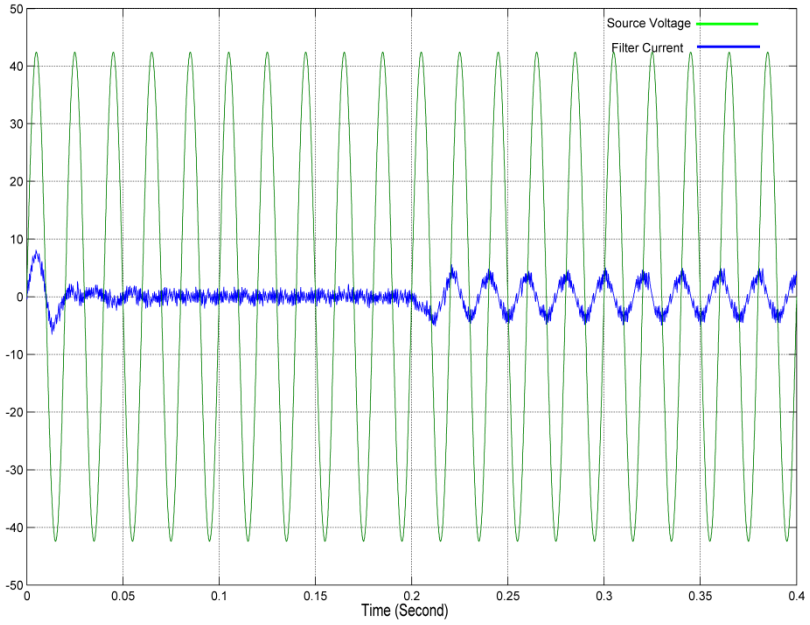

Figure 5.25 Non-active current theory with SPWM controller, filter current versus source voltage, DSP co-working with MATLAB

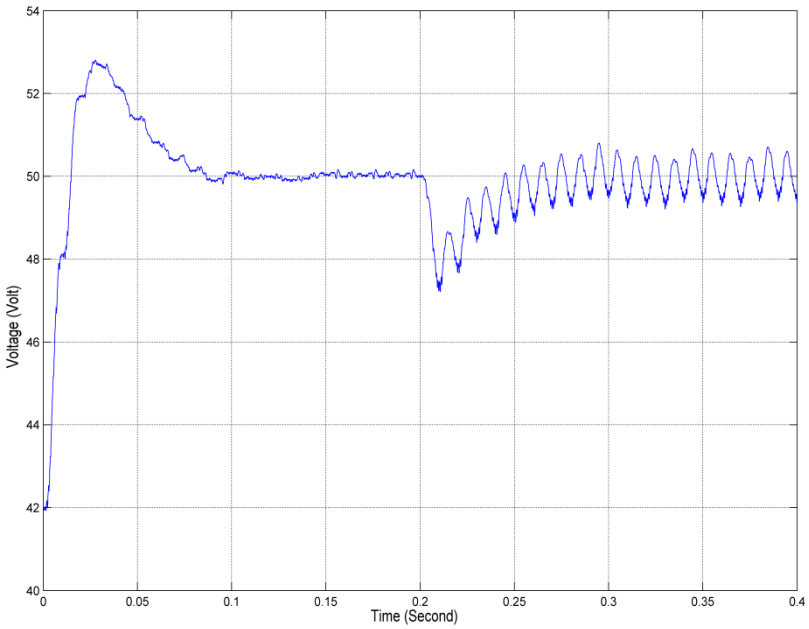

Figure 5.26 Cascade PI controller, DC link variation, DSP co-working with MATLAB

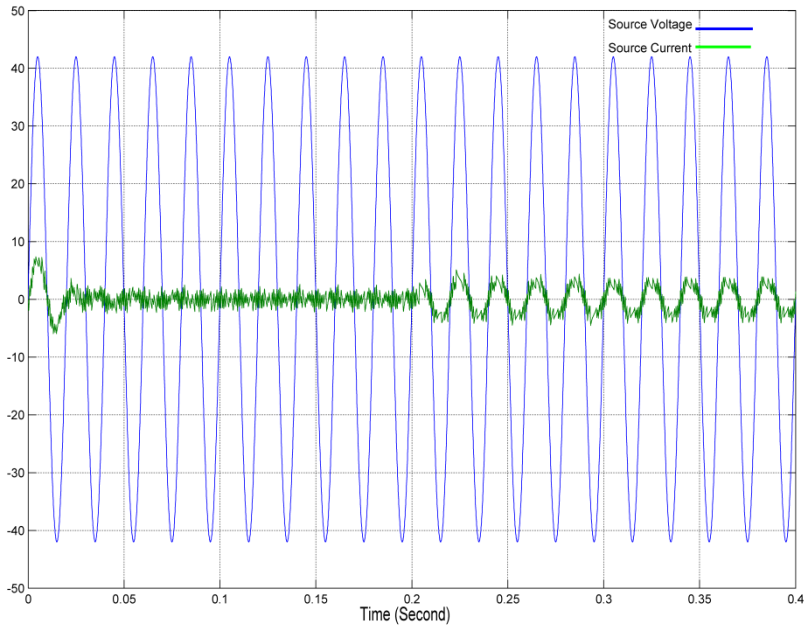

Figure 5.27 Cascade PI controller, source current versus source voltage, DSP co-working with MATLAB

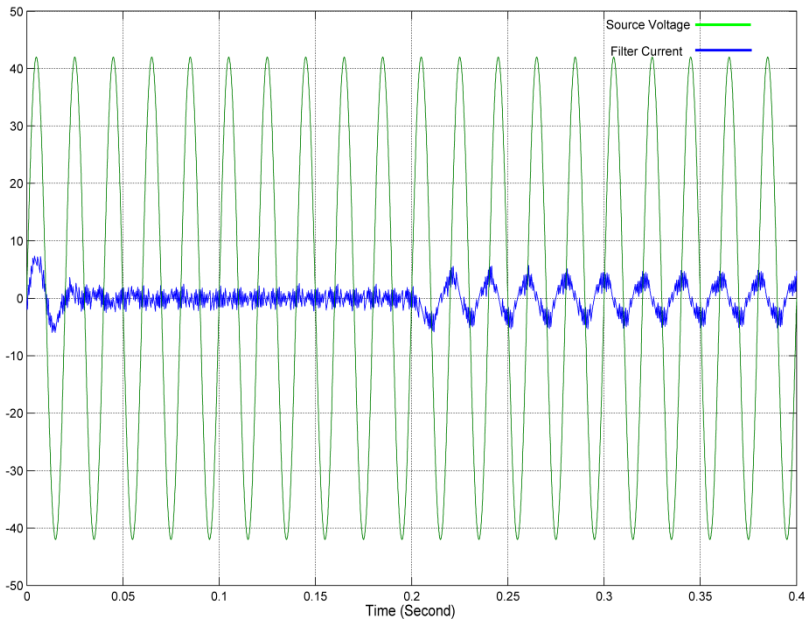

Figure 5.28 Cascade PI controller, filter current versus source voltage, DSP co-working with MATLAB

5.3 Stand-Alone DSP Based Experimental Setup

Laboratory prototype comprises of blow parts is established:

- Voltage and current measurement circuit
- Buffer circuit
- DSP board
- IGBT driver circuit
- IGBT with antiparallel diode based boost type Voltage Source Inverter (VSI)
- DC link capacitor
- Coupling inductance

For voltage and current sensing Voltage Transducer LV 25-P and Current Transducer LA 100-P are used respectively. Measured voltage and current are not in desired range to be used as DSP input channels, then buffer circuit comprises of Op-Amp, capacitor and resistance is used in order to modify measured data in 0-3.3V voltage range, compatible to 12bit DSP Ac to Dc Converter (ADC) channels. CCS 3.3 software is used to establish control methods in C/C++ language and by utilizing “on cheap flash programming” tool, it is executed to DSP flash memory. Four

IRG4PH50KD IGBTs are implemented in H-bridge single-phase VSI. Utilized IGBTs are voltage control devices which 15-20V Gate-to-Emitter voltage satisfies Collector to Emitter conduction. DSP output signal are around 3–3.5 volts and did not provide this voltage range, consequently, IGBT drive circuit is implemented by means of IR2113 high and low side driver. Between driver circuit and DSP board the isolation between DSP board and VSI (power circuit) is realized by means of 6N138 optocouplers. For DC capacitor and coupling inductance 450V/4700μF and three 1.8~2 mH in series are used respectively.

5.3.1 Insertion of Deadtime

In real implementation IGBTs or other switching devices have not ideal characteristics and have some delay time during turning on and off. Typically turn off delay and fall time in these devices are more longer than turn on delay and rise time, because of this fact switches in H-bridge inverters in one leg turn on faster than the complimentary switch turn off and this causes short circuit on DC bus and may burn IGBT or damage them and other parts of circuit. To avoid this phenomenon and guarantee the safety of VSI system and keep each switching power device in parallel reliably driven, it is common to insert dead-time when producing PWM waves and to place isolation parts, drivers, amplifiers between DSP and VSI. Commonly this deadtime interval is considered around 3μs and in this implementation deadtime is inserted to the gate signals in software programming and it is considered as 4μs, where 4μs and in worse situation 3μs deadtime between turn on and turn off signals is observed from oscilloscope. Here the worse situation means the situation that optocouplers or drive circuit between DSP and VSI cause some delay in the signals and deteriorate the exact 4 μs deadtime that is implemented in software. Figure 5.29 and Figure 5.30 are shown the recorded gate signals in the implemented circuit. Figures' scale is 1μs, first the turn off signal comes and after 4 μs the turn on signal has been sent to the gate of IGBTs.

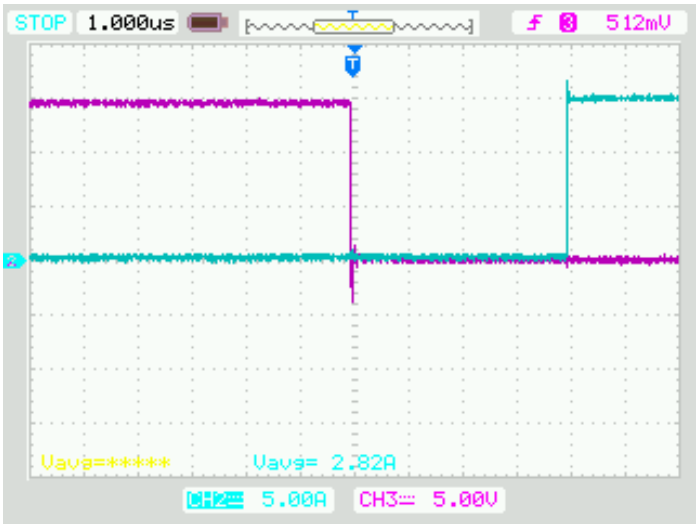

Figure 5.29 Observed 4 µs deadtime from IGBT end, experimental results

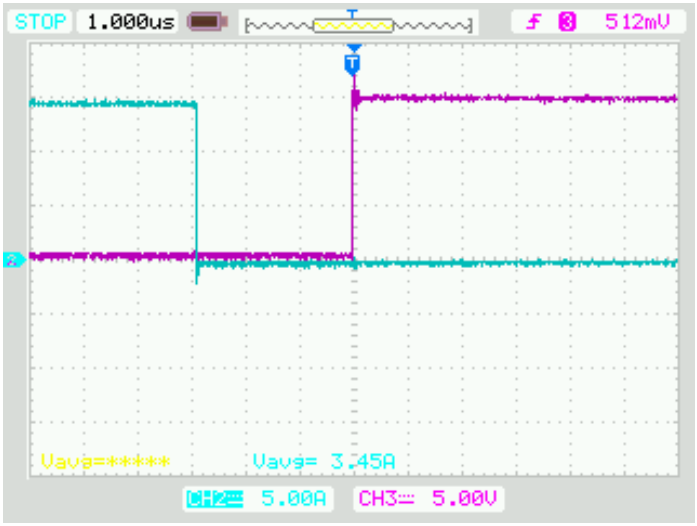

Figure 5.30 Observed 3µs deadtime from IGBT end, experimental results

5.3.2 Experimental Results

5.3.2.1 Instantaneous Reactive Power Theory with Hysteresis Current Controller

The circuit firstly is tested under no-load, transient and steady state behavior of DC link voltage has been observed. Parallel resistive-inductive (R-L) load is connected to the system and source voltage versus source current, source voltage versus filter current are recorded.

Source voltage versus load current is shown in Figure 5.31 which is common for all three implemented control strategies. Load current lagging the source voltage and absorbs 52.5Watt active power and 52.5VAR reactive power.

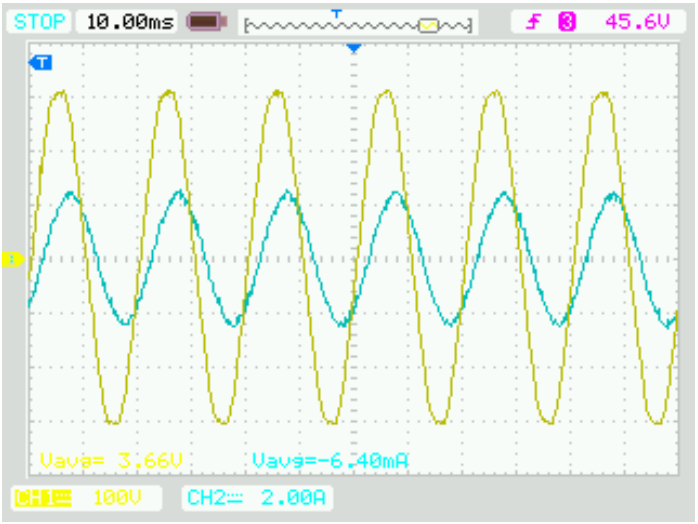

Figure 5.31 Source voltage versus load current in laboratory setup, experimental results

p-q theory with hysteresis current controller has been implemented in DSP based laboratory prototype with exactly the same setup that is represented in 5.1.1 and the DC link variation with source current and source voltage is shown in Figure 5.32

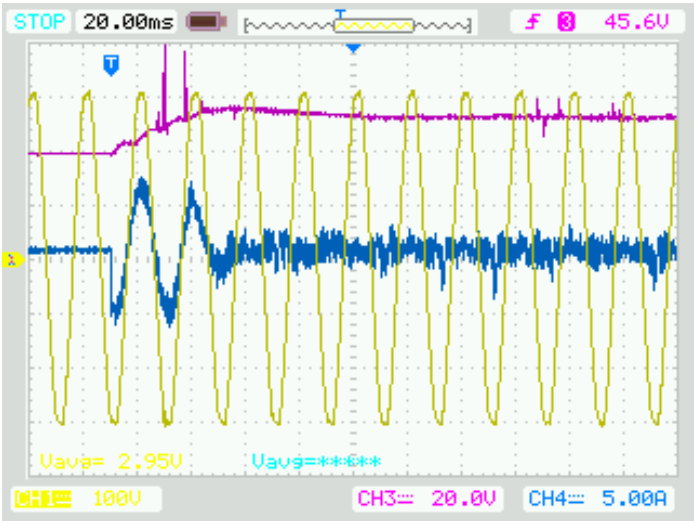

Figure 5.32 p-q theory with hysteresis current controller, DC link & source voltage & source current, experimental results

Figure 5.32 shows the satisfactory response of PI controller with hysteresis current controller which in less than two period of fundamental frequency boosts the DC link to 50 volt and from Figure 5.2 and Figure 5.3 the simulation results are almost the same with experimental ones where PI controller in one and half period of time responses and boosts the DC link to reference value.

Source voltage versus source current and source voltage versus filter current are illustrated in Figure 5.33 and Figure 5.34 respectively.

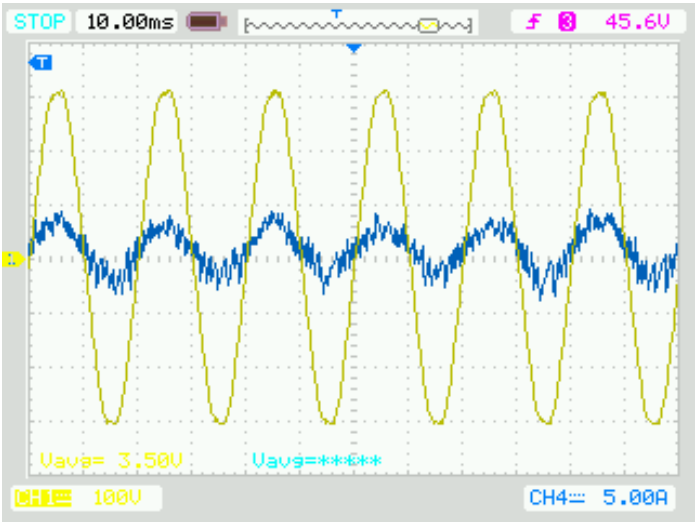

Figure 5.33 p-q theory with hysteresis current controller, source voltage versus source current, experimental results

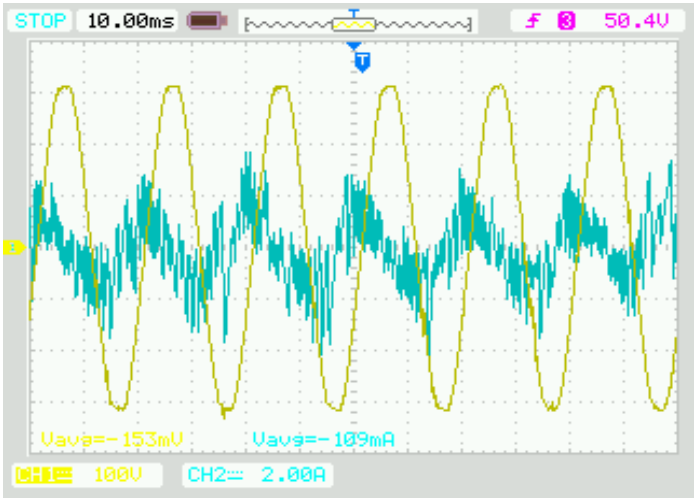

Figure 5.34 p-q theory with hysteresis current controller, source voltage versus filter current, experimental results

From oscilloscope records 25-30 switching per period are observed in source current waveform (1.25-1.5 kHz) which fairly coincides with Simulink FFT analyses result. Figure 5.33 shows that source current is in-phase with source voltage and reactive power compensation is achieved, also in Figure 5.34 filter current has 90º phase difference with source voltage and it illustrates that VSI produces reactive power and inject reactive current to the system to compensate reactive current of the load.

5.3.2.2 Non-active Current Theory with SPWM controller

In p-q theory implementation sampling time is considered 83.33µs however, non-active current theory with the SPWM controller implementation has taken more time to execute in DSP therefore sampling time is set to 100µs. the same set up in 5.1.2 is implemented in DSP flash programming DC link transient and steady-state variation, source current versus source voltage and filter current versus source voltage are shown in Figure 5.35 ,Figure 5.36 and Figure 5.37 respectively.

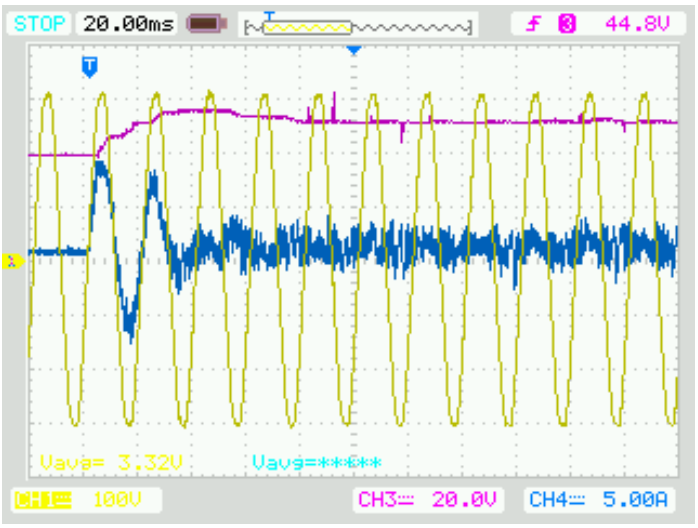

Figure 5.35 Non-active current theory with SPWM controller, DC link & source voltage & source current, experimental results

DC link is boosted to its reference value in one and half period of time and is completely coincide with simulation results in Figure 5.8 and Figure 5.9.

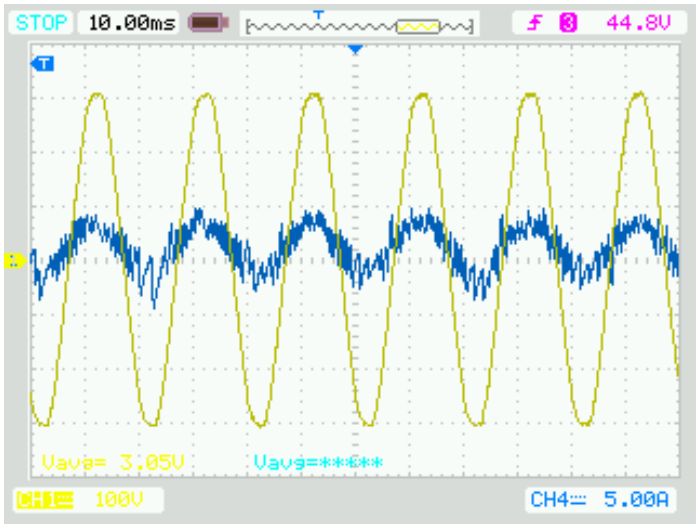

Figure 5.36 Non-active current theory with SPWM controller, source current versus source voltage, experimental results

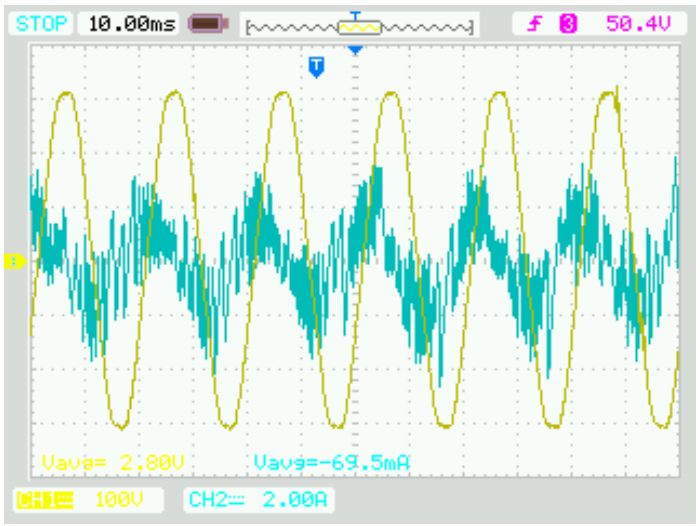

Figure 5.37 Non-active current theory with SPWM controller, filter current versus source voltage, experimental results

From above figures it is obvious that source current is in phase with source voltage and filter current is reactive current to compensate the reactive current of load. Experimentally reactive power and current is compensated and constant DC link voltage is satisfied by this control method. Switching frequency is around 1.25kHz (PWM carrier frequency) and matches the simulation results.

5.3.2.3 Cascade PI controller

Finally the proposed cascade PI controller with same setup that represented in 5.1.3 is implemented in DSP flash programming and experimental results gave credibility to proposed control method. Laboratory experimental results are represented below.

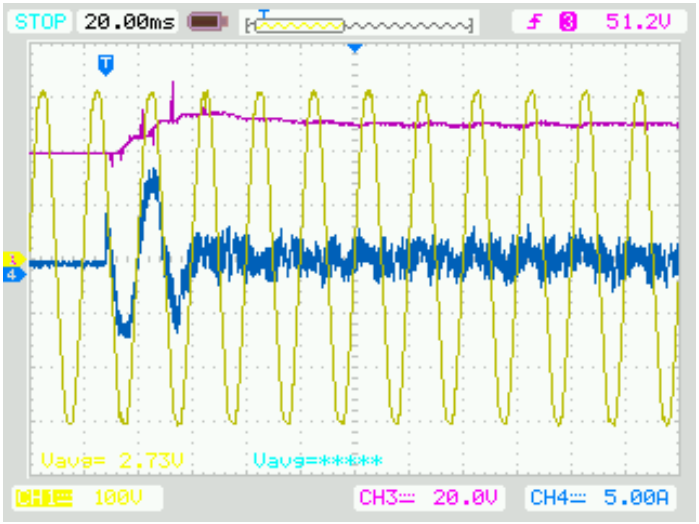

Figure 5.38 Cascade PI controller, DC link & source voltage & source current, experimental results

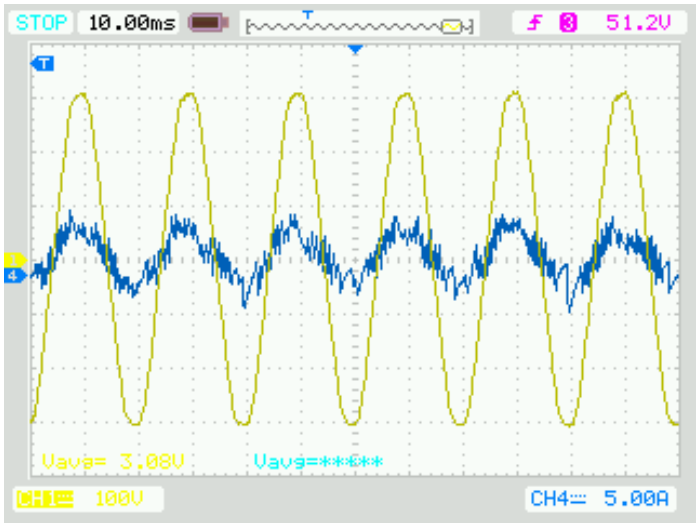

Figure 5.39 Cascade PI controller, source current versus source voltage, experimental results

From Figure 5.38 DC link in one and half period of time is boosted to 50 volt and it is completely coincide with simulation results in Figure 5.14 and Figure 5.15.

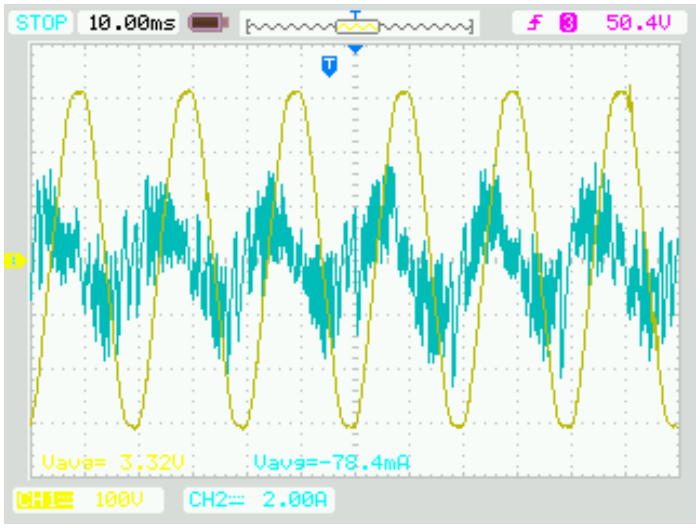

Figure 5.40 Cascade PI controller, filter current versus source voltage, experimental results

Figure 5.39 depicts that source current is in phase with source voltage and reactive power compensation is achieved properly and it is evident from Figure 5.40 that VSI is produced reactive current in order to supply reactive part of load then only active part of load is supplied by source voltage.

CHAPTER SIX
CONCLUSION

In this thesis instantaneous reactive power theory (p-q theory) and non-active current theory as two well-known control methods for STATCOM and APF are analyzed and some misinterpretations, limits and issues of these theories have been cleared up in chapter three. According to analyses it has been shown that under highly distorted source voltage or with non-linear load current reactive power and reactive current calculation of these theories is not accurate enough to be implemented for compensation purpose. In chapter four switching function based on SPWM control method is extracted for single phase STATCOM and extracted switching functions is implemented in space-state model of single phase STATCOM or APF both in MATLAB script programming and Simulation. Simulation results are verified the switching function and the model. By deep investigating the model it has been seen that DC link PI controller and current controller are key points in this scheme and the constant DC link and proper reactive power compensation can be achieved by just two cascade PI controller without any extra calculation for reactive power and reactive current, based on this experiment novel cascade PI controller for single phase STATCOM has been designed and effectiveness of the proposed method both in simulation and experiment is proven.

In the laboratory prototype experimental works, the simulation and model results are verified by experimental ones in p-q theory, non-active current theory and cascade PI control implementation. During experimental works it has been clarified that sampling time is a crucial factor in these configuration and control methods. Non-active current theory with SPWM controller needs more calculation burden in DSP programming than p-q theory with hysteresis current controller, and in this control method higher sampling time leads to smoother reference voltage and it leads to faster and more reliable switching which will leads to smoother filter and source current with lower Total Harmonic Distortion (THD).

In p-q theory with hysteresis current theory it has been observed that in 83.33μs sampling time, current controller could not able to properly limit the filter current between hysteresis bound and recorded hysteresis bound is wider than what was set in program. Higher sampling time leads to faster response of the controller and consequently filter current can properly meet hysteresis bound and smoother filter and source current can be produced. Higher sampling time can be attained by utilizing more powerful DSPs to decrease execution time or implementing optimization techniques in order to avoid repetitive calculation in each period and decrease calculation burden in DSP and enhance the performance of the system.

Also multi-level VSIs with cascade VSIs can be implemented in order to increase switching frequency and voltage level. Hybrid configuration is preferred because high frequencies can be filtered out by means of series PF and APF or STATCOM is responsible for low order harmonics and reactive power.

REFERENCES

Aghanoori, N., Mohseni, M. & Masoum,M. A.S. (2011). Fuzzy approach for reactive power control of dfig-based wind turbines, *Innovative Smart Grid Technologies Asia, Institute of Electrical and Electronics Engineers Power and Energy Society*, 1-6.

Akagi, H., Kanazawa, Y. & Nabae, A. (1984). Instantaneous reactive power compensation switching devices without energy storage component. *Institute of Electrical and Electronics Engineers Transaction on Industry Application, IA-20(3),* 625-630.

Akagi, H. (1994). Trends in active power line conditioners, *Institute of Electrical and Electronics Engineers Transaction on Power Electronics, 9,* 263–268.

Akagi, H., Watanabe, E. H. & Aredes, M. (2007). *Instantaneous power theory and application to power conditioning* (1th ed.). Institute of Electrical and Electronics Engineers Press: Wiley Interscience.

Avik, B. & Chandan, C. (2009). Adaline controlled 3-phase 3-wire shunt active power filter with enhanced performance using the capacitor voltage feedback, *Institute of Electrical and Electronics Engineers International Conference on Industrial Technology*, 1 – 6.

Bandal, V. S. & Madurwar, P. N. (2012). Performance analysis of shunt active power filter using sliding mode control strategies, *12th International Workshop on Variable Structure Systems*, 214 – 219.

Bhattacharya, S. & Divan, D. (1995). Design, implementation of a hybrid series active filter system, *Proceedings of the Institute of Electrical and Electronics Engineers Power Electronics Specialists Conference*, 189–195.

Bhattacharya, S., Veltman, A., Divan,D. M. & R Lorenz,. D. (1995). Flux based active filter controller, *Conference Record Institute of Electrical and Electronics Engineers- Industry Applications Society Annual Meeting*, 2483–2491.

Bose, B. K., (1990). An adaptive hysteresis-band current control technique of a voltage-fed PWM inverter for machine drive system, *Institute of Electrical and Electronics Engineers Transaction on Industrial Electronics, 37 (5)*, 402- 408.

Cataliotti, A., Genduso, F., Raciti, A. & Galluzzo, G. R. (2007). Generalized PWM VSI control algorithm based on a universal duty-cycle expression: theoretical analysis, simulation results, and experimental validations, *Institute of Electrical and Electronics Engineers Transaction on Industrial Electronics, 54 (3)*, 1569–1580.

Chen, C. & Divan, D. M. (1991). Simple topologies for single-phase AC line conditioning, *Conference Record Institute of Electrical and Electronics Engineers- Industry Applications Society Annual Meeting*, 911–917.

Choi, J. H., Park, G. W. & Dewan, S. B. (1995). Standby power supply with active power filter ability using digital controller, *Proceedings Institute of Electrical and Electronics Engineers the Applied Power Electronics Conference*, 783–789.

Cirrincione, M., Pucci, M., Vitale, G. & Miraoui, A. (2009). Current harmonic compensation by a single-phase shunt active power filter controlled by adaptive neural filtering, *Institute of Electrical and Electronics Engineers Transactions on Industrial Electronics, 56* (8), 3128 – 3143.

Czarnecki, L. S. (1987). What is wrong with the Budeanu concept of reactive and distortion power and why it should be abandoned. *Institute of Electrical and Electronics Engineers Transactions on Instrumentation and Measurement, im-36 (3)*, 834-837

Dahono, P. A. (2008). New hysteresis current controller for single-phase full-bridge inverters, *The Institution of Engineering and Technology Power Electronics, 2 (5),* 585 – 594.

Epstein, E., Yair, A. Alexandrovitz, A. (1979). Analysis of a reactive current source used to improve current drawn by static inverters. *Transactions on Industrial Electronics and Control Instrumentation, 23 (2),* 172-177

Fei, J., Li, T. & Zhang, S. (2012). Indirect current control of active power filter using novel sliding mode controller, *Institute of Electrical and Electronics Engineers 13th Workshop on Control and Modeling for Power Electronics*, 1 – 6.

Fryze, S. (1932). Wirk-, blind-, und scheinleistung in elektrischen stromkreisen mit nicht-sinusoidalen verlauf von strom und spanning. *Elektrotechnische Zeitschrift, 25–27.*

Grady, W. M., Samotyj,M. J. & Noyola, A. H. (1990). Survey of active power line conditioning methodologies, *Institute of Electrical and Electronics Engineers Transaction on Power Delivery, 5,* 1536–1542.

Gyugyi, L. & Strycula, E. (1976). Active AC power filters, *Conference Record Institute of Electrical and Electronics Engineers- Industry Applications Society Annual Meeting,* 529-535

Harashima, F., Inaba, H. & Tsuboi, K. (1976). A Closed-loop control system for the reduction of reactive power required by electronic converters, *Institute of Electrical and Electronics Engineers Transactions on Industrial Electronics and Control Instrumentation, 23 (2),* 162-166

Hayashi, Y., Sato, N. & Takahashi, K. (1988). A novel control of a current source active filter for AC power system harmonic compensation, *Conference Record*

Institute of Electrical and Electronics Engineers- Industry Applications Society Annual Meeting, 837–842.

Hong, R.C., Chang, G. W., Chao, C. Y., Chu, Y. B. & Chen, C. I. (2010). Incorporating hardware-in-the-loop simulation and ADALINE for shunt active power filter design, *The 5th Institute of Electrical and Electronics Engineers Conference on Industrial Electronics and Applications,* 492 – 497.

IEEE Std 1459™-2010. (2010). IEEE Standard Definitions for the Measurement of Electric Power Quantities Under Sinusoidal, Nonsinusoidal, Balanced, or Unbalanced Conditions. *Institute of Electrical and Electronics Engineers Power & Energy Society*

Jeraldine Viji, A., Pushpalatha, R. & Rekha, M. (2011). Comparison of an active harmonic compensator with PWM and delta modulation under distorted voltage conditions, *International Conference on Recent Advancements in Electrical, Electronics and Control Engineering,* 82 – 86.

Jou, H. L. (1995). Performance comparison of the three-phase active power filter algorithms, Proceedings Institute of Electrical and Electronics Engineers Generation, *Transmission, Distribution, 142 (6),* 646–652.

Kamran, F. & Habetler, T. G. (1998). A novel on-line UPS with universal filtering capabilities, Proceedings *Institute of Electrical and Electronics Engineers Power Electronics Specialists*, 500–506.

Kawabata, T., Miyashita, T. & Yamamoto, Y. (1990). Dead beat control of three phase PWM inverter, *Institute of Electrical and Electronics Engineers Transaction on Power Electronics, 5 (1),* 21– 28.

Liu, J., Yang, J. & Wang, Z. (1999). A new approach for single-phase harmonic current detecting and its application in a hybrid active power filter. *Institute of*

Electrical and Electronics Engineers Annual Conference of the Industrial Electronics Society, 2, 849-854

Lyon, V. (1935). [Discussion to H. L. Curtis and F. B. Silsbee paper "Definitions of power and related quantities," AIEE Transactions, vol. 54, no. 4, pp. 394–404, Apr. 1935], *Electrical Engineering*, 1121.

Marco, O. S., Alejandro, R. P. & Marving, A. J. (2003). Dynamic analysis of active filters using chaos theory, *Proceedings of the American Control Conference, 3*, 2413 – 2418.

Martin, D. & Santi, E. (2012). Auto tuning of digital deadbeat current controller for grid tied inverters using wide bandwidth impedance identification, *Annual Institute of Electrical and Electronics Engineers Applied Power Electronics Conference and Exposition,* 277 – 284.

Moran, S. (1989). A line voltage regulator/conditioner for harmonic-sensitive load isolation, *Conference Record Institute of Electrical and Electronics Engineers-Industry Applications Society Annual Meeting,* 945–951.

Moran, L., Werlinger, P. Dixon, J. & Wallace, R. (1995). A series active power filter which compensates current harmonics, voltage unbalance simultaneously, *Proceedings Institute of Electrical and Electronics Engineers Power Electronics Specialists Conference,* 222–227.

Nasiri, A. & Emadi, A. (2003). Modeling, simulation, and analysis of active filter systems using generalized state space averaging method, *The 29th Annual Conference of the Institute of Electrical and Electronics Engineers Industrial Electronics Society, 3*, 1999-2004

Nastran, J., Cajhen, R., Seliger, M. & Jereb, P. (1994). Active power filter for nonlinear AC loads, *Institute of Electrical and Electronics Engineers Transaction on Power Electronics, 9,* 92–96

Quinn, C. A., Mohan, N. & Mehta, H. (1993). A four-wire, current-controlled converter provides harmonic neutralization in three-phase, four-wire systems, *Institute of Electrical and Electronics Engineers Applications of Power Electronics Conference*, 841-846.

Raymond B. Sepe, J. (1993). A unified approach to hysteretic and ramp-comparison current controllers, *Conference Record of the Institute of Electrical and Electronics Engineers Industry Applications Society Annual Meeting, 1*, 724 – 731

Saadat, H. (2004). *Power system analysis* (2nd ed.). McGraw-Hill.

Saeedifard, M, Iravani, R. & Pou, J. (2007). Analysis and control of dc-capacitor-voltage-drift phenomenon of a passive front-end five-level convertor, *Institute of Electrical and Electronics Engineers Transactions on Industrial Electronics, 54 (6)*, 3255- 3266.

Singh, B., Al-Haddad, K. & Chandra, A. (1999). A Review of active filters for power quality improvement, *Institute of Electrical and Electronics Engineers Transactions on Industrial Electronics, 46 (5),* 960-971

Singh, B. & Solanki, J. (2009). An implementation of an adaptive control algorithm for a three-phase shunt active filter, *Institute of Electrical and Electronics Engineers Transactions on Industrial Electronics, 56 (8),* 2811- 2820.

Tsang, K. M. & Chan, W. L. (2005). Cascade controller for DC/DC buck converter, *Institute of Electrical and Electronics Engineers Proceedings Electric Power Applications, 152 (4),* 827 – 831.

Tsang, K. M. & Chan, W. L. (2006). Design of single phase active power filter using analogue cascade controller, *Institute of Electrical and Electronics Engineers Proceedings Electric Power Applications, 153 (5),* 735 – 741.

Tsang, K. M., Chan, W. L. & Tang, X. (2013). Multi-level shunt active power filter using modular cascade h-bridge and delay firing, *Taylor & Francis Electric Power Components and Systems, 41 (6),* 605 - 617.

Wang, X., Liu, J. J., Hu, J., Meng, Y. & Yuan, C. (2008). Frequency characteristics of the d-q synchronous-frame current reference generation methods for active power filter, *7th International Conference on Power Electronics,* 945 –950.

Xu, Y., Tolbert, L.M., Chiasson, J.N., Campbell, J.B. & Peng, F.Z. (2007). A generalised instantaneous non-active power theory for STATCOM. *The Institution of Engineering and Technology Electric Power Application,* 853 – 861

Xu, Y., Tolbert, L. M., Kueck, J. D. & Rizy, D. T. (2010), Voltage and current unbalance compensation using a static VAR compensator, *The Institution of Engineering and Technology Power Electronics, 3 (6),* 977-988.

Yazdani, D., Bakhshai, A., Joos, G. & Mojiri, M. (2008). An adaptive notch filtering approach for harmonic and reactive current extraction in active power filters, industrial electronics, *34th Annual Conference of Institute of Electrical and Electronics Engineers,* 535 – 538.

APPENDICES

Appendix A

Budeanu's Active and Reactive Power Definition

For a nonsinusoidal voltage and current that contain wide range of harmonic content, Budeanu by means of Fourier series and in harmonic domain defined active and reactive power as the multiplication of each voltage and current in the same frequency and neglected cross multiplication.

For voltage and current that defined as

$$v(t) = \sqrt{2} \sum_{h=1,2,3}^{n} V_h \sin(h\omega t) \tag{A.1}$$

$$i(t) = \sqrt{2} \sum_{h=1,2,3}^{n} I_h \sin(h\omega t - \varphi_h) \tag{A.2}$$

Budeanu defined active and reactive power like

$$p = \sum_{h=1,2,3}^{n} V_h I_h \cos(\varphi_h) = \sum_{h=1,2,3}^{n} P_h \tag{A.3}$$

$$q = \sum_{h=1,2,3}^{n} V_h I_h \sin(\varphi_h) = \sum_{h=1,2,3}^{n} Q_h \tag{A.4}$$